Patterns of recent sedimentation in Hudson Bay

By

Samantha Huyghe

A Thesis submitted to the Faculty of Graduate Studies of The University of Manitoba in partial fulfilment of the requirements of the degree of
MASTER OF SCIENCE

Department of Earth Sciences
University of Manitoba
Winnipeg

Abstract

Hudson Bay is a large Arctic/sub-Arctic shelf sea that covers an area of approximately 841,000 km^2, and is estuarine in character, with a large watershed and more than 40 rivers discharging into the bay. Sediment core data for 18 new cores in Hudson Bay was used to understand the processes effecting sedimentation in the bay. This data was interpreted together with sedimentation rates and inventories of ^{210}Pb and ^{137}Cs from previously published articles, archived cores, and geophysical data from the past four decades. Geophysical data shows that the bulk of sedimentation occurs offshore, between 100 and 150 m depth, on the east and northwest coasts of the bay, localized depressions along the southern coast between 50 and 100 m depth, and basins in the center of the bay. Inventories of ^{210}Pb and ^{137}Cs are variable but overall show a trend of lower inventories in the northwest to higher inventories in the southeast. Both geophysical and geochemical data show that sedimentation in the bay is largely transient with sediment deposits at the base of slopes, in localized depressions, and near the mouths of rivers.

Acknowledgements

First, I would like to sincerely thank my advisor Dr. Zou Zou Kuzyk for her support, patience, kindness, and encouragement throughout my degree. I would also like to thank my committee members, Dr. Ian Ferguson, and Dr. David Lobb for their suggestions, insight and for assistance with data analysis. I also wish to thank Dr. Patrick Lajeunesse, and Gabriel Joyal for access to their subbottom datasets.

Thanks are extended to Stephen Ciastek, Punarbasu Chaudhuri, Nolan Snyder, Teresinha Wolfe, Matt Donaldson, Catherine van Doorn, and Marie Pierrejean for their assistance in sample prep and field work. Special thanks to Anthony Buckley, Maureen Soon, Eva Slavicek, Michelle Kamula, and Masoud Goharrokhi for sample analysis and analytical protocols. I am also very thankful to the crew of the CCGS Amundsen for all of their work to ensure that I could obtain my samples.

I would like to thank BaySys, NSTP, ArcticNet/Amundsen Science, and Dr. Kuzyk for their financial support, without which this study would not have been possible. Special thanks to Tonya Burgers and Inge Deschepper for the zoom work sessions over the pandemic, you both helped me stay focused and motivated. Finally, I sincerely thank all of my loved ones for their unwavering support and cheerleading over the course of this degree, I would not have been able to do it without all of you.

Contents

Abstract ii

Acknowledgements iii

List of Figures vi

List of Tables viii

Chapter 1 Introduction 1

Objectives and Anticipated Significance 5

Thesis Structure 6

Chapter 2 Literature Review 7

Shelf Seas and Sedimentation 7

Sedimentation in Hudson Bay 8

Geological Setting 10

Application of Radioisotopes for Studying Modern Sedimentation 12

^{210}Pb 12

^{137}Cs 13

Previous Work 14

Chapter 3 Methods 16

Geophysical Data Review 16

Sediment Core Collection 20

Particle Size Analysis 24

Organic Carbon Analysis 24

Radioisotope Analysis 24

Calculations of Sedimentation Rates 26

Chapter 4 Results 28

Subbottom seismic profiles 28

Sediment Core Data 34

Particle Size Distribution 34

Carbon and nitrogen content 37

Porosity profiles 43

Profiles of Pb-210, Ra-226, and Cs-137 46

Inventories of ^{210}Pb and ^{137}Cs 51

Sedimentation rates estimated by modelling ^{210}Pb profiles 53

Chapter 5 Discussion 59

Distribution of depositional basins across Hudson Bay 59

Sediment core properties and sedimentation parameters in Hudson Bay 64

Northwestern Hudson Bay Cores 64

Southern Hudson Bay Cores 65

Eastern Hudson Bay Cores 66

Comparison with other published cores 67

Chapter 6 Conclusion 73

Chapter 7 References 75

Appendix 1: Table of Sediment Deposits from Geophysical Data 84

Appendix 2: Total Nitrogen vs Depth Plots 111

List of Figures

Figure 1-1: Map of Hudson Bay with collected cores (filled circles), previous cores (empty circles), and bathymetry. Bathymetric contours are 15m, 30m, 40m, 50m, 60m, 70m, 80m, 90m, 100m, 150m, 200m, and 250m. Scale 1:12,000,000..... 4

Figure 2-1: Simplified bedrock geology of Hudson Bay. Orange and pinks are Precambrian crystalline bedrock and blues and greens are Paleozoic carbonates. 12

Figure 3-1: a) Map of 3.5 kHz subbottom data. Light blue lines are 1977 and 1978 data and the remaining colours are 2003-2018 ArcticNet data. Scale 1:12,500,00. b) An example of the 3.5 kHz data from the ArcticNet data set showing the internal reflectors visible in these new data. 18

Figure 3-2: An example of one subbottom line displayed in (a) SeismiGraphix, (b) PostSurvey, and (c) SegyJp2Viewer 19

Figure 3-3: Distribution of sediment cores in Hudson Bay. Filled circles are new cores analyzed for this thesis and empty circles with italic and underlined labels are previously

published cores. Bathymetric contours are 15m, 30m, 40m, 50m, 60m, 70m, 80m, 90m, 100m, 150m, 200m, and 250m..... 22
Figure 4-1: Frequency distribution of sediment deposits located along seismic lines across water depth bins (a), latitudinal bins (b), and longitudinal bins (c). 29
Figure 4-2: Sediment deposits (red) and examined subbottom lines (dark grey). Blue lines show bathymetry of Hudson Bay. 31
Figure 4-3: Sediment deposits (red) and bedrock geology. Orange and pinks are Precambrian crystalline bedrock and blues and greens are Paleozoic carbonates. 32
Figure 4-4: Typical sediment deposits along the southeast coast of Hudson Bay. 33
Figure 4-5: Typical subbottom deposits in eastern Hudson Bay. 34
Figure 4-6: Typical subbottom deposits in southwestern Hudson Bay. 34
Figure 4-7: Typical subbottom deposits in northwestern Hudson Bay. 34
Figure 4-8: Photo of the coarse-grained materials at the surface of core 32. 35
Figure 4-9: Particle size distribution in surface samples throughout Hudson Bay. Yellow denotes gravel sized particles, grey denotes sand, orange denotes silt, and blue denotes clay. 36
Figure 4-10: Vertical profiles of organic carbon in the sediment cores. 40
Figure 4-11: Vertical profiles of carbon to nitrogen ratios. 42
Figure 4-12: Porosity profiles in the sediment cores. 45
Figure 4-13: Profiles of Ra-226 and Pb-210 in the sediment cores. 48
Figure 4-14: Profiles of Cs-137 and excess Pb-210 in the cores. 50
Figure 4-15: 210Pb inventories throughout Hudson Bay. Inventories are in dpm cm^{-2} 52
Figure 4-16: ^{137}Cs inventories throughout Hudson Bay. Inventories are in dpm cm^{-2} and adjusted to the year 1963. 53

Figure 4-17: Fits of the two-layer advective-diffusive model to measured excess ^{210}Pb profiles in the cores. 58
Figure 5-1: Sediment deposits identified from subbottom data overlying Zevenhuizen and Josenhans (1990) stratigraphic unit map 61
Figure 5-2 Cross sections of the slope gradients in Hudson Bay 62
Figure 5-3: Bottom currents in Hudson Bay simulated by the NEMO ocean model (Figure courtesy of Paul Myers, University of Alberta). 63
Figure 5-4 Cross section of the Midbay Bank and its proximity to cores 36 and 38. Top left: Subbottom image where core 38 was taken. Bottom left: Cross section of Midbay Bank (red line) Right: Map showing location of core 38 66
Figure 5-5: Spatial trends of ^{210}Pb in Hudson Bay based on the observed inventories and various smoothing methods. Courtesy of Dr. Ian Ferguson at the University of Manitoba. ... 70
Figure 5-6: Spatial trends of ^{137}Cs in Hudson Bay based on the observed inventories and various smoothing methods. Courtesy of Dr. Ian Ferguson at the University of Manitoba. .. 71
Figure 5-7: Excess ^{210}Pb inventories vs ^{137}Cs inventories. This figure includes inventories for new cores as well as previously published cores. ^{137}Cs data were adjusted to 1963. 72

List of Tables

Table 3-1. Core IDs, year obtained, coordinates, bottom depth, and core length 21
Table 4-1. Percentage of clay, silt, sand, and gravel sized particles in the surface sediment sample of each sediment core. 37

Table 4-2. Carbon and nitrogen data for the surface sections of each core 38

Table 4-3. Sedimentation rates and other modelled parameters in the cores. 55

Chapter 1 Introduction

Sedimentation rates control the accumulation and preservation (burial) of materials on the sea floor. In offshore or pelagic settings, sedimentation rates inform us about links between pelagic and benthic systems. In more coastal settings, sedimentation rates inform us about the intensity of sediment supply from rivers or coastal erosion (Déry et al., 2005; Duboc et al., 2017). However, it is not uncommon to find large spatial variation in sedimentation rates because of variation in sediment sources, transport processes, and depositional environment (Leivuori & Niemistö, 1995). Vastly different sedimentation rates can occur under situations of very similar sediment supply if the depositional regime is different. Within ocean basins and even across a single continental shelf, variations in topography, bottom roughness, slope gradients, and even the orientation of features relative to bottom currents creates tremendous diversity in depositional setting (de Haas et al., 2002).

Often, one of the ultimate applications of sedimentation rates is for constructing budgets for carbon or for various types of contaminants (De Haas et al., 1997; C. Michelle Kamula et al., 2020; Leivuori & Niemistö, 1995). The total sediment sink for the particular ocean area of interest is generally calculated by taking the sedimentation rates determined at a number of locations (i.e., from a number of discrete sediment cores), and 'scaling them up' to the total area of interest using some kind of map of surficial sediment distribution or other surface properties (cf., Cooper & Grebmeier, 2018). An area with a strong sediment sink has potential to be a strong sink for organic carbon or for burying contaminants. Sediment budgets also provide means of projecting the significance of various perturbations that could come about, for example through human impacts or climate change.

Arctic shelves are tricky places for interpreting radioisotope profiles and assessing sedimentation rates for the purposes of establishing sediment budgets. Arctic shelves and other northern shelf seas tend to be largely floored by relict sediments (Andrews & Tedesco, 1992; De Haas et al., 1997). Radionuclides such as ^{137}Cs and ^{210}Pb that can be used to date sediment cores are often present in lower initial concentrations in Arctic sediments because of great distance from source areas or low annual precipitation and hence scavenging from the atmosphere or low vertical particle fluxes and hence low scavenging from the water column (J. N. and E. K. M. Smith, 1982; Thibodeau et al., 2017). Furthermore, the application of

radioisotopes to date shelf sediment cores is complicated by bioturbation, which may mix tracer signals downwards in a sediment column just as rapidly as accumulating materials bury these signals, particularly in areas of low sedimentation (H. Josenhans et al., 1988). Two tracers often may be used together to estimate both sedimentation and mixing rates. If this is not possible, i.e., if rates just cannot be calculated because the assumptions implicit in applying the tracers are not met, then at the very least, it is possible to use the vertical profiles of tracers in sediment cores to assess sediment inventories or stocks – sums expressing how much material is held in a certain depth interval of the sediment column. Comparing sediment inventories of tracers can provide quite a bit of insight into the processes that are most important at particular locations, even if they do not allow estimation of a 'sediment sink' (Kuzyk et al., 2013).

Despite the challenge, Arctic shelves are places where better understanding of sedimentation rates is urgently needed. In Canada's eastern Arctic and Scandinavia, these areas are undergoing fundamental change due to relatively high rates of residual isostatic rebound from previous glaciation (Shilts, 1986). Arctic shelf areas are also highly susceptible to impacts from ongoing climate change and hydroelectric development (Duboc et al., 2017; Hochheim & Barber, 2014), as well as proposed shipping and leisure traffic as the shelf waters become ice free for longer spans of time.

In 2009, the first steps were taken towards developing sediment and organic carbon budgets for the Hudson Bay System, a large inland shelf sea at the southern margin of the Arctic which is undergoing rapid change in both ice environments and watershed processes (Hochheim & Barber, 2014; Ridenour et al., 2019). The average sedimentation rate from 13 sediment cores combined with an estimate of the area of active sedimentation in the Bay (~15% of the seafloor), yielded a sediment sink in Hudson Bay of 138 (±64)×10^6 t a^{-1} (Kuzyk et al., 2009). The known sediment sources could account for only about one-third of the apparent sediment sink implying a large imbalance, possibly explained by a large contribution of resuspended and laterally transported sediments to the burial flux. This sedimentary regime would place Hudson Bay in stark contrast to other northern shelves and severely limit its potential to act as a carbon and contaminant sink. Major uncertainties in this preliminary

estimate of the sediment sink included sparse sediment core data especially in the northwest quadrant of the bay and a lack of geophysical (sub-bottom) data particularly for coastal areas.

In this thesis, I present new radionuclide and supporting physical (particle size) and geochemical (organic carbon) data from 18 sediment cores collected across Hudson Bay (Figure 1-1). Most cores were collected as part of the 2018 NSERC-Manitoba Hydro "BaySys" project, which sought to explore the influences of both climate change and hydroelectric development within the Hudson Bay System. I use the profiles and inventories of the radioisotopes to determine sediment mixing and accumulation rates, to assess the intensity of scavenging and burial, and to detect riverine sediment influence. Secondly, I combine this new sediment core data with previously published radionuclide inventories and sedimentation rates and assess spatial and statistical trends within the combined data sets. Lastly, I interpret presence/absence of surficial sediment deposits from all known publicly available seismic data lines collected across Hudson Bay between 1977 and 2018 (representing tens of thousands of kilometres) to assess how sedimentation is distributed on the regional scale.

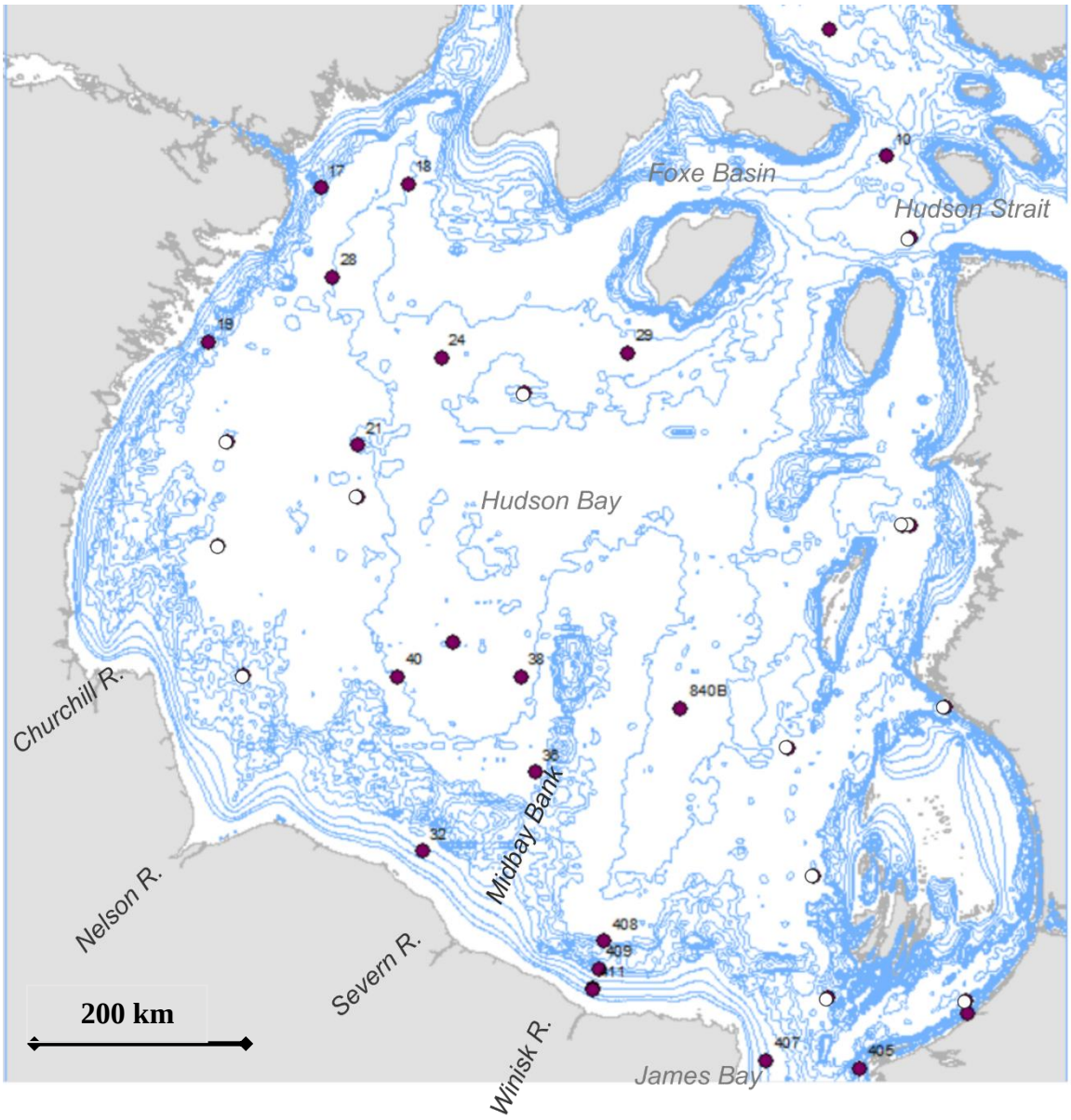

Figure 1-1: Map of Hudson Bay with collected cores (filled circles), previous cores (empty circles), and bathymetry. Bathymetric contours are 15m, 30m, 40m, 50m, 60m, 70m, 80m, 90m, 100m, 150m, 200m, and 250m. Scale 1:12,000,000

In past studies of sediment deposition and attempts to construct sediment budgets in Hudson Bay, there have been some critical gaps in the data that led to large uncertainties in conclusions. Josenhans et al. in their 1988 paper provided a good map of the locations and types of sediment within the bay but they lacked data for coastal regions. In Kuzyk et al. 2009, a limited number of cores was used, together with the Josenhans and Zevenhuizen 1990 map, to estimate the total sediment sink in Hudson Bay but cores were completely lacking for the northwestern and western portions of the bay as well as the area of the Winisk Trough and was also scarce along the southern and eastern shores. The preliminary sediment budget estimates included in Kuzyk et al., 2009 have been used as a basis for crafting a mercury budget for Hudson Bay (Hare et al., 2008) and a carbon budget (Capelle et al., 2020). These applications reinforce the need for improved understanding of sedimentation in Hudson Bay as a basis for future re-evaluation of the sediment sink and its role in mercury and carbon cycling.

Objectives and Anticipated Significance

This study aims to reassess sedimentation and its primary controls within Hudson Bay by filling in gaps about modern sediment coverage with the analysis of more geophysical data and re-evaluating average and ranges of sedimentation rates using a larger and more geographically distributed database of sediment cores. Specific objectives are as follows:

1. Revisit the previous estimate of the sediment sink for Hudson Bay
    a. Map sediment deposits from subbottom data
    b. Characterize surface and near-surface sediments using bulk properties and radioisotopes
    c. Where possible, determine sedimentation and mixing rates using vertical profiles of radioisotopes.
2. Use new and previous data to help determine the processes leading to spatial variation in sedimentation in Hudson Bay

Thesis Structure

This thesis is structured in six chapters. The first chapter is an introduction to the thesis and the objectives. The second chapter is a literature review section to introduce the study area and application of radioisotopes to determine sediment mixing rates in modern marine sediments. The third chapter is the methods and data collection section of the thesis. The fourth and fifth chapters consist of the results and discussion, respectively. The sixth chapter contains the conclusions. Following the sixth chapter are the references and appendices.

Chapter 2 Literature Review

Shelf Seas and Sedimentation

Continental shelves are areas of submerged continent that are shallower than 200 m (Mackenzie et al., 1988). These continental shelf areas can form large seas such as the North Sea, Baltic Sea, and Hudson Bay. They are typified by high sedimentation rates, which support high burial rates of carbon and other elements, meaning they are disproportionately important, relative to their surface area, as sinks in global elemental budgets such as the carbon budget (de Haas et al., 2002; Mackenzie et al., 1988). Thus, to be able to understand the fate of carbon or the fate of other elements or pollutants that cycle in association with carbon, it is important to determine sedimentation rates in the world's shelf seas. Shelf sediments also provide a number of other important ecosystem services, including habitat for marine life ranging from benthos to marine mammals such as walruses.

Sedimentation rates in shelf seas are fundamentally controlled by sediment supply. Sediment is supplied to continental shelf seas by many sources with main ones being river runoff, coastal erosion, ice rafting, and marine primary production (Kuzyk et al. 2009). Globally, river runoff is thought to provide 95% of the sediment entering the ocean (Syvitski et al., 2003); however, in arctic shelf areas, where thawing permafrost destabilizes shorelines, the sediment introduced by coastal erosion can exceed that supplied by river runoff (Stein & Macdonald, 2004). Continental shelf seas are also major sites of marine primary production (de Haas et al., 2002).

Sedimentation patterns in shelf seas tend to be complex. Along the continental shelves of eastern and northern North America, there are large areas showing little net active deposition and most surficial sediments are relict or reworked relict sediments (Piper, 1991). In some shelf areas, very little fine-grained sediment derived from coastal erosion and rivers escapes from the coastal zone (Piper 1991). In other systems, fundamental controls such as physiography and glacial isostatic adjustment, and wave driven resuspension are important processes controlling the distribution of sediment deposits (Suteerasak et al., 2017). In arctic areas, ice rafting and iceberg scour reworking of Quaternary sediments is common (Piper, 1991; Whitehouse et al., 2007).

Sedimentation in Hudson Bay

Hudson Bay is a marine body of water in central Canada that has an area of approximately 841,000 km^2 and an average depth of 125 m (Kuzyk et al., 2009). The Laurentide ice sheet covered the Hudson Bay area during the last glaciation in the late Wisconsinan and formed the Tyrrell Sea about 8,000 years ago when the ice sheet melted (Pelletier *et al.*, 1968). As a result of this glaciation and subsequent deglaciation, Hudson Bay is undergoing isostatic rebound. The rate of uplift in southern Hudson Bay was around 10 m per century during deglaciation and has slowed to about 1 m per century at present (Lavoie et al., 2002).

Sediment is supplied to and deposited in Hudson Bay by several different processes. The first process is sediment input from rivers discharging into the Bay. Hudson Bay receives approximately 713 km^3 of river run-off per year and an associated estimated $11.6x10^6$ Tg sediment (Kuzyk et al., 2009). The Hudson Bay watershed covers approximately $3.7x10^6$ km^2 of Canada throughout Alberta, Saskatchewan, Manitoba, Ontario, Quebec, and Nunavut (Déry et al., 2005) and comprises over 40 major rivers (Godin et al., 2017). Although sediment discharge from the bay's rivers has not been studied systematically, the rivers draining the Hudson Bay Lowlands in southwest Hudson Bay and James Bay are rapidly incising into fine-grained, uplifting glacial sediments (Cumming, 1968) and, in satellite imagery, appear much more reflective than rivers draining Canadian Shield. In the case of the largest river, the Nelson River that discharges to west Hudson Bay, Lake Winnipeg traps much of the sediment from the watershed implying that sediment discharged to Hudson Bay is mostly generated by bank erosion and algal production in reservoirs along the lower reaches of the river (Goharrokhi et al., 2021; and see also the MSc thesis of Tassia Stainton, 2019). In James Bay, a southern extension of Hudson Bay, southern rivers are under the influence of the great clay belt (Dresser, 1913) resulting in extremely high suspended sediment loads (de Melo et al., in review).

Sediment is also redistributed by currents, which circulate in a generally counterclockwise direction in Hudson Bay (Pelletier et al., 1968). The counter-clockwise coastal current is strong along the east coast of the bay particularly in fall (Saucier et al., 2004). In May and June, the flow pattern in eastern Hudson Bay reverses and the currents

flow in a clockwise direction, while currents in western Hudson Bay still flow counter clockwise, causing flow convergence near James Bay (Ridenour et al., 2019). Bottom currents have not been reported.

A third important set of processes affecting sediment deposition is ice scour and ice rafting. Hudson Bay is covered in sea ice for much of the year. Ice forms between late October and December and melts between May and July depending on location within the bay (Hochheim & Barber, 2014). The mobile pack ice near the shore moves counterclockwise around the Bay and when the ice melts, it deposits the sediment it has accumulated (Pelletier et al., 1968). There is also more recent evidence (Barber et al., 2021; Landy et al., 2017) showing that the ice is thicker in the southern or southeastern portion of the bay both during winter and during summer when overall ice extent is very low because of widespread melt. A large amount of pack ice often collects in southern Hudson Bay in June because of northerly and northwesterly winds moving the ice southward throughout winter, with the consequence that there is potential for a significant amount of sediment-laden ice to melt in the southern area just west of James Bay. Although the source of the sediment in the pack ice is not known, suspension freezing during ice formation is suspected to be important. The very thick ice that results from dynamic processes throughout winter (e.g., pack ice colliding with itself or with landfast ice) means that the ice in Hudson Bay may interact with the seabed at much greater water depths than would be expected from the thermodynamic ice thickness of 1.0-1.5 m. The late-melting ice observed in southwest Hudson Bay by Barber et al. (2021) had an average freeboard of 2.2 m, which corresponds to an estimated total thickness of 18 m. In eastern Hudson Bay, a zone of maximum ice scouring was found at water depths between 8 and 12 m and corresponded to a zone of maximum erosion of Holocene sediments (Hequette et al., 1999). Bottom scouring by dragging ice keels is believed to resuspend the sediments, and near-bottom currents subsequently redistribute the resuspended sediments.

There are large differences between coastal and interior Hudson Bay in terms of river influence, sea ice cover (landfast vs. mobile pack ice), primary production and many other factors that may be expected to affect sedimentation. Coastal Hudson Bay is subject to processes within the Riverine Coastal Domain (RCD), which is a narrow, shallow, feature that transports freshwater along Arctic coasts (Carmack et al., 2016). The RCD presumably

affects how land-derived sediment is transported within the bay although little is known about this region because early studies (e.g., as reported in Josenhans et al., 1988) largely avoided these poorly charted areas. The interior of the bay contains mostly glacial sediment deposits and has glacial features that are preserved on the seafloor (Lajeunesse & St-Onge, 2008; Pelletier, 1986). The glacial sediment deposits consist of glaciomarine sediments deposited during the retreat of the Laurentide Ice Sheet, paraglacial deposits and postglacial deposits (Haberzettl et al., 2010).

Biological material is also very important to sedimentation. Hudson Bay has many areas that have high primary production (Sibert et al., 2011), which allows for more particle scavenging, i.e., uptake of ^{210}Pb (and other particle-reactive substances) dissolved in the water column, and subsequently more deposition (Appleby, 2001). The northwestern portion of Hudson Bay is the location of a large recurrent polynya during the winter (Saucier et al., 2004), which appears to be a significant hotspot of spring primary production (Matthes et al., 2021). Spatial patterns of primary production and export of produced material to the seabed in Hudson Bay have been modeled; however, changing ice conditions throughout the bay (Hochheim & Barber, 2014; Landy et al., 2017; Sibert et al., 2011) mean that the blooms are subject to change in the future.

In addition to the natural processes governing sedimentation rates and patterns in Hudson Bay, there are also anthropogenic factors. Due to hydroelectric development, there has been a change in the amount and timing of river runoff entering Hudson Bay as well as the energy with which the water enters the bay (Dery et al. 2005). It has been suggested that hyperpycnites - deposits from hyperpycnal flows related to ice jam formation on the Lower Nelson River - have decreased due to dam construction on this river (Duboc et al., 2017). Due to climate change the seasonal ice cover in Hudson Bay is exhibiting freeze-up approximately a month later and breakup a month earlier than it used to (Gagnon & Gough, 2005), which may potentially lead to a change in sediment sources and sinks in Hudson Bay.

Geological Setting

The bedrock beneath Hudson Bay is comprised of the Precambrian Superior Province and Trans Hudson Orogen, and the Paleozoic Hudson Bay Platform (Donaldson, 1986; Norris,

1986) (Figure 2-1). The Superior Province, which makes up the bedrock of the east coast of Hudson Bay, largely consists of Archean and Proterozoic granitic plutons and gneisses as well as a lesser amount of metamorphosed basalt and sedimentary rocks (Donaldson, 1986; Henderson, 1989).

The Trans Hudson Orogen comprises the western coast of Hudson Bay and is also mostly granitoid igneous rocks and gneisses (Donaldson, 1986). It is comprised of the Rae Craton, Hearne Craton, and the Chesterfield Craton (Pehrsson et al., 2013). Hudson Bay Platform is composed of Ordovician, Silurian, and Devonian age shallow marine facies, the bulk of which are limestones (Norris & Sanford, 1968). There is also a coal rich Cretaceous formation to the southwest of James Bay that is contributed into the bay by Moose River (Nicolas & Armstrong, 2017).

The two widely dissimilar rock types have weathered and eroded to produce different landscapes southwest vs. east of the bay and the contrasts apparently also extend to the continental shelf as pronounced variations in bottom physiography in various parts of the bay. Coastal areas in the south, where the bedrock is composed of carbonate rocks, are more susceptible to erosion than both the western and eastern coasts that are composed of more resistant crystalline bedrock.

Ridges and valleys on the seafloor indicate an old drainage system; the valleys are U-shaped, indicating that they were eroded by glaciation (Pelletier et al., 1968). In the Wisconsinan age, several glacial advances took place with sea water entering the area when the glacier receded (H. Josenhans et al., 1988; Shilts, 1982, 1986). This created many episodes of erosion followed by the deposition of till (Shilts, 1982). As the glacier receded for the final time it deposited more till and exposed the U-shaped valleys and ridges created by the glacier, which were then infilled with seawater (Pelletier, 1968). Many of these features are still present today, affecting where sediment is deposited in the bay (Pelletier, 1986).

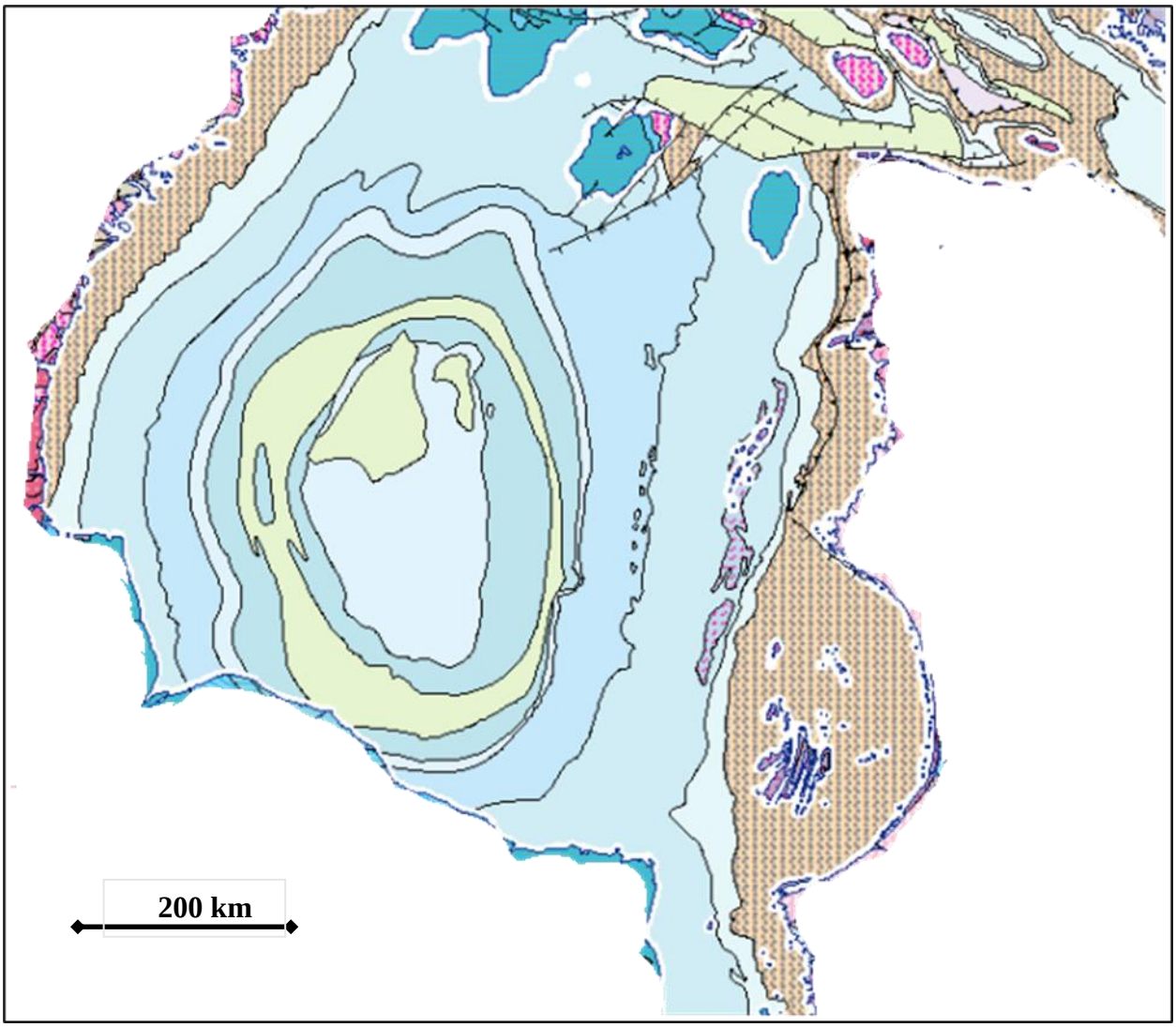

Figure 2-1: Simplified bedrock geology of Hudson Bay. Orange and pinks are Precambrian crystalline bedrock and blues and greens are Paleozoic carbonates.

Application of Radioisotopes for Studying Modern Sedimentation

^{210}Pb

^{210}Pb is a radioisotope that is commonly used in dating sediment cores. Lead-210 is a naturally occurring radioisotope that is part of the Uranium-238 decay series (Appleby & Oldfield, 1992). The ^{210}Pb content in sediment is comprised of two components, supported ^{210}Pb and unsupported ^{210}Pb, which make up the total ^{210}Pb content. Supported ^{210}Pb is derived from *in situ* decay of ^{226}Ra in bottom sediments whereas unsupported ^{210}Pb is derived

from the atmosphere (Kuzyk et al., 2009). Unsupported ^{210}Pb has two sources: particle scavenging and runoff. Some of the ^{222}Rn produced by the decay of ^{226}Ra escapes from the bottom sediment and is released into the atmosphere (Appleby & Oldfield, 1992). The ^{222}Rn then decays into ^{210}Pb and is reintroduced to the water column through precipitation. The lead is then scavenged by particles and deposited on the bottom of the body of water. Unsupported ^{210}Pb from runoff occurs when ^{210}Pb is introduced to the system through precipitation on land into the watershed or from the decay of ^{226}Ra in soil (Appleby, 2001). A large inventory of unsupported ^{210}Pb in a core means that the area is depositional whereas if there is only a small amount of unsupported ^{210}Pb it is likely that the area experiences a lot of erosion or resuspension (Kuzyk et al. 2009). Where there are deep ocean basins with long water residence times and low particle production and settling processes, dissolved ^{210}Pb produced by decay of dissolved ^{226}Ra may accumulate in the water column, leading to the process of 'boundary scavenging' around the margins, where the ^{210}Pb-rich water mass encounters settling particles and rapid removal of ^{210}Pb occurs (Kuzyk et al., 2013)

Once a sediment core is obtained, sediment subsections or slices may be analyzed to determine the downcore profile of ^{210}Pb. A typical ^{210}Pb profile in recently deposited marine sediments shows excess ^{210}Pb decreasing exponentially (with decay) to background levels deeper in the core. This interpretation of a decrease in ^{210}Pb with depth being due solely to accumulation of sediment at the seabed and decay of previously deposited ^{210}Pb makes the assumption of steady-state deposition, meaning that ^{210}Pb is being deposited at a constant rate (Appleby and Oldfield, 1992). This assumption is used when modelling ^{210}Pb in a two-layer advection-diffusion model such as the one used later in this thesis. A two-layer advection-diffusion model assumes steady-state as well as a top layer that is subject to bioturbation from benthic organisms and a lower layer where bioturbation does not take place (Kuzyk et al., 2015). In a natural system, variation in the rate of ^{210}Pb deposition may be caused by changes in particle size or composition, which alters the initial activity ^{210}Pb, or fluctuations in the amount of material being deposited (sediment flux).

^{137}Cs

Cesium 137 is a useful tracer for estimating sediment fluxes as well as a useful check on ^{210}Pb sedimentation rates because it does not naturally occur in the environment. ^{137}Cs is a

human made radionuclide that derives from nuclear fission (Foster et al., 2006; Kuzyk et al., 2013; Walling & He, 2000). It was introduced into the environment primarily during the period of nuclear weapons testing during the peak of the Cold War. Due to the large amount of ^{137}Cs released into the atmosphere during this time, it can be used globally as a marker of the 1950s to approximately 1963 when many countries agreed to faze out the use of nuclear weapons (Zaborska et al., 2010). More recent sources of ^{137}Cs are due to resuspension and transport through watersheds and runoff (Oughton et al., 1997).

Profiles of ^{137}Cs typically show no cesium at the bottom of the core followed by a pulse of ^{137}Cs followed by a steady decrease to the surface. Cores that have a secondary increase near the surface are likely getting a freshwater watershed source of ^{137}Cs deposited into the area (J. N. and E. K. M. Smith, 1982). Cores that have little or no ^{137}Cs might have been subject to erosion or the ^{137}Cs might have migrated in dissolved phase out of the sediments (Oughton et al., 1997). A third alternative is that the ^{137}Cs decayed out completely based on its short half life of 30.2 years (Wright et al., 1999).

Previous Work

Previous geophysical works in Hudson Bay were done using Huntec, sidescan, airgun, and 3.5kHz seismic data (Josenhans et al., 1988, Zevenhuizen & Josenhans, 1990) and sidescan data alone (Henderson, 1989) to map the postglacial sediment in Hudson Bay. Henderson (1989) found that post-glacial sedimentation was restricted to <100 m depth and was often reworked by rivers and marine currents. Josenhans et al. 1998 used primarily Huntec to analyze the sediment type determining whether it was glacial till, glaciomarine, or postglacial sediment and 3.5kHz data to extrapolate from the Huntec data to map the sediment type throughout the bay. They determined that glaciomarine and postglacial sediments are largely restricted to localized depressions and river mouths with glacial till throughout the bay. More in-depth studies have been done in portions Maclean et al., (1992) conducted a study of Hudson Strait and Ungava Bay using Huntec and determined that there were large basins that were the location for accumulation of postglacial sediment though those basins were still glaciomarine predominantly. Gonthier et al., (1993) conducted a study near the mouth of the Great Whale River using sidescan, 3.5 kHz profilers, and Huntec. They

determined that the sedimentation in the area has up to 50 m of Quaternary sediment in some locations but only units 4 and 5 are postglacial.

Previous geochemical studies in Hudson Bay include Duboc et al.'s (2017) study of sediment cores in the Churchill and Nelson estuaries, Thibodeau et al.'s (2017) study on low Pb accumulation in Hudson Bay, Hulse & Bentley's (2012) ^{210}Pb budget of the Great Whale River delta, and Kuzyk et al.'s (2009) preliminary sediment budget for Hudson Bay. Duboc *et al.* (2017) found evidence of hyperpycnites in cores from the estuaries of the Nelson and Churchill rivers, indicating that ice jams caused damming and then large influxes of sediment into the estuary. However, since hydroelectric damming has taken place, the hyperpycnites have stopped occurring indicating that the control in water flow has also changed the sediment influx into Hudson Bay. Thibodeau *et al.* (2017) found low levels of lead in Hudson Bay despite increased anthropogenic lead inputs in the last century. They determined that there was low vertical export of lead due to low primary production. Hulse & Bentley (2012) determined that there was an offshore shift in sediment deposition near the mouth of the Great Whale River. They also determined that 77% of the sediment delivered by the river was being deposited even further offshore or elsewhere in the bay. They concluded that the warming climate could cause more energetic conditions allowing for sediment to be carried further from its source. Kuzyk et al. (2009) estimated a sediment sink of 138 (±64) x 10^6 t a^{-1} and calculated that only one third of that is from contemporary sediment sources to the bay. This indicates that resuspension is a major factor in the sediment sink in Hudson Bay.

Chapter 3 Methods

Geophysical Data Review

Geophysical data was obtained from Nature Resources Canada and Professor Patrick Lajeunesse's team at Laval University, which has conducted a seabed mapping program throughout the Canadian Arctic as part of ArcticNet (2003-2018). Data were collected from areas of interest for oceanographic research as well as marine geology. All the data is 3.5 kHz acoustic soundings obtained through underway systems on various vessels. The bulk of the data for offshore areas is from 1977 and 1978, which was digitized by NRCan.

Overall, there was more than 100,000 km worth of data analyzed for this thesis. Figure 3-1 shows the distribution of the data with the light blue lines denoting the 1977 and 1978 data and remainder of the colours denoting the ArcticNet mapping. I analysed these data by eye (Hougardy, 2014; Josenhans & Zevenhuizen, 1990) using a photo viewer program with the goal of identifying surficial unconsolidated deposits. As reference, I used a combination of previous works on Hudson Bay (Henderson, 1989; H. Josenhans et al., 1988; Pelletier, 1986) and other seismic survey studies (Hougardy, 2014; Todd et al., 1998). Older data was analysed using the method of classification that was used in Josenhans *et al.* 1988 due to the nature of the quality of the scans of the subbottom data. These data sets were largely lower quality jpeg files in which reflections were not clearly visible unless they were strong reflections. For example, it was often difficult to determine if the sediment deposits were one layer overlying bedrock due to the lack of reflectors in many of the deposits. Due to the low resolution of this data, the lack of reflections could indicate either largely homogenous unit (no interbedded sands) (Hougardy, 2014) or that the scanned image does not display layers that are present.

Newer data from 2003-2018 collected from the CCGS Amundsen is high quality (see, for example, Figure 3-1b) and was able to be viewed in three programs SEGYJp2 launcher (NRCan), SounderSuite: PostSurvey (Knundsen), and SeismiGraphix (SeismiGraphix). I used these programs to pick out recent sedimentation again by eye using all three programs in

tandem to be able to zoom in with higher resolution to confirm the presence of a deposit (SeismiGraphix), get a crisp, clear image of the whole line (PostSurvey), and access the metadata attached to the lines (SEGYJp2 launcher). Below in Figure 3-2 are screenshots of the same subbottom file on all three programs. SeismiGraphix (Fig. 3-2a) clearly has the greatest amount of detail in the image itself, but it does not provide latitude and longitude for any given point. PostSurvey (Fig. 3-2b) also shows detail quite well, but it does not have any depth information or scale bars on the image which makes it difficult to get any information about a selected deposit. SEGYJp2 launcher (Fig. 3-2c) is the only program of the three that stitches the line together properly if something interfered with the signal and provides all the metadata for any given point selected. However, it does not provide as high quality of an image and the zoom function makes the image blurry much faster than the other two programs. Therefore, it was often necessary to use a combination of two or all three to acquire the most accurate determination of whether a sediment deposit was present or not.

The newer data and ability to view data in multiple programs allowed for higher confidence in the presence of deposits picked out of the 2003-2018 data. It was also easier with the newer data to view units within a sediment deposit as well as being able to see a thin drape of sediment with more ease. It is not likely that deposits thinner than 5m can be reliably detected and the lack of an appearance of sediment in those areas does not mean that the seafloor is just exposed bedrock. An example of the newer data is shown in Figure 3-1b, where it is possible to see a lower reflection unit overtop of a higher reflection unit indicating that the upper unit is likely mud compared to a sandier unit below it (cf., Hougardy. 2014). The identified sediment deposits from all data sets were logged (Appendix 1) and plotted on a map of Hudson Bay. Notes were made regarding the character of the deposit, discrete vs. continuous, thin vs. thick as well as characteristics of reflections (Appendix 1).

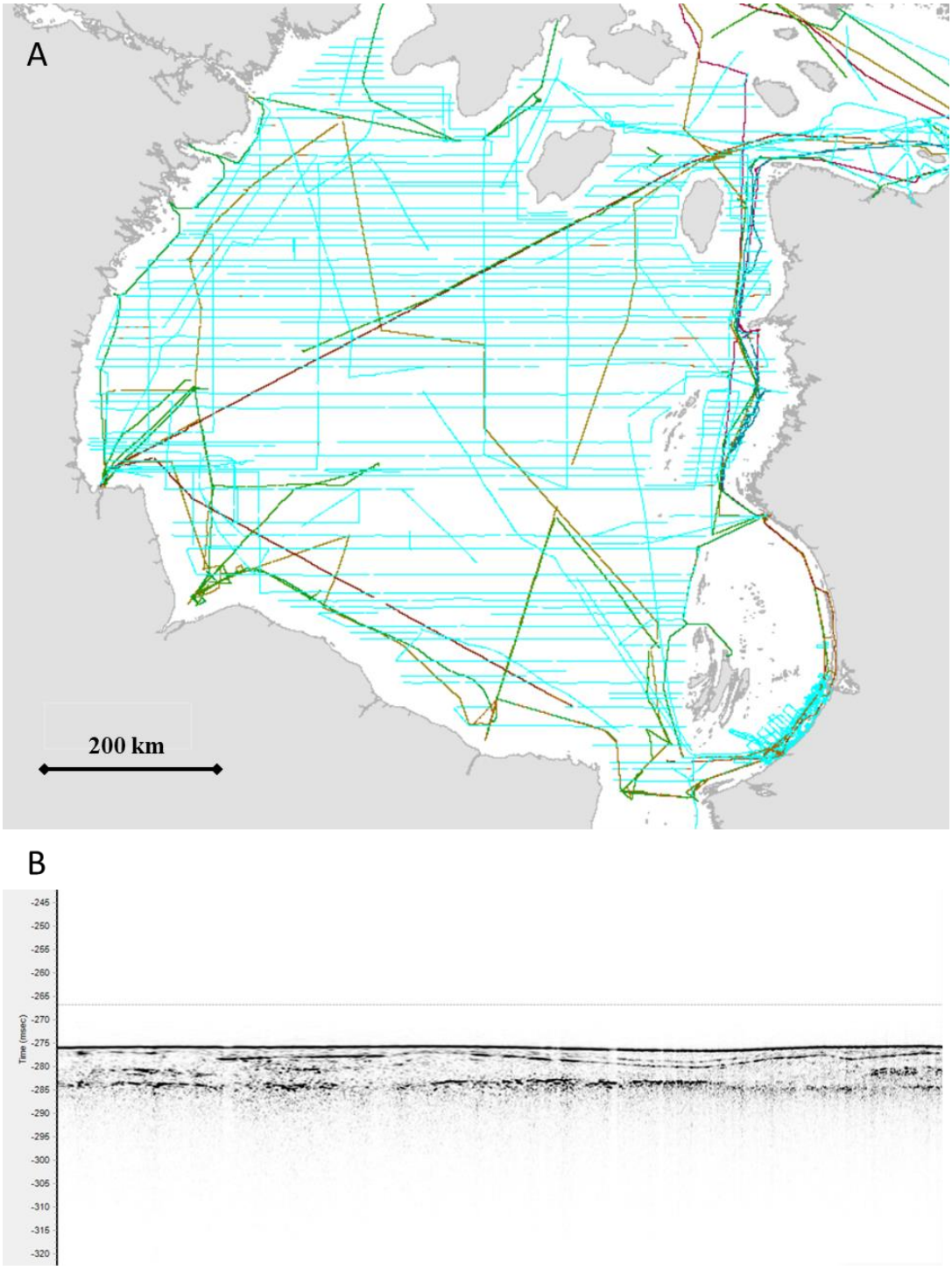

Figure 3-1: a) Map of 3.5 kHz subbottom data. Light blue lines are 1977 and 1978 data and the remaining colours are 2003-2018 ArcticNet data. Scale 1:12,500,00. b) An example of the 3.5 kHz data from the ArcticNet data set showing the internal reflectors visible in these new data.

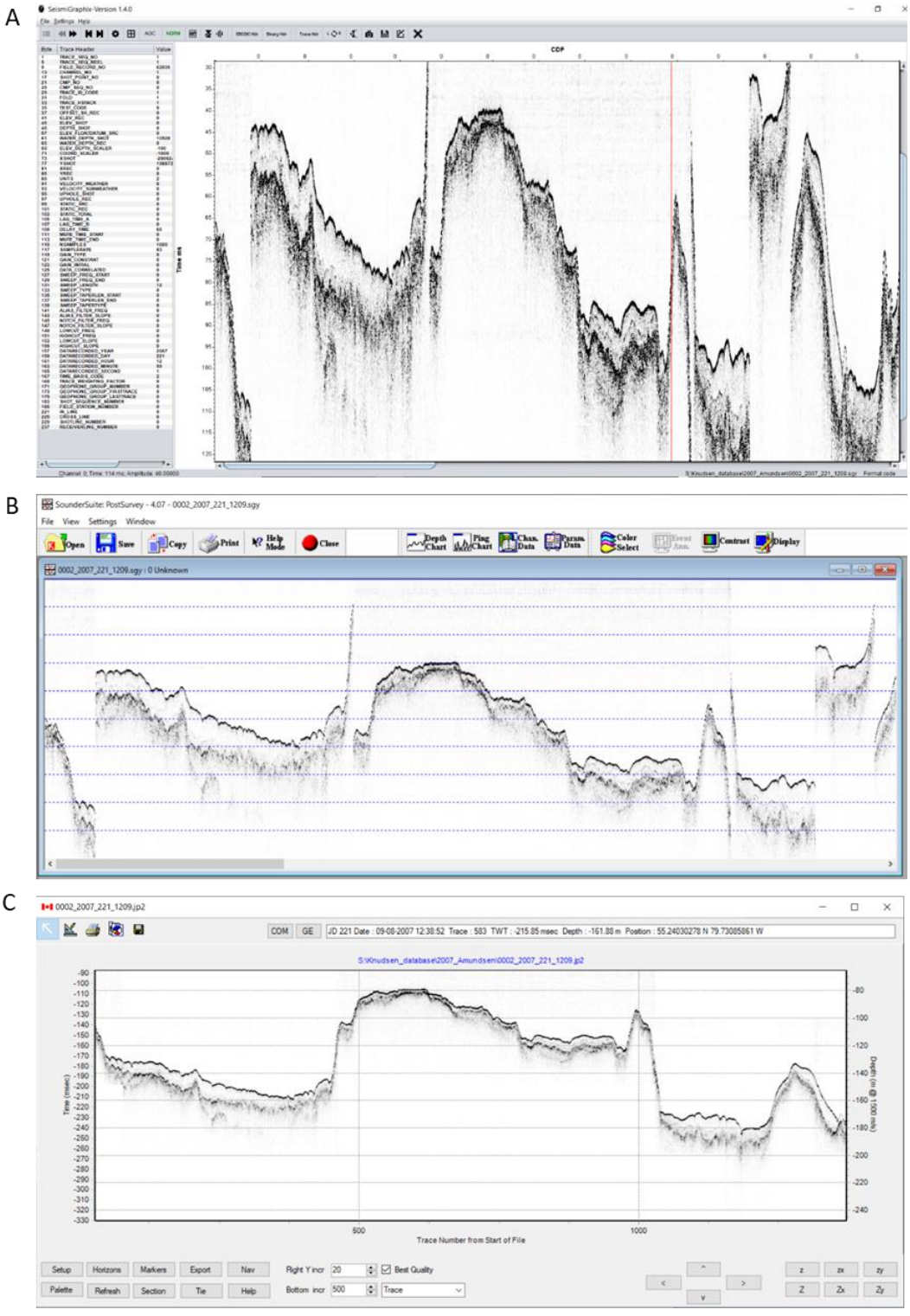

Figure 3-2: An example of one subbottom line displayed in (a) SeismiGraphix, (b) PostSurvey, and (c) SegyJp2Viewer

Sediment Core Collection

Eighteen new and previously unstudied cores were analyzed for this thesis (Table 3-1). Five of the cores (405, 407, 408, 409, 411) were previously collected aboard the CCGS Amundsen Icebreaker between August 10 and 12, 2007. These cores were obtained from the entrance to James Bay and the coastal area near the Winisk River in southwest Hudson Bay (Figure 3-3). Core 840B was collected aboard the CCGS Amundsen during the summer of 2013 from a location west of the Belcher Islands (Figure 3-3). The remainder of the cores (n=12) were collected aboard the CCGS Amundsen during the BaySys cruise in summer 2018.

A box corer was used to collect all the sediment cores and push cores were then taken by hand from each box. Sites for sampling during the 2018 Amundsen cruise were selected by the science steering committee onboard the vessel during meetings, and the decision whether to box core was made based on real-time sub-bottom data from the acquisition room to help avoid areas that had a rough subbottom that could damage the box corer or areas that did not appear to have a significant amount of sediment. Push cores were taken only if the surface of the mud in the box corer was undisturbed and there was still surface water above the sediment surface indicating that the box corer had properly sealed. The geographic emphasis with the new cores was northwest Hudson Bay (cores 17, 18, 19, 21, 24, and 28) and southwest Hudson Bay west of the Midbay Bank (cores 32, 36, 38, and 40) (Figure 3-3). This distribution complements the distribution of previously studied cores (Kuzyk et al., 2009; Thibodeau et al., 2017), which emphasized the central and eastern portions of the bay (see empty circles in Figure 3-3). The 12 new cores were obtained from bottom depths between 34 and 203 m. The core lengths that were recovered varied from 24 to 36 cm (Table 3-1).

Table 3-1. Core IDs, year obtained, coordinates, bottom depth, and core length

Core IDs	Year	Latitude (N)	Longitude (W)	Water Depth (m)	Length of Core (cm)	Bottom Water Salinity (PSU)
405	2007	54.67400	-79.9523	62	37.5	30.5
407	2007	54.76417	-81.7163	27	31	29.7
408	2007	56.03733	-84.7403	103	26	32.6
409	2007	55.73983	-84.8338	58	30	31.2
411	2007	55.52883	-84.9505	26	30	27.2
840B	2010	58.41100	-83.3030	175	26	32.0
10	2018	63.45071	-79.4452	203	22.5	32.6
17	2018	63.18458	-90.0337	92	31	32.9
18	2018	63.71968	-88.4021	122	28.5	33.4
19	2018	61.84316	-92.1328	86	32.5	33.0
21	2018	60.91407	-89.3385	149	26.5	33.0
24	2018	61.70548	-87.7845	186	36	33.0
28	2018	62.41676	-89.8175	162	24	33.1
29	2018	61.74867	-84.2958	177	34	32.8
32	2018	56.97127	-88.1301	34	27.5	31.1
36	2018	57.77581	-86.0279	127	34.5	32.6
38	2018	58.72343	-86.2957	180	33.5	33.1
40	2018	58.24775	-88.5965	90	27.5	32.6

The cores were immediately extruded and subsectioned and the samples frozen. Cores were subsectioned into 1 cm slices for the first 10 cm of the core, 2 cm slices for the following 10 cm, and 5 cm slices from 20 cm to the bottom of the core, with a few exceptions. Cores 17, 18, and 19 were subsectioned into 1 cm slices for the first 10 cm and then 2 cm slices for the remainder of the core due to visible changes in grain size and colour in the sediment. Core

840B was subsectioned into 0.5 cm slices for the first 10 cm and 1 cm slices for the remainder of the core.

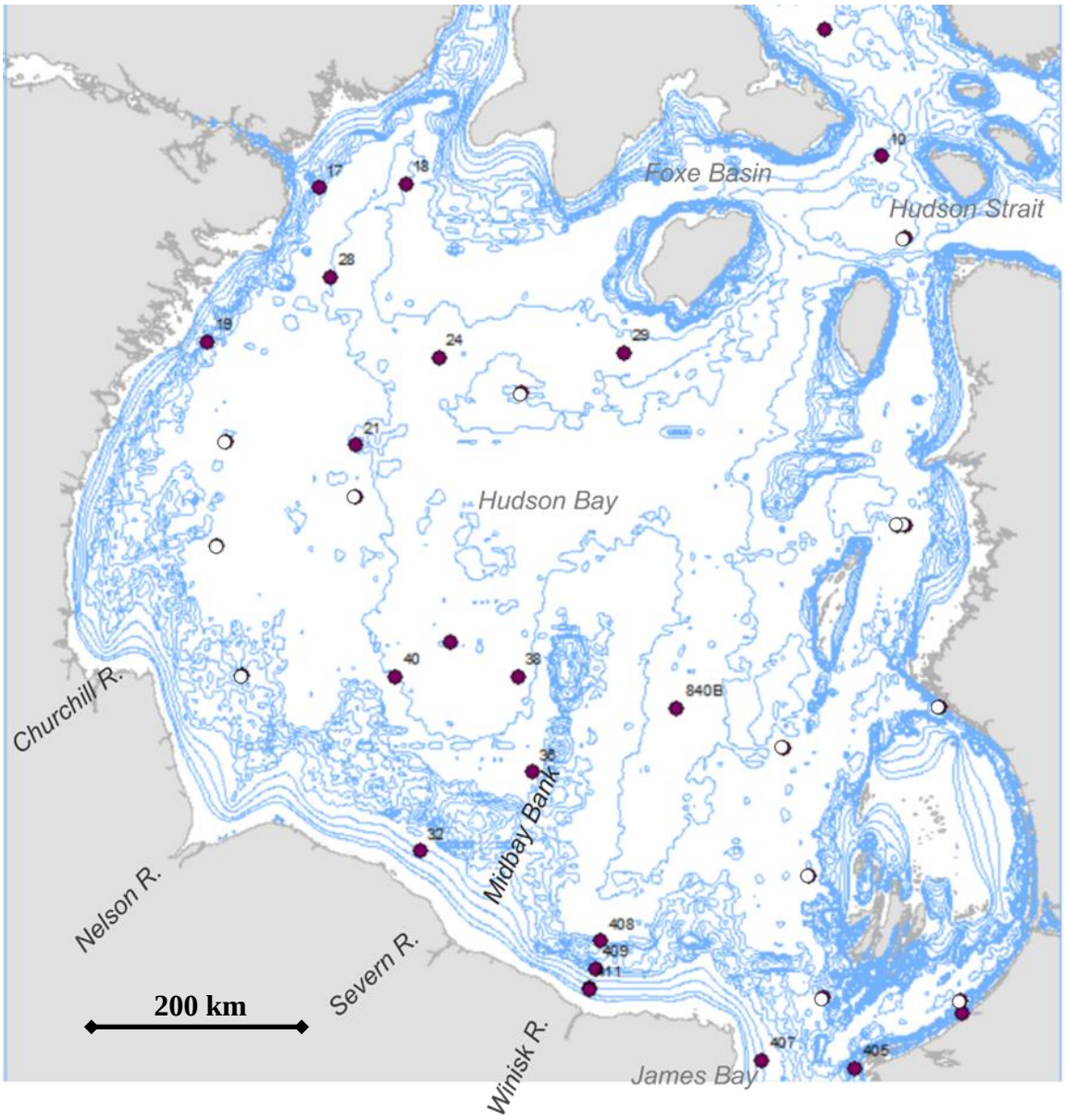

Figure 3-3: Distribution of sediment cores in Hudson Bay. Filled circles are new cores analyzed for this thesis and empty circles with italic and underlined labels are previously published cores. Bathymetric contours are 15m, 30m, 40m, 50m, 60m, 70m, 80m, 90m, 100m, 150m, 200m, and 250m.

Once all the samples were back in Winnipeg, the sediment was thawed and subsampled into 20 ml vials. The sediment samples in the vials were freeze dried at -55°C for 3-4 days at the University of Manitoba to remove the water from the samples. Wet and dry weights were recorded for each sample to allow for porosity calculations using equations 1 through 4. The dry weights of the sediment were then salt corrected using the bottom salinity obtained from CTD data on the rosette from each coring site and equations 5 through 8.

Equation 1

$$\frac{Wet\ Wt. - Dry\ Wt.}{Wet\ Wt.} = W$$

Equation 2

$$((W + (W * S)/1000))/\rho = V_w$$

Equation 3

$$\frac{\left(1 - W - \frac{W * S}{1000}\right)}{\rho_s} = V_s$$

Equation 4

$$\frac{V_w}{V_w + V_s} = \Phi$$

Equation 5

$$Mass\ of\ solid = 1 - W$$

Equation 6

$$Mass\ of\ salt = \frac{W * S}{1000}$$

Equation 7

$$Mass\ of\ salt\ free\ solid = Mass\ of\ solid - Mass\ of\ salt$$

Equation 8

$$Factor\ of\ salt = \frac{Mass\ of\ solid}{Mass\ of\ salt\ free\ solid}$$

Where W = proportion of moisture, S = salinity (psu), V_w = volume of water per unit mass of total sample, V_s = volume of solid per unit mass of total sample, ρ = *in situ* density of the salt water ρ_s = density of sediment grains (constant used here is 2.65g/cm^3), and Φ = porosity.

Particle Size Analysis

Particle size analysis was done on the surface samples of all 18 of the cores on the Mastersizer 2000 in the Richardson building at the University of Manitoba. Gravel sized particles were removed from the sample by eye. One gram of each sample was placed into a beaker with hydrogen peroxide for 24 hours and then placed on a hot plate to boil off the H_2O_2. This process removes the organic portion from the sample so that only the sediment is analyzed (Goharrokhi et al., 2021). The sample was then dispersed with sodium hexametaphosphate before being analyzed (Goharrokhi et al., 2021).

Organic Carbon Analysis

Seventeen out of the 18 cores were sent to the University of British Columbia (UBC) to be analyzed for % total nitrogen and % total carbon (which is broken down into the % of carbonate carbon and the % of organic carbon). Five to six slices of each core at approximately 5 cm intervals were analyzed using a Carlo Erba NA-1500 Elemental Analyzer (c.f. Verardo et al., 1990). The precision of the instrument is +/-0.3% for OC and +/- 1.6% for N (Verardo et al., 1990)

Radioisotope Analysis

The activities of ^{210}Pb, ^{226}Ra, and ^{137}Cs in the sediment core sections were counted using a combination of gamma and alpha spectrometry at the Environmental Radioisotope Lab (ERL) at the University of Manitoba. To prepare the sediment samples for radioisotope analysis by gamma spectrometry, freeze dried and ground samples were put into petri dishes and weighed. The samples were then sealed for 21 days to allow secular equilibrium to develop between ^{226}Ra and its radon progeny (^{222}Rn) nuclide ^{214}Pb (Murray et al., 1987). The samples in the petri dishes were measured for ^{137}Cs by counting gamma emissions at 661

keV. ^{210}Pb and ^{226}Ra were measured for some samples (cores 10, 17,18, 24, 405, 407, 408, 409, and 411) by counting gamma emissions at 46.5 keV and 352 keV, respectively. Samples were counted for 12-48 hours for ^{137}Cs and 24 hours for ^{210}Pb. Detector efficiency and self-absorption were corrected by counting reference material distributed by the International Atomic Energy Agency (IAEA) within petri dishes of the same geometry (Cutshall et al., 1983).

Particular attention was paid to QA/QC because the radioisotope activities in the sediments were very low. For ^{137}Cs, repeatability of the gamma analysis was assessed by analyzing 11 samples in duplicate. ^{137}Cs was not detected in eight of 11 samples during the first round of analysis and four of 11 samples during the second round of analysis. The values detected during only the second round of analysis averaged 0.136 dpm/g, which implies that this value reflects the practical limit of detection for the analysis. For the three samples that contained detectable ^{137}Cs during both rounds of analysis, the average relative percent difference for the pairs of analyses was 37%. Note that the ^{137}Cs activity was low (average 7.3 Bq/kg) in the set of samples that were analyzed repeatedly, which implies that 37% provides an outside estimate for the repeatability of the analysis. Better repeatability for ^{137}Cs in the order of 8.8% is typically found at ERL for sediment samples containing higher ^{137}Cs activity levels (c.f. C.M. Kamula et al., 2017). For ^{210}Pb, the lab's typical repeatability with the gamma spectrometer is 6% (cf., Kamula et al., 2017). Here, repeated analysis of one slice of core 40, which contained low ^{210}Pb activity, yielded a coefficient of variation (relative standard deviation) of 19% (n=5). Subsequent analysis of the same low-level samples by alpha revealed that gamma results for ^{210}Pb were biased low reflecting poor detection of very low levels. The cores that were affected by this showed almost no difference when both the gamma and alpha data were modelled. All the cores that were originally run on gamma have been run on alpha and that data replaced the gamma data with the exception of core 32 which had such low levels of ^{210}Pb that there would be negligible differences between the two.

For alpha spectrometry, the method involves measuring ^{210}Pb indirectly by determining the activity of its daughter isotope ^{210}Po. It is assumed that ^{210}Pb and ^{210}Po are in secular equilibrium. The isotope peak of ^{210}Po is compared with a known activity peak of the isotope tracer ^{209}Po. Sediment samples were prepared for alpha analysis by measuring 0.7-1.0 g of

dry sediment into a 100 ml beaker. Then 200 µl of ^{209}Po tracer and 30 ml of 6N HCl were added to each sample and the sample placed on a hot plate for 3-5 hours at 180^{o}C. The beakers were removed from the hotplate and swirled to mix the solution, then allowed to cool and settle. The clear liquid was decanted into a 250 mL beaker which already contained 50 ml of distilled water and 5 mL of 10% ascorbic acid. A silver disc with a sample ID etched onto it was placed into the beaker unmarked side up and the samples were placed back on the hot plate with a watch glass at 80^{o}C overnight. The next day, the samples were allowed to cool to room temperature, the liquid was poured off and the discs were rinsed with distilled water and allowed to air dry. The discs were then counted on the alpha counter for 48-72 hours. Five samples of the same slice of one of the cores (core 36) run on different detectors on the alpha spectrometer revealed a repeatability of 10%. Sightly better repeatability (6%) has been found previously for samples containing higher activities of ^{210}Pb and all analyzed on the same detector (Kamula et al., 2017).

Throughout the thesis, radioisotope results are reported in units of disintegrations per minute per gram of dry sediment (dpm/g) after correcting the dry sediment mass for salt content. Unsupported or excess ^{210}Pb was calculated as the difference between measured ^{210}Pb and ^{226}Ra for those cores analyzed by gamma. In the remaining cores, excess ^{210}Pb was calculated as the difference between the measured ^{210}Pb activity in each slice and supported ^{210}Pb estimated as the average activities deep in the cores.

Calculations of Sedimentation Rates

For cores that appeared to meet the assumptions of steady-state sedimentation, sedimentation rates were derived from excess ^{210}Pb profiles using a two-layer advection diffusion model to account for biomixing and compaction with depth (cf. Kuzyk et al., 2015). The model assumes that there is a constant supply of ^{210}Pb to the seafloor and that there is an upper section of the core that is biomixed by benthic creatures and a deeper unmixed layer where the ^{210}Pb decays to background level undisturbed (Appleby, 2001; Kuzyk et al., 2015). The model used Eq. 9 above the surface mixed layer (SML) and Eq. 10 below the SML. The SML was identified by eye as the portion of the core near the sediment surface where ^{210}Pb

activities were constant or near constant with depth (c.f. Kuzyk et al., 2015). In cores where ^{137}Cs was detected, validation of the sedimentation rates was attempted using MatLab (cf. Kamula *et al.*, 2017). The modelling of ^{137}Cs assumes that there is no ^{137}Cs prior to 1954 with an influx between 1954 and 1963, and then decreasing towards the surface after the cessation of nuclear testing in 1963. If the sedimentation rate derived from the ^{210}Pb dating, fits the sedimentation rate of ^{137}Cs then the sedimentation rate is validated.

Equation 9

$$\omega\left(\frac{\partial C}{\partial z}\right) - \left(\frac{\partial}{\partial z}\right) * K_b \left(\frac{\partial C}{\partial z}\right) = -\lambda C$$

Where ω is the sediment velocity (cm/yr), C is the excess ^{210}Pb activity (dpm/ cm^3), z is the depth, K_b is the diffusion coefficient (cm^2/yr), and λ is the radioisotope decay constant (0.03114/yr).

Equation 10

$$\omega = -\lambda/m$$

Where w is the sediment velocity (cm/yr), λ is the radioisotope decay constant (0.03114/yr), and m is the slope of the natural log of the excess ^{210}Pb.

Equation 11

$$r = \rho_s(1 - \Phi)w$$

Where r is the sedimentation rate (g/cm/yr), ρ_s is the density of sediment (2.65 g/cm^3), Φ is the mean porosity, and w is the sediment velocity.

Chapter 4 Results

Subbottom seismic profiles

In total, only 414 distinct sediment deposits were located along the thousands of kilometers of inspected seismic data lines. Figure 4-1 summarizes the frequency distribution of the deposits across water depth, latitude, and longitude. Sediment deposits were not located in areas shallower than 50 m although, in places, seismic surveys went into as little as 20 m water depth. However, over the depth range of 50 to 212 m, the greatest number of deposits were in the shallowest (50 to 82 m) depth category (Figure 4-1). There is a general decrease in sediment deposits with increasing water depth. The distribution of deposits with latitude is bimodal: there are a large number of sediment deposits in the most southerly portion of the bay (south of 56.38°N) and also a significant number of deposits broadly distributed across the middle latitudes of the bay between 57.68°N and 61.58°N (Figure 4-1). There is also a trend with respect to longitude with the bulk of the sediment deposit located in the east between -80.8°E and -78.6°E.

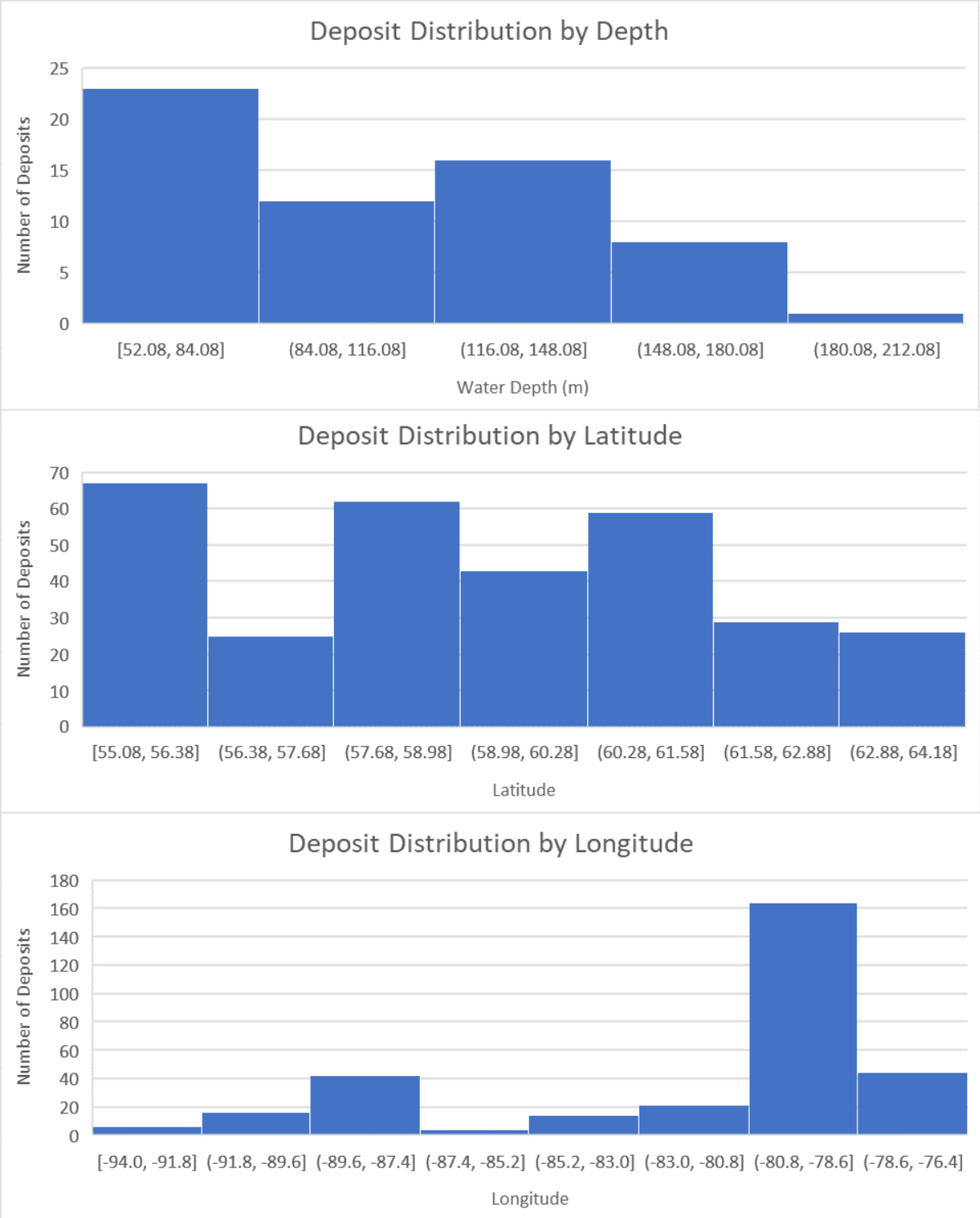

Figure 4-1: Frequency distribution of sediment deposits located along seismic lines across water depth bins (a), latitudinal bins (b), and longitudinal bins (c).

The geographic distribution of located sediment deposits is shown with respect to water depth contours in Figure 4-2 and simplified bedrock geology in Figure 4-3. Most of the located deposits occur in southeastern and eastern Hudson Bay (Figure 4-2), with the densest distribution of deposits lying along the southeast coast between the entrance to James Bay and the Nastapoca River. In this region, deposits are very densely distributed (nearly continuous) along two seismic lines that parallel the coast, approaching as close as 6 km in some places (Figure 4-2). Deposits are also densely distributed along a seismic line that crosses the entrance to James Bay and extends west to the Winisk River mouth. Near the Winisk River mouth, two across-shore seismic lines also showed very dense distributions of deposits (Figure 4-2). Outside southeast Hudson Bay, several other small areas in east and northeast Hudson Bay have densely distributed deposits. There is a band of nearly continuous deposits along a seismic line running roughly north south, just northwest of the Belcher Islands, and there is a second band of dense deposits in northeast Hudson Bay to the southeast of Mansel Island (Figure 4-2). In general, there are quite a few clusters of dense deposits along almost all seismic lines running alongshore or across-shore in northeast Hudson Bay, especially between Mansel Island and the Povungnituk river mouth. Some of these located deposits appear to coincide with the bottom of the slope (Figure 4-2), while others are near the mapped geological contact the Paleozoic limestone (blue) and Precambrian crystalline bedrock (pink) (Figure 4-3).

In southwest Hudson Bay, deposits are sparse compared to southeast and east Hudson Bay. There are deposits concentrated near the mouth of the Nelson-Hayes Rivers and the Churchill River. However, deposits come no closer than 42 km from shore on the western side. There are also deposits near the base of the slope.

In northwestern Hudson Bay, the majority of sediment deposits occur well beyond (offshore from) the base of the slope (>100 m). A number of deposits lie in a band offshore from Chesterfield Inlet in relatively deep water well beyond the base of the slope (Figure 4-2). This band of deposits appears to lie near the mapped geological contact between Silurian and Devonian limestone deposits (both in blue) (Figure 4-3).

There are relatively few localized deposits in central Hudson Bay. However, on two separate sets of survey lines, deposits are found in one very deep area in the north-central part

of the bay (Figure 4-2). Not a single deposit was found along the seismic line extending NNE from the Winisk River across to the Mansel Island area.

Figure 4-2: Sediment deposits (red) and examined subbottom lines (dark grey). Blue lines show bathymetry of Hudson Bay.

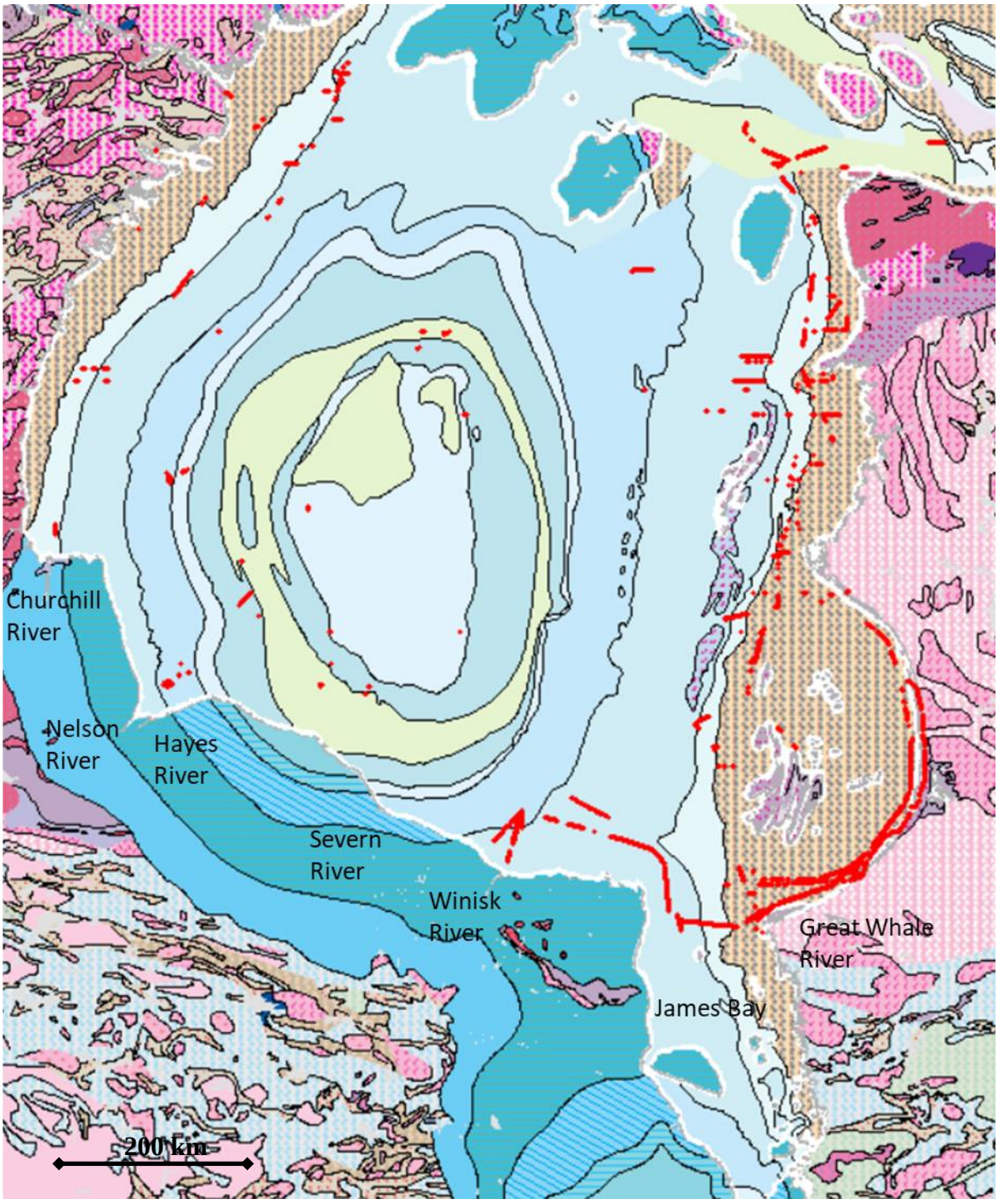

Figure 4-3: Sediment deposits (red) and bedrock geology. Orange and pinks are Precambrian crystalline bedrock and blues and greens are Paleozoic carbonates.

Sediment deposits throughout the bay do not all appear the same in terms of thickness, surface reflection, and presence of internal reflectors. Along the southeast coast of Hudson Bay, the sediment deposits are thin, continuous drape with occasional wavy reflections within the deposits (Figure 4-4).

In eastern Hudson Bay, there are many large, deep sediment deposits and long expanses of contiguous deposits (Figure 4-5). Deposits in the east range from continuous, thick deposits in large troughs to discrete, thick deposits where there is rougher bottom topography. The deposits in eastern Hudson Bay also show clearer internal reflectors that are typically linear or wavy parallel.

Southwestern Hudson Bay is characterized by fairly smooth subbottom with sediment deposits in localized shallow but laterally extensive depressions (Figure 4-6). The sediment in the southwest is either discrete, thin deposits in localized depressions or a continuous, thin drape of sediment over 10s of kilometers. The bathymetry in this area indicates a much gentler slope and little relief. Figure 4-6 shows a continuous thin drape of sediment deposited in between relative topographic highs, which are only a few metres higher than the base of the depression.

Northwestern Hudson Bay is characterized by a rough, uneven subbottom with deposits in localized depressions within larger troughs. The northwest is also typified by discrete, thin deposits and often the deposits show no reflectors within them. When the deposits do show reflectors, they are ponded/onlap reflectors within small troughs and faint linear reflectors where there is a stretch of flatter topography.

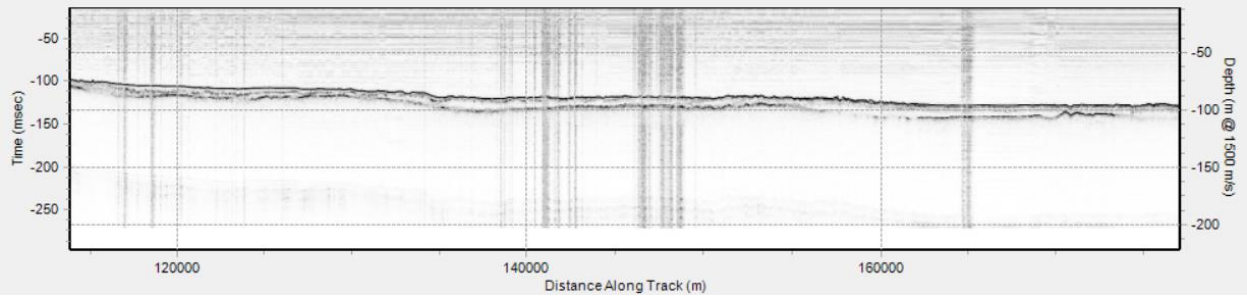

Figure 4-4: Typical sediment deposits along the southeast coast of Hudson Bay.

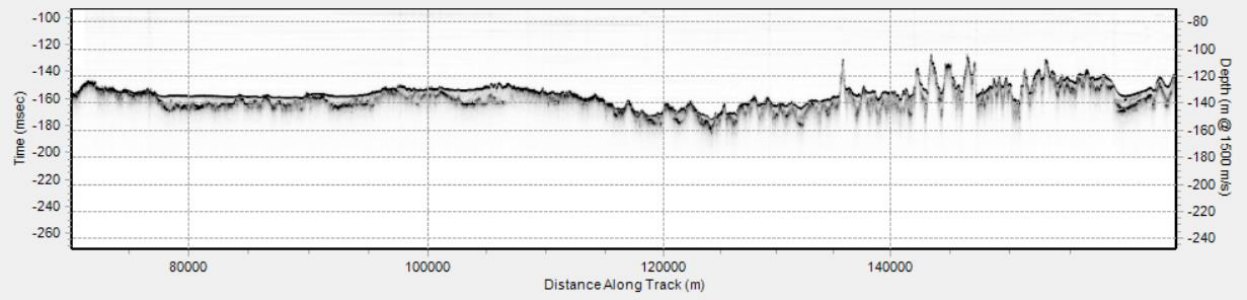

Figure 4-5: Typical subbottom deposits in eastern Hudson Bay.

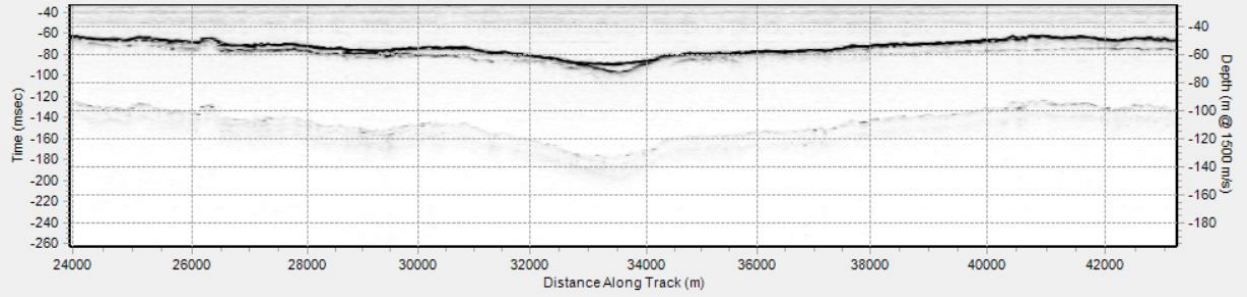

Figure 4-6: Typical subbottom deposits in southwestern Hudson Bay.

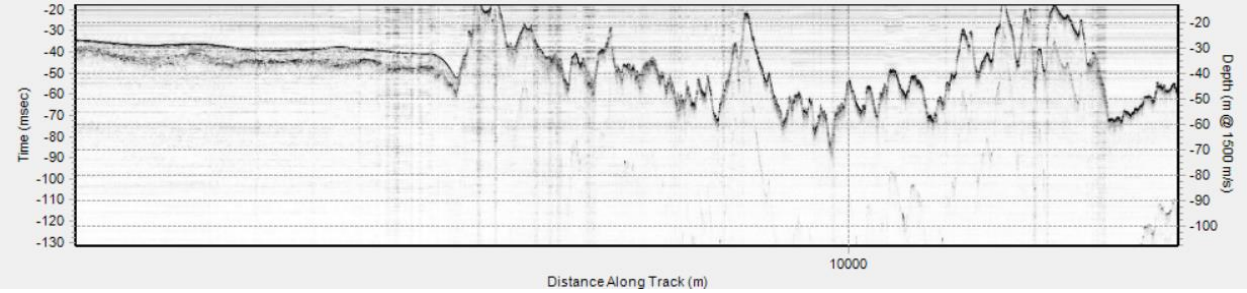

Figure 4-7: Typical subbottom deposits in northwestern Hudson Bay.

Sediment Core Data

Particle Size Distribution

Because we attempted to avoid coring at sites where coarse materials were evident in the real-time multibeam backscatter data, most recovered cores were generally muddy. However, at one site (32), where there was a large accumulation of sediment-laden ice at the time of

sampling, the box recovered pebble- and cobble-sized particles (Figure 4-8). The pebble- and cobble-sized particles only occurred at the surface; however, visibly sandy layers were found throughout the core. The pebble sized particles were hand-picked out of the surface sample and estimated to represent about 15% (by volume) of the sediment matrix.

Figure 4-8: Photo of the coarse-grained materials at the surface of core 32.

Particle size analysis of the surface samples of the remaining sediment cores revealed a wide range of particle sizes. All the samples had either sand or silt as the dominant particle size (Table 4-1). The proportion of sand sized particles ranged from 0 to 99%, silt sized particles ranged from 0.3 to 84.6%, and clay sized particles ranged from 0 to 35.8%. Sand dominated (>92%) in core 10, at the entrance to Hudson Bay, and in the nearshore area in the northwest portion of the bay (cores 17, 18, and 19) (Figure 4-9). Sand also contributed significant proportions (9.6-48.5%) to the surface sediments in cores 21, 24 and 28 in deeper water in the northwest portion of the bay (Figure 4-9). Sand also was present in proportions greater than 2.5% in all the cores from water depths less than 100 m in southwest Hudson Bay (Table 4-1).

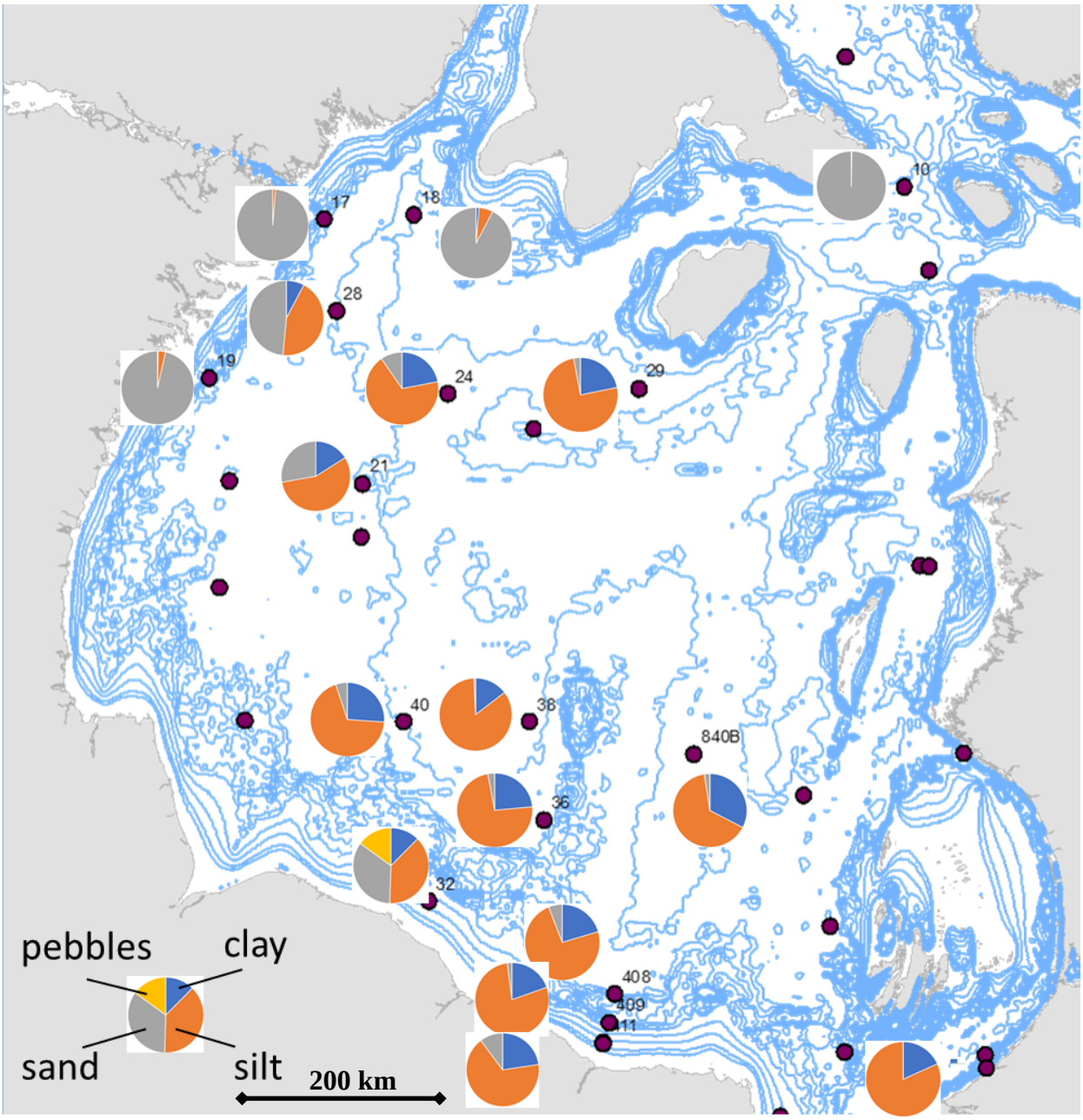

Figure 4-9: Particle size distribution in surface samples throughout Hudson Bay. Yellow denotes gravel sized particles, grey denotes sand, orange denotes silt, and blue denotes clay.

Table 4-1. Percentage of clay, silt, sand, and gravel sized particles in the surface sediment sample of each sediment core.

Core	%Clay	%Silt	%Sand	%Gravel
405	18.2	81.8	0.0	0.0
407	19.4	74.3	6.3	0.0
408	20.4	73.6	5.9	0.0
409	19.6	78.4	2.0	0.0
411	22.6	67.1	10.3	0.0
840B	32.6	65.0	2.5	0.0
10	0.0	0.3	99.7	0.0
17	0.0	1.3	98.7	0.0
18	1.3	6.3	92.4	0.0
19	0.3	3.3	96.5	0.0
21	16.1	56.2	27.7	0.0
24	22.0	68.4	9.6	0.0
28	7.7	43.8	48.5	0.0
29	21.8	75.2	2.9	0.0
32	12.4	38.1	34.5	15.0
36	23.5	73.5	3.0	0.0
38	14.6	84.6	0.8	0.0
40	26.1	68.8	5.1	0.0

Carbon and nitrogen content

Five to six sections across 17 sediment cores were analyzed for inorganic carbon, organic carbon, and nitrogen content. The percentage of organic carbon in the surface sediment sections ranged from <0.1% to 1.11% (Table 4-2). Cores 17, 19 and 32 had very low levels of organic carbon (≤0.4%) and at most 0.041% total nitrogen.

Vertical profiles of organic carbon within the cores varied widely among the cores (Figure 4-10). Decreases in organic carbon with depth occurred in cores 10, 17, 19, 21, 24, 28, 36, 38 and 40. In core 18, there was no vertical trend in organic carbon. In core 29, organic carbon decreased with depth to a subsurface minimum and then increased with depth in the lower portion of the core. In core 32, organic carbon increased with depth down to maximum values at the base of the core (Figure 4-10). Total nitrogen had similar vertical profiles to organic carbon (Appendix 2). Throughout the cores, the nitrogen content was low at between 0 and 0.2%.

Molar ratios of carbon to nitrogen varied widely in the sediments with values ranging from less than 6 to nearly 80. In surface sediment sections, Molar C:N ratios showed variable

vertical trends within cores but in many cases increased with depth (Figure 4-11). Cores 24 and 38 had anomalously low surface C:N ratios but beneath this layer C:N ratios decreased with depth. C:N ratios also decreased with depth in core 40.

Table 4-2. Carbon and nitrogen data for the surface sections of each core

Core	Slice Depth (cm)	%OC	%TN	C:N
405	0-1	1.06	0.143	7.39
407	0-1	0.39	0.070	5.57
408	0-1	0.78	0.069	11.3
409	0-1	0.73	0.070	10.4
411	na	na	na	na
840B	0-0.5	0.81	0.107	7.60
10	0-1	0.71	0.108	6.60
17	0-1	0.34	0.041	8.27
18	1-2	0.66	0.080	8.31
19	1-2	0.35	0.043	8.02
21	0-1	0.97	0.137	7.07
24	0-1	1.00	0.170	5.88
28	0-1	1.11	0.164	6.76
29	0-1	0.80	0.117	6.78
32	1-2	0.07	<0.029	2.48
36	0-1	0.96	0.136	7.09
38	1-2	1.02	0.184	5.56
40	0-1	1.07	0.166	6.47

na – not available

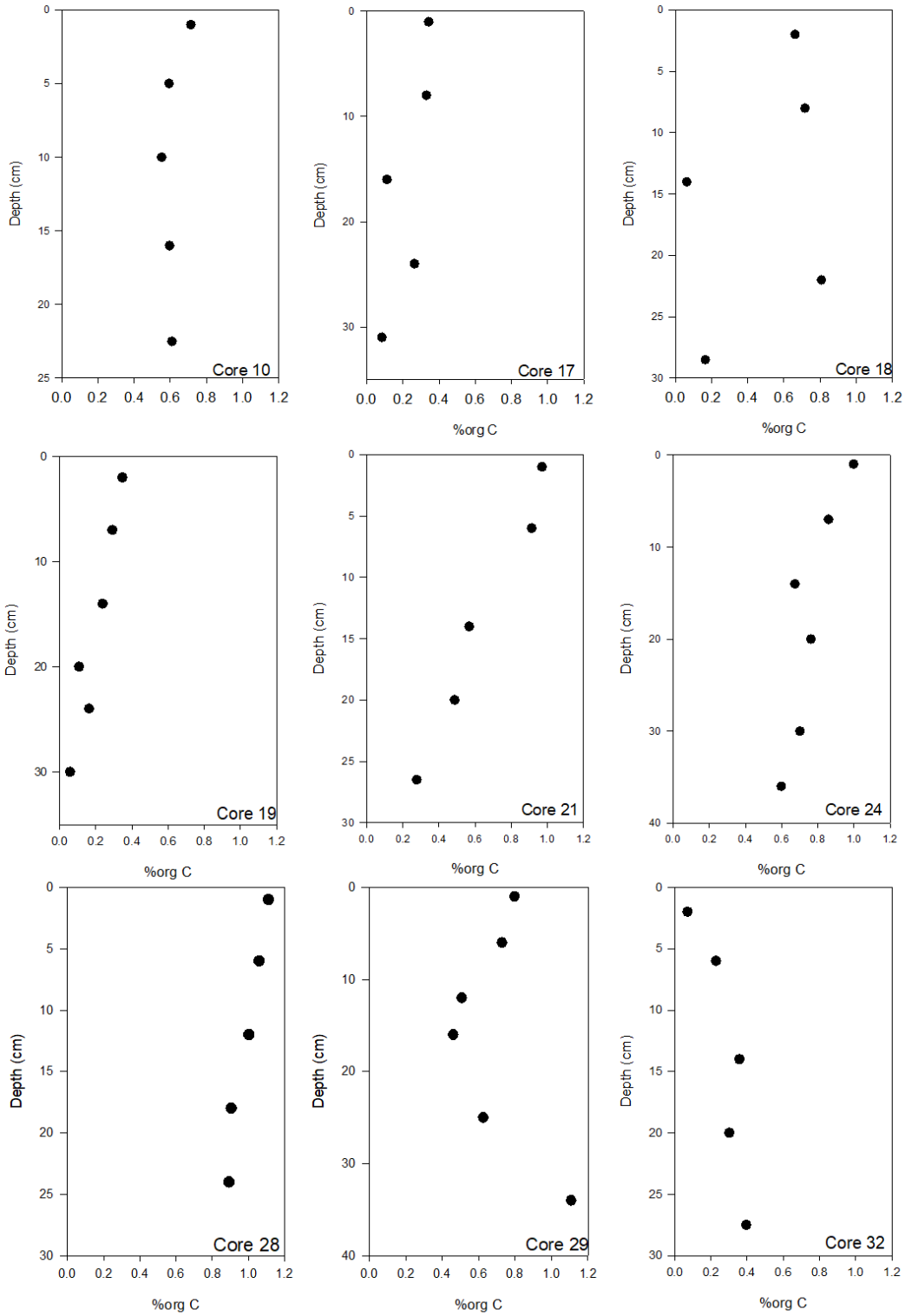
Core 10
Core 17
Core 18
Core 19
Core 21
Core 24
Core 28
Core 29
Core 32
Depth (cm)
%org C

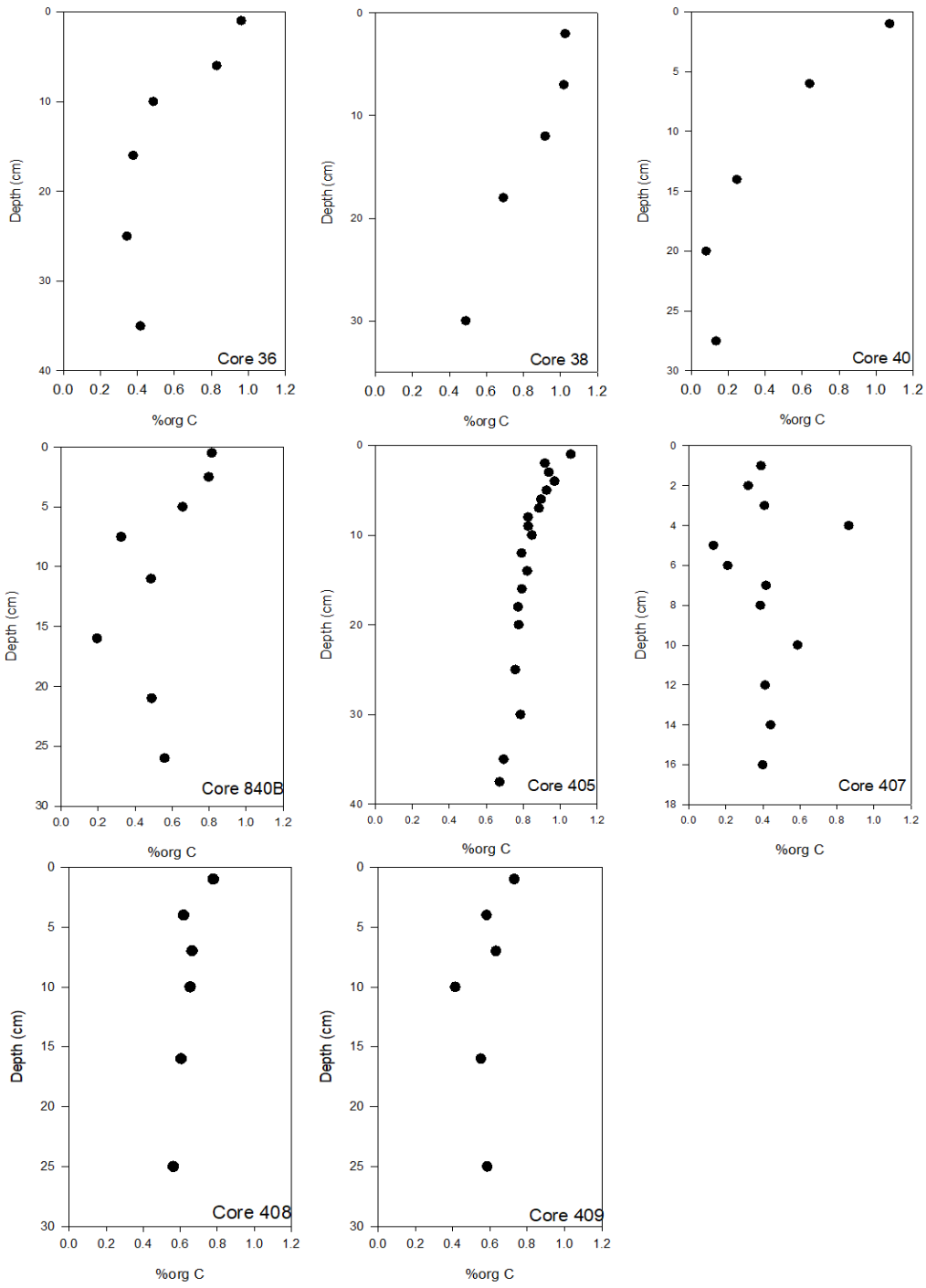

Figure 4-10: Vertical profiles of organic carbon in the sediment cores.

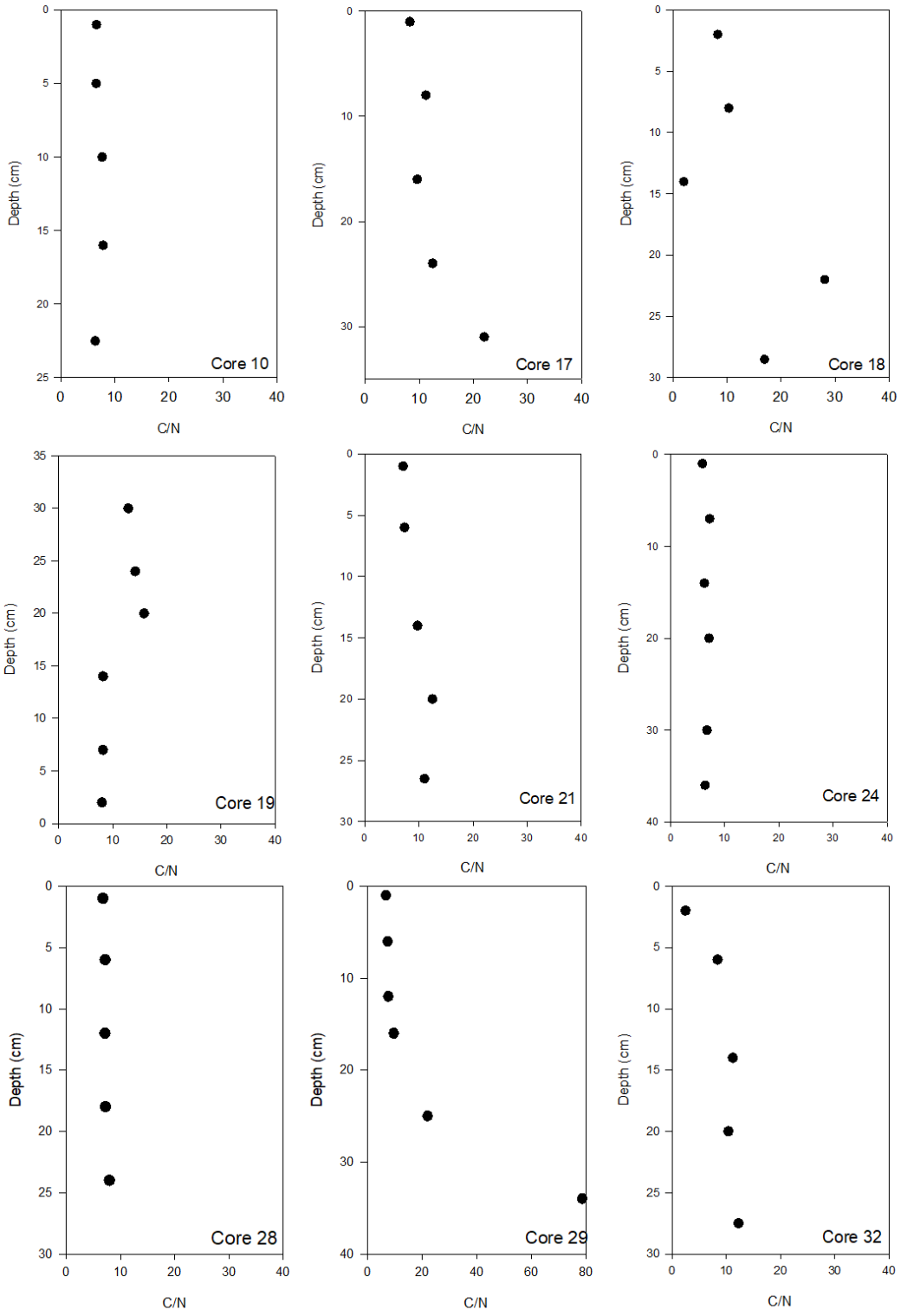
Depth (cm)
C/N
Core 10
Core 17
Core 18
Core 19
Core 21
Core 24
Core 28
Core 29
Core 32

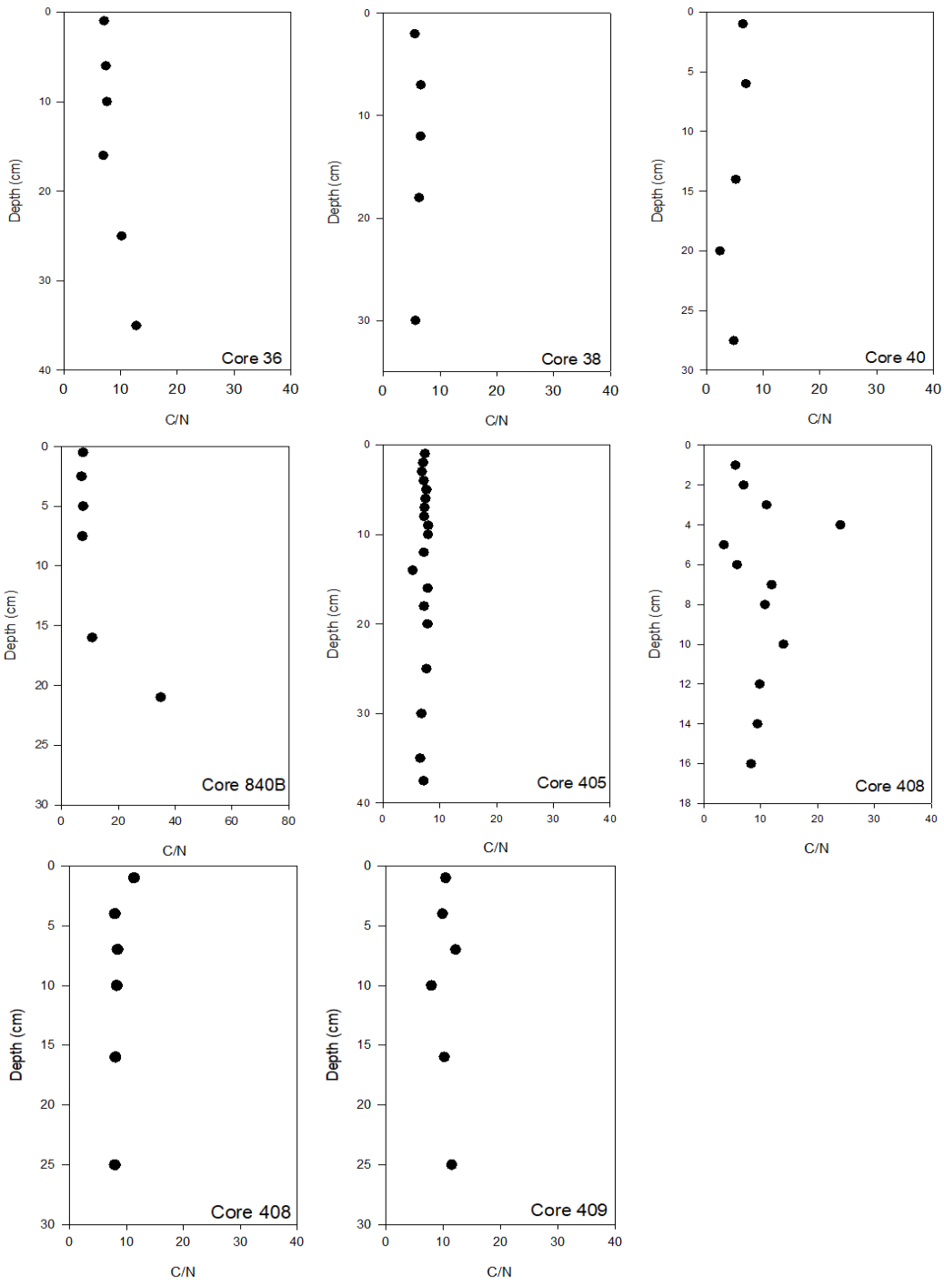

Figure 4-11: Vertical profiles of carbon to nitrogen ratios.

Porosity profiles

Thirteen of the 18 cores showed a typical porosity profile wherein porosity decreased with depth below the surface until a point in the central portion of the core and then stayed near constant with depth throughout the lower portion of the core (Figure 4-12). Cores 10, 17, 18, and 19 showed a decrease in porosity in the shallow subsurface layers and then an *increase* in porosity starting around 10 cm depth and extending down to the base of the core. Core 32, which contained the pebbles on the surface (Figure 4-8), showed a reverse profile wherein porosity *increased* with depth over the entire length of the core. In all five cores with atypical profiles, there were relatively large fluctuations in porosity over the length of the core.

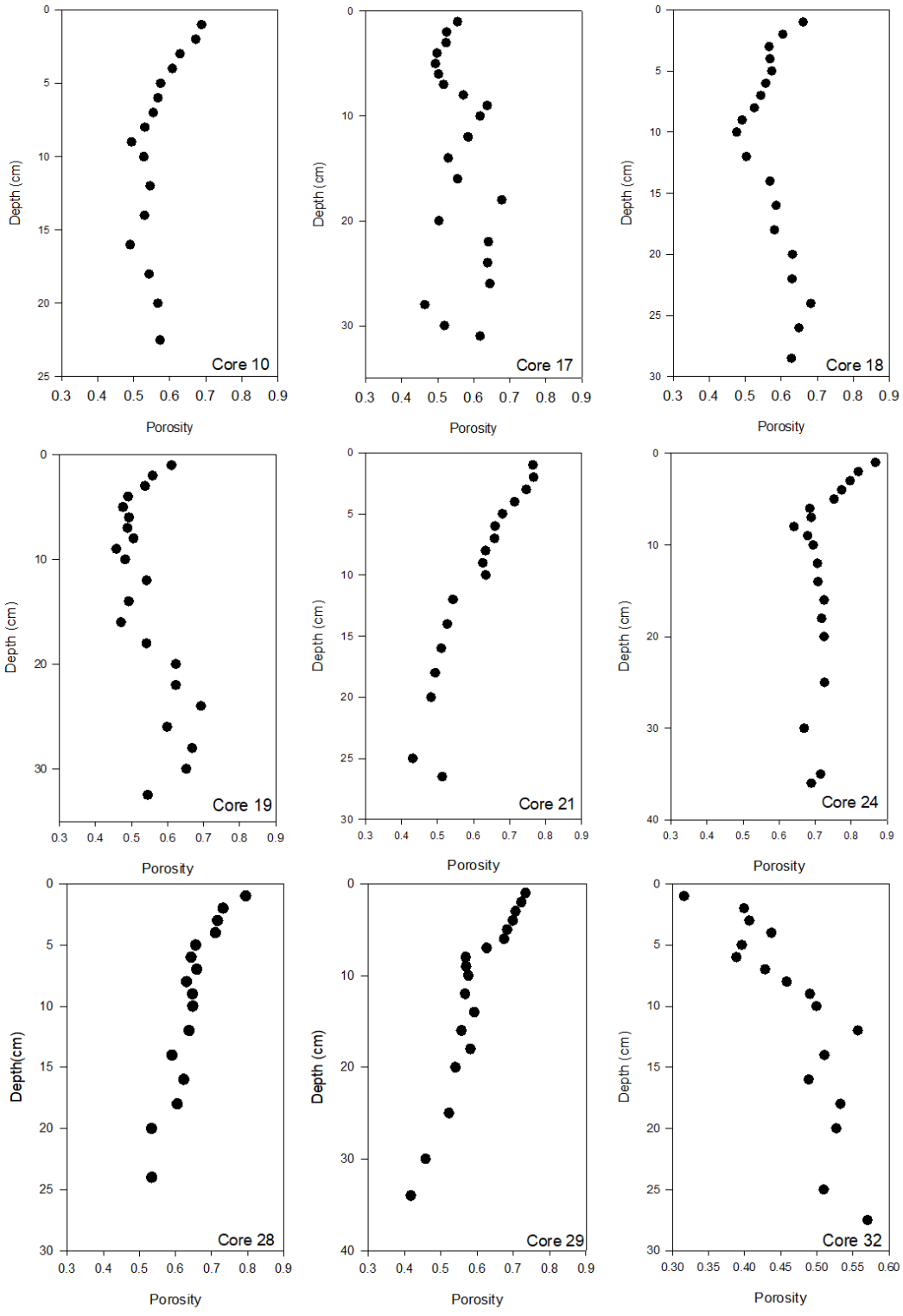
Depth (cm)
Porosity
Core 10
Core 17
Core 18
Core 19
Core 21
Core 24
Depth(cm)
Core 28
Core 29
Core 32

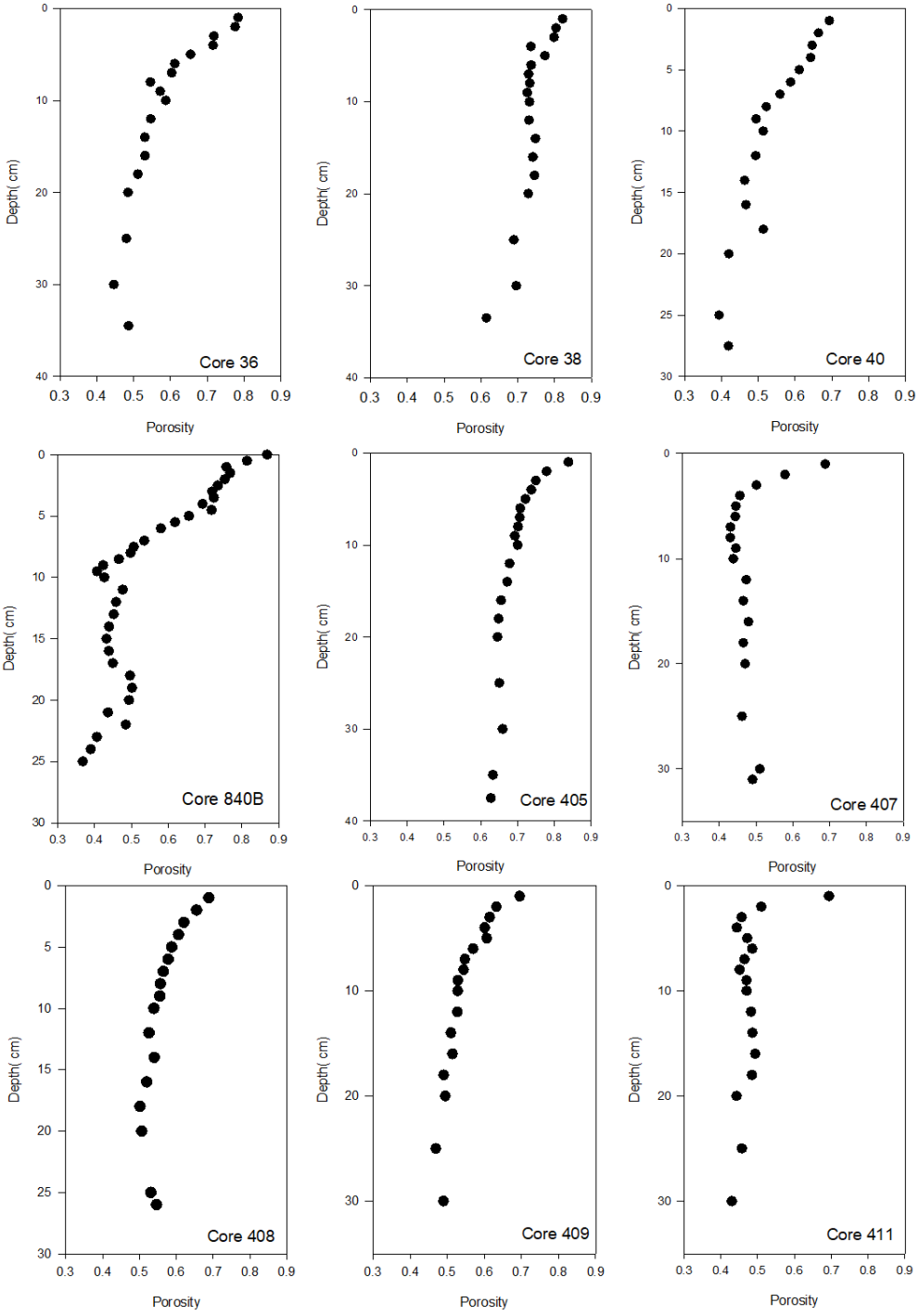

Figure 4-12: Porosity profiles in the sediment cores.

Profiles of Pb-210, Ra-226, and Cs-137

Activities of ^{226}Ra measured throughout nine of the cores were relatively constant with depth within each core (Figure 4-13). Activities of ^{210}Pb were higher than activities of ^{226}Ra in the upper portions of the cores and decreased with depth in most cases reaching similar levels to ^{226}Ra in deep sections of the cores (Figure 4-13). Where ^{226}Ra was not measured, it was assumed based on previous results for Hudson Bay that low, constant levels of ^{210}Pb found deep in the cores were representative of supported or "background" ^{210}Pb levels. Profiles of excess ^{210}Pb calculated from total ^{210}Pb minus ^{226}Ra or total ^{210}Pb minus "background" ^{210}Pb if ^{226}Ra was not available are shown in Figure 4-14. Ten of the 18 cores showed a typical profile where excess ^{210}Pb levels decreased with depth down to depths of between 4 and 12 cm. In one core (405), excess ^{210}Pb remained high and steadily decreased with depth throughout the recovered thickness of sediment. This indicates a high rate of deposition or downward mixing of the surface-deposited ^{210}Pb in that area. Negative values in figure 4-14 are a result of subtracting small numbers from each other and are within the error. The negative numbers could also be a result of the error incurred by averaging the total ^{210}Pb near the bottom of the core that are determined to be supported ^{210}Pb by eye when using alpha data opposed to subtracting the ^{226}Ra from the total ^{210}Pb when using gamma data.

^{137}Cs was detected only in 9 of the 18 cores. It was generally absent from the deepest sections of the cores. Seven of the cores showed only one or two subsurface sections that contained ^{137}Cs with the sections above these depths returning to nondetectable ^{137}Cs. Core 40 showed an increase of ^{137}Cs continuously from its introduction at 7 cm to the surface (Figure 4-14). In core 405, ^{137}Cs was detected in every slice with the amount decreasing towards the surface of the core.

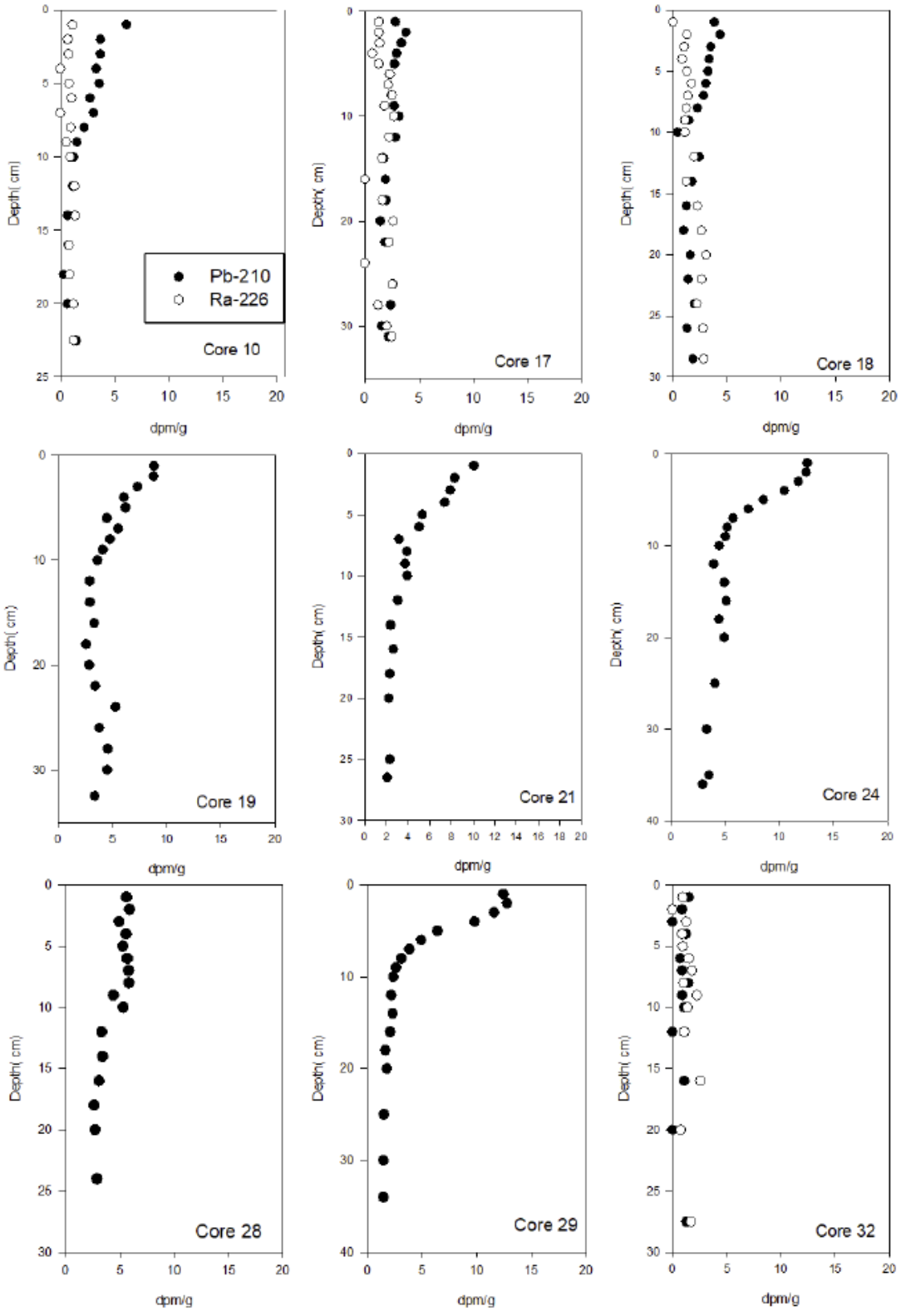
Depth(cm)
dpm/g
Pb-210
Ra-226
Core 10
Core 17
Core 18
Core 19
Core 21
Core 24
Core 28
Core 29
Core 32

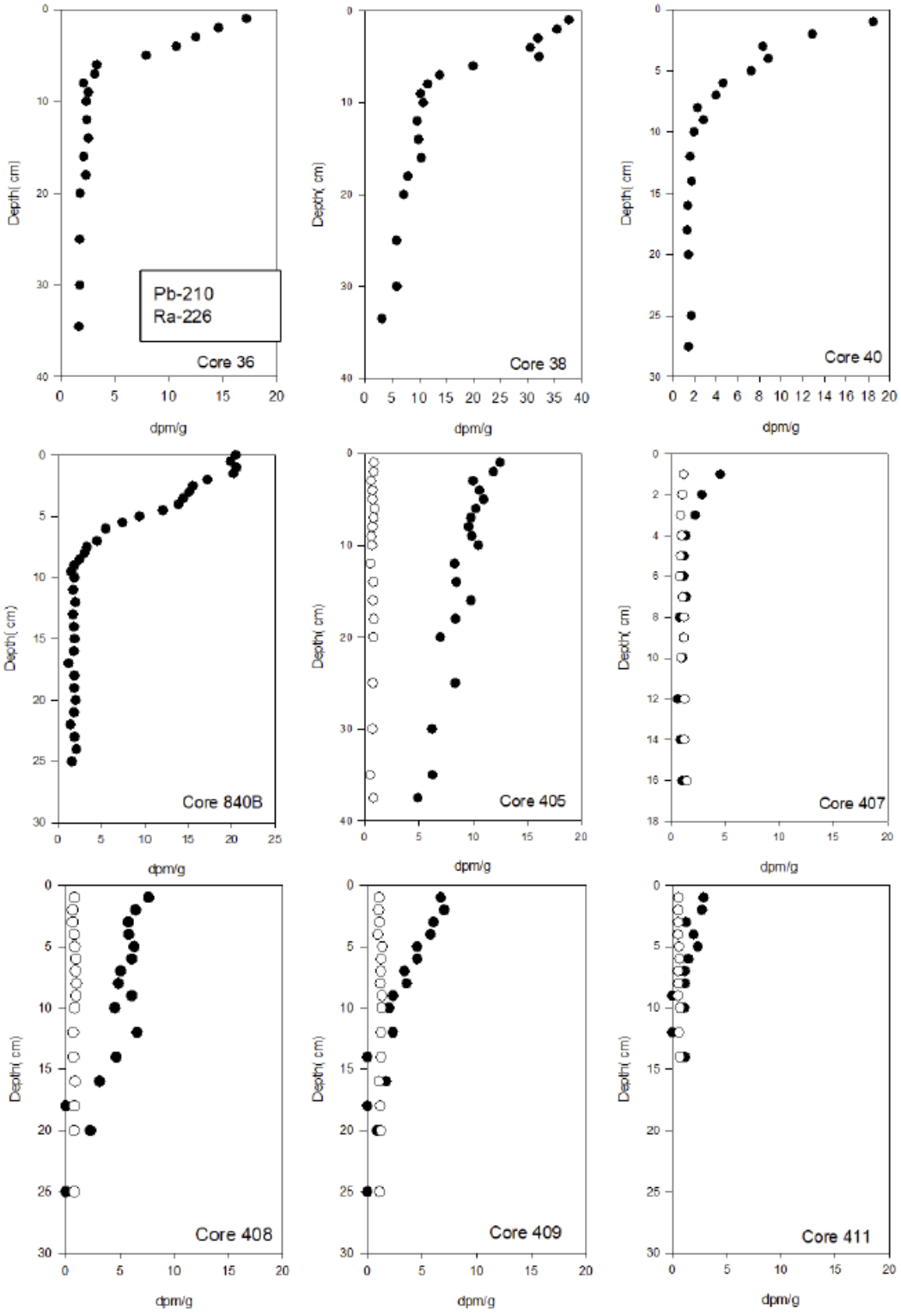

Figure 4-13: Profiles of Ra-226 and Pb-210 in the sediment cores.

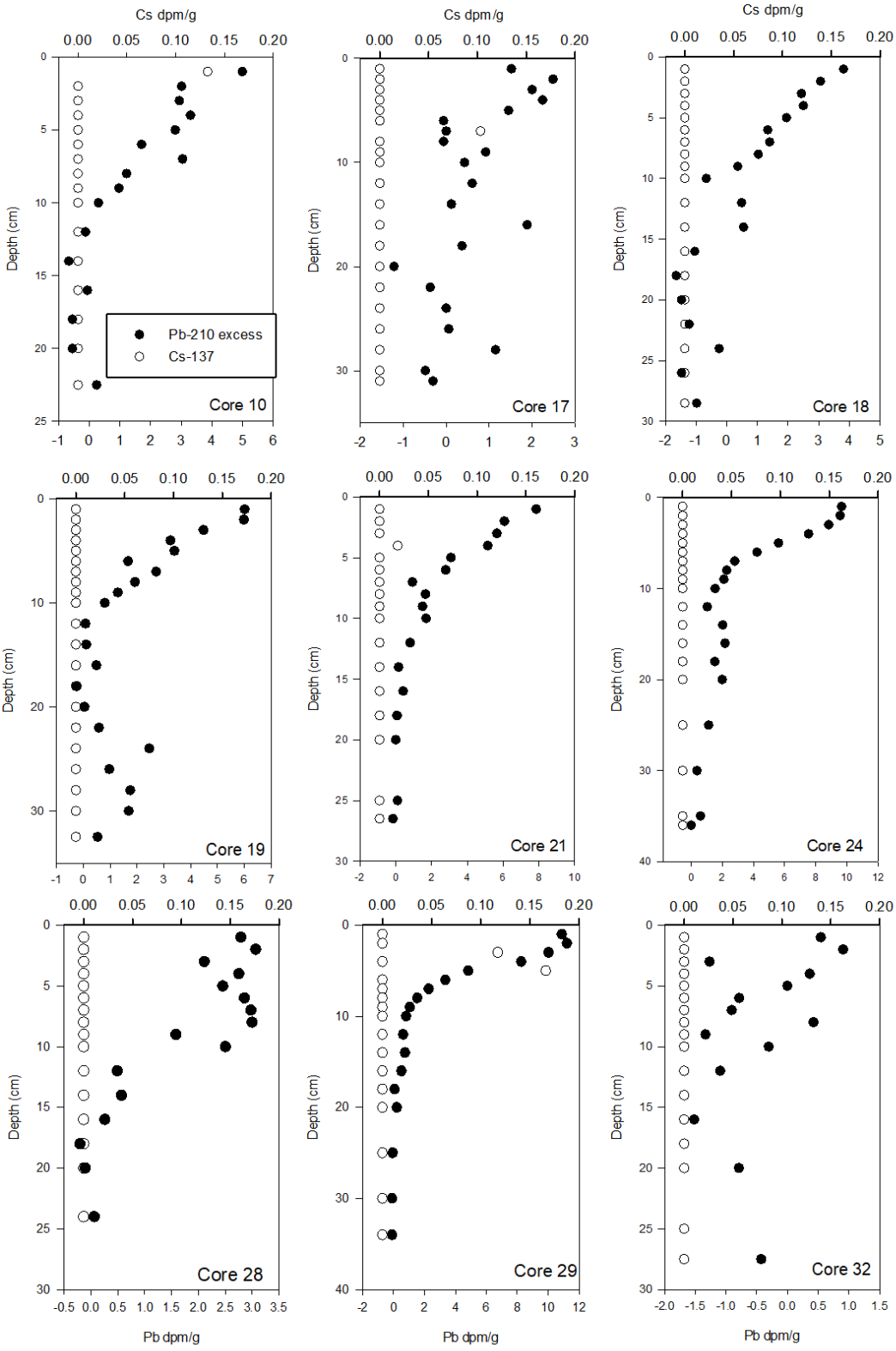
Cs dpm/g
Depth (cm)
Pb-210 excess
Cs-137
Core 10
Core 17
Core 18
Core 19
Core 21
Core 24
Core 28
Core 29
Core 32
Pb dpm/g

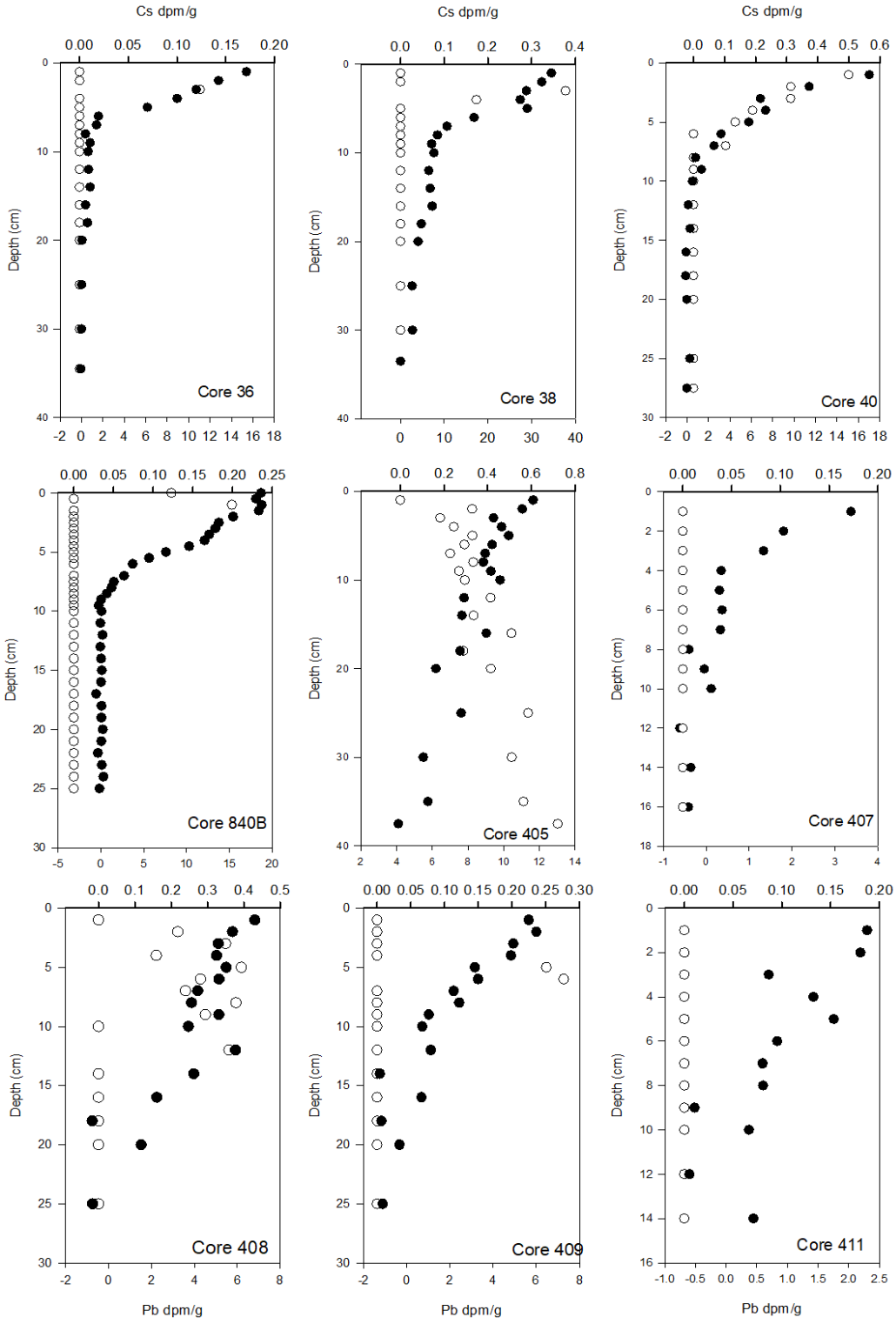

Figure 4-14: Profiles of Cs-137 and excess Pb-210 in the cores.

Inventories of ^{210}Pb and ^{137}Cs

Inventories of $^{210}Pb_{ex}$ and ^{137}Cs were calculated by summing over the length of the cores the product of the mass-depth (g cm^{-2}) of each sediment section and the section's excess ^{210}Pb ($^{210}Pb_{ex}$) or ^{137}Cs activity (dpm g^{-1}). Note that the calculated inventories for core 405 underestimate the total inventories in this core because background levels were not reached. The inventories for $^{210}Pb_{ex}$ and ^{137}Cs are plotted in Figures 4-15 and 4-16, respectively, together with previously published values following correction of the ^{137}Cs inventories for decay. Plotted ^{137}Cs inventories were all normalized to 1963. Previous published data were sourced from various workers (Kuzyk et al., 2009; Thibodeau et al., 2017).

Inventories of $^{210}Pb_{ex}$ across Hudson Bay sediments ranged over almost two orders of magnitude from 3.6 dpm cm^{-2} in core 32 to more than 237.0 dpm cm^{-2} in core 405 (Figure 4-15). There were large inventories also in core 38 in the south-central offshore region of the bay. Aside from these sites of very high inventory (cores 405 and 38), there was no obvious spatial pattern in the inventories. A number of locations distributed throughout the bay had inventories of 50-100 dpm cm^{-2}.

Inventories of ^{137}Cs ranged from 0 to 16.5 dpm cm^{-2} with maximum values in core 405 (Figure 4-16). The inventories have a clear spatial pattern with higher values in the southern portion of the bay. Generally, the higher ^{137}Cs inventories occurred in cores close to the coast and sediments in the central portion of the bay had low or negligible inventories.

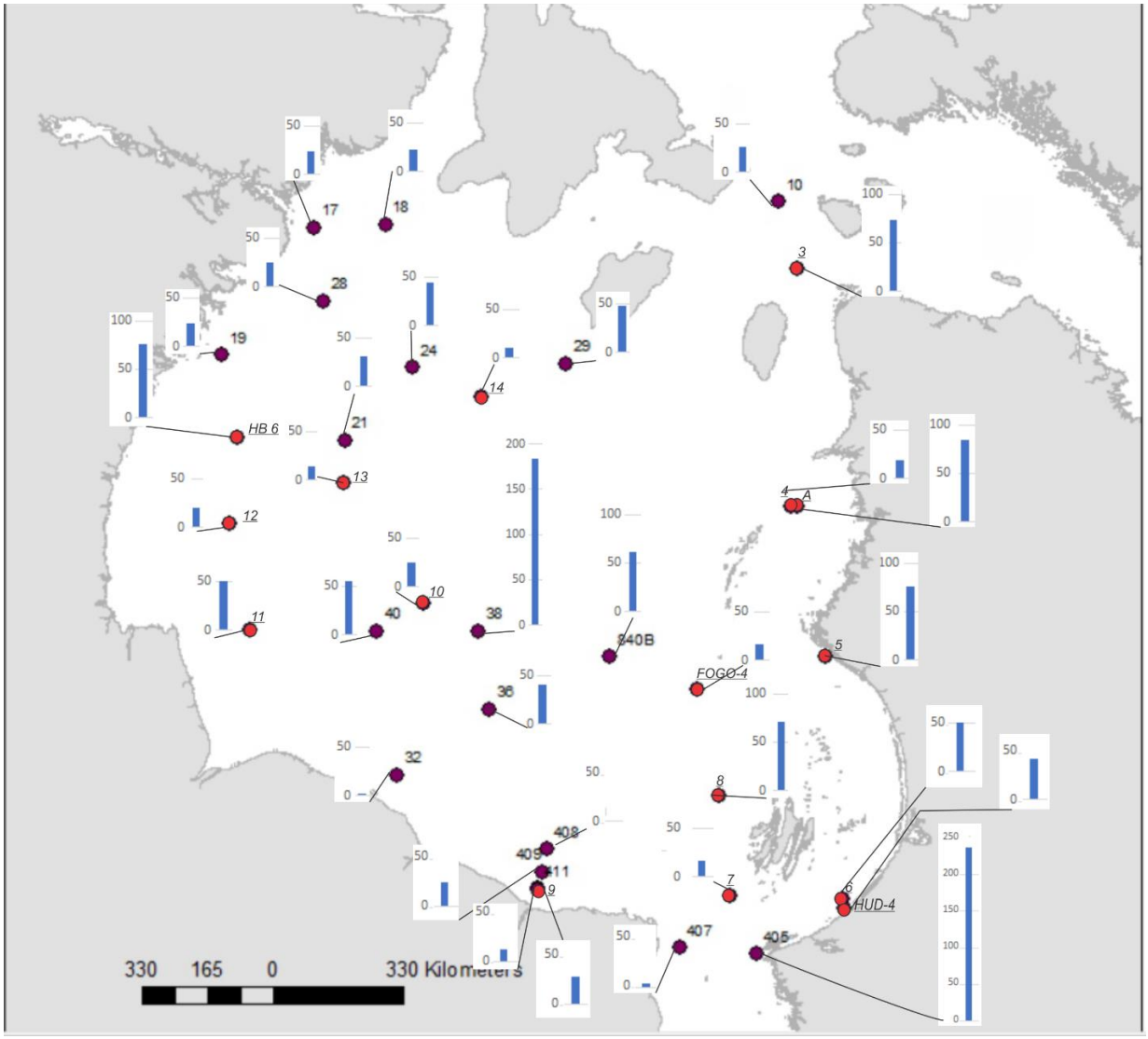

Figure 4-15: 210Pb inventories throughout Hudson Bay. Inventories are in dpm cm^{-2}

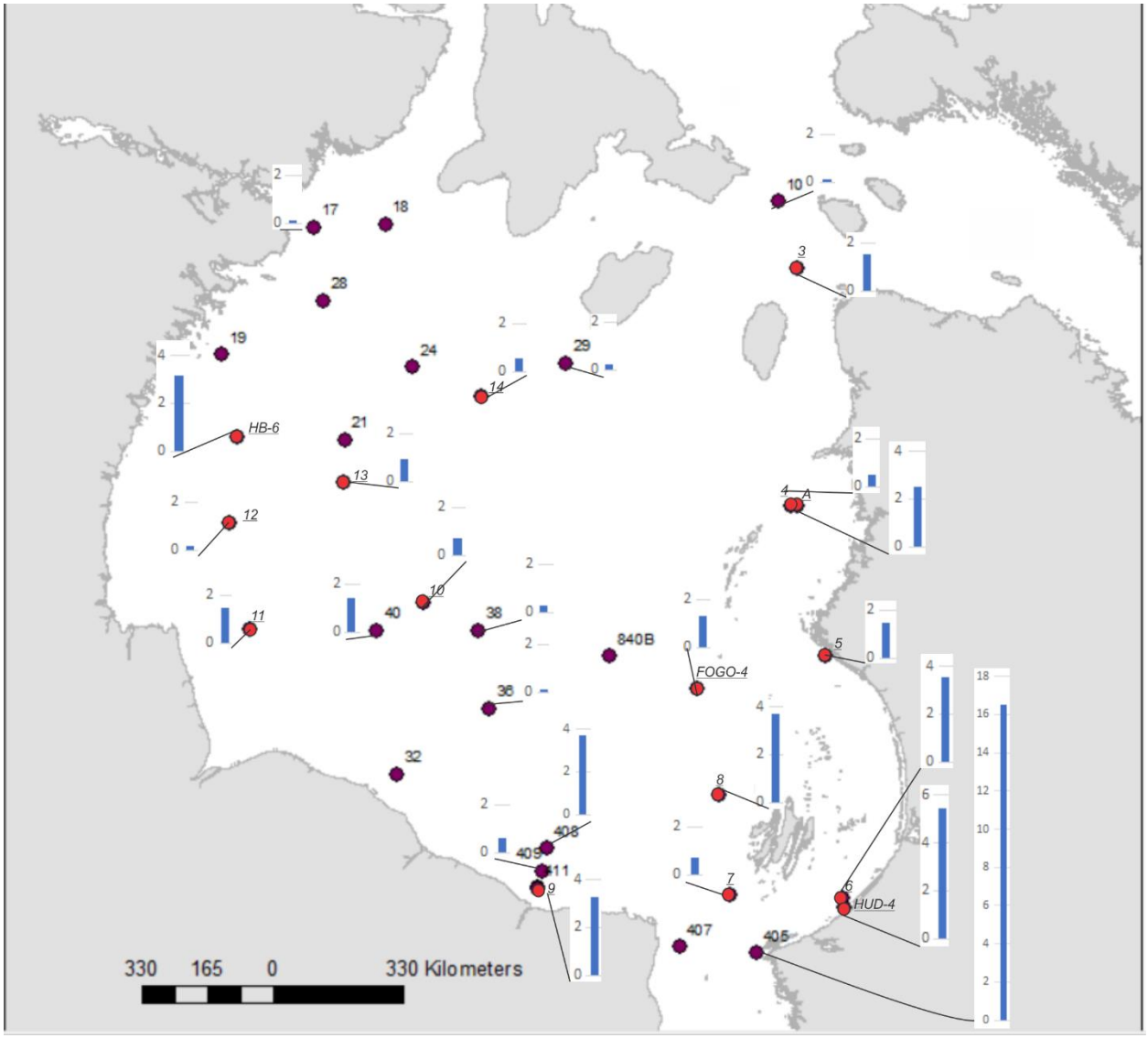

Figure 4-16: ^{137}Cs inventories throughout Hudson Bay. Inventories are in dpm cm^{-2} and adjusted to the year 1963.

Sedimentation rates estimated by modelling ^{210}Pb profiles

Figure 4-17 shows attempts to fit the two-layer advective-diffusive model to the measured excess ^{210}Pb profiles in the cores. Although the model accounts for both sedimentation and mixing (Kuzyk et al., 2009), careful consideration was given to the validity in applying the model across all sediment cores. The model assumes steady-state in sedimentation, i.e., that there is a steady supply of sediment and ^{210}Pb to the surface of the

seabed, and that mixing within the sediment column occurs at a steady rate until a specific depth and then is negligible below that (Robbins, 1978; Lavelle *et al.*, 1985). Due to evidence in the porosity profiles or other sediment core data of failure to meet these assumptions, six of the cores could not be validly dated using their ^{210}Pb profiles and the selected model. Cores 10, 17, 18, 19, 24, and 32 all show a reversal in their porosity profiles indicating that porosity does not decrease with depth but rather increases or changes between higher and lower porosity. Many of these cores also show irregular ^{210}Pb profiles implying non-steady state sedimentation. Several also had very low ^{210}Pb activities, which increases the error in the measurement, or shallow penetration of ^{210}Pb in the sediment column. After excluding those cores for which the assumption of steady-state sedimentation clearly is invalid, twelve of the 18 original $^{210}Pb_{ex}$ profiles (Figure 4-17) were modelled to estimate sedimentation rates in the cores (Table 4-3). Calculated sedimentation rates ranged from 0.05 – 1.50 cm yr^{-1} (Table 4-3). Mixing rates for the surface layer and other parameters were also estimated to obtain the best possible fit between the simulated and observed profile. The uncertainties in the sedimentation rates given in Table 4-3 represent only those uncertainties obtained from the 95% confidence limits determined from linear regression analysis of $^{210}Pb_{ex}$ vs. depth and represent minimum uncertainties in the rates. Caution is required if using any of the presented rates because they were not able to be validated using ^{137}Cs profiles (cf., Smith, 2001) due to a lack of detected ^{137}Cs in most of the sediment cores.

Table 4-3. Sedimentation rates and other modelled parameters in the cores.

Core	Water Depth (m)	$\Phi_{average}$	SML (cm)	w (cm yr^{-1})	r (g cm^{-2} yr^{-1})	C_0 (dpm cm^{-3})	K_{b1} (cm^2 yr^{-1})
10	203	0.57	6	0.05 (0.02-0.35)	0.06 (0.03-0.44)	16	2.5
17	92	0.56	3	0.11 (0.08-0.27)	0.13 (0.08-0.30)	4.5	5.0
18	122	0.58	3	0.10 (0.12-1.09)	0.22 (0.12-1.14)	8	2.0
19	86	0.55	6	0.07 (0.05-0.15)	0.05 (0.03-0.11)	7	4.0
21	149	0.61	3	0.14 (0.10-0.22)	0.15 (0.11-0.23)	7	1.0
24	186	0.73	3	0.12 (0.11-0.14)	0.10 (0.08-0.11)	8	20
28	162	0.65	9	0.10 (0.04-0.15)	0.10 (0.04-0.15)	8	25
29	177	0.60	2	0.10 (0.09-0.11)	0.10 (0.10-0.11)	13	4.0
32	34	0.47		n/a	n/a		
36	127	0.59	3	0.07 (0.05-0.13)	0.08 (0.06-0.14)	18	1.0
38	180	0.74	4	0.09 (0.06-0.13)	0.06 (0.04-0.09)	42	20
40	90	0.54	4	0.08 (0.05-0.13)	0.09 (0.07-0.16)	19	0.20
840B	175	0.55	4.5	0.06 (0.05-0.08)	0.07 (0.06-0.09)	31	10

Core	Water Depth (m)	$\Phi_{average}$	SML (cm)	w (cm yr^{-1})	r (g cm^{-2} yr^{-1})	C_0 (dpm cm^{-3})	K_{b1} (cm^2 yr^{-1})
405	62	0.69		1.50 (1.34-3.19)	1.39 (1.36-3.25)		
407	27	0.48	0	0.10 (0.06-0.24)	0.14 (0.09-0.35)	3	0.1
408	103	0.56	12	0.13 (0.06-0.24)	0.11 (0.07-0.28)	21	10
409	58	0.55	3	0.12 (0.10-0.36)	0.19 (0.12-0.44)	8	6.0
411	26	0.48	4	0.09 (0.03-0.15)	0.13 (0.05-0.21)	5	4.0

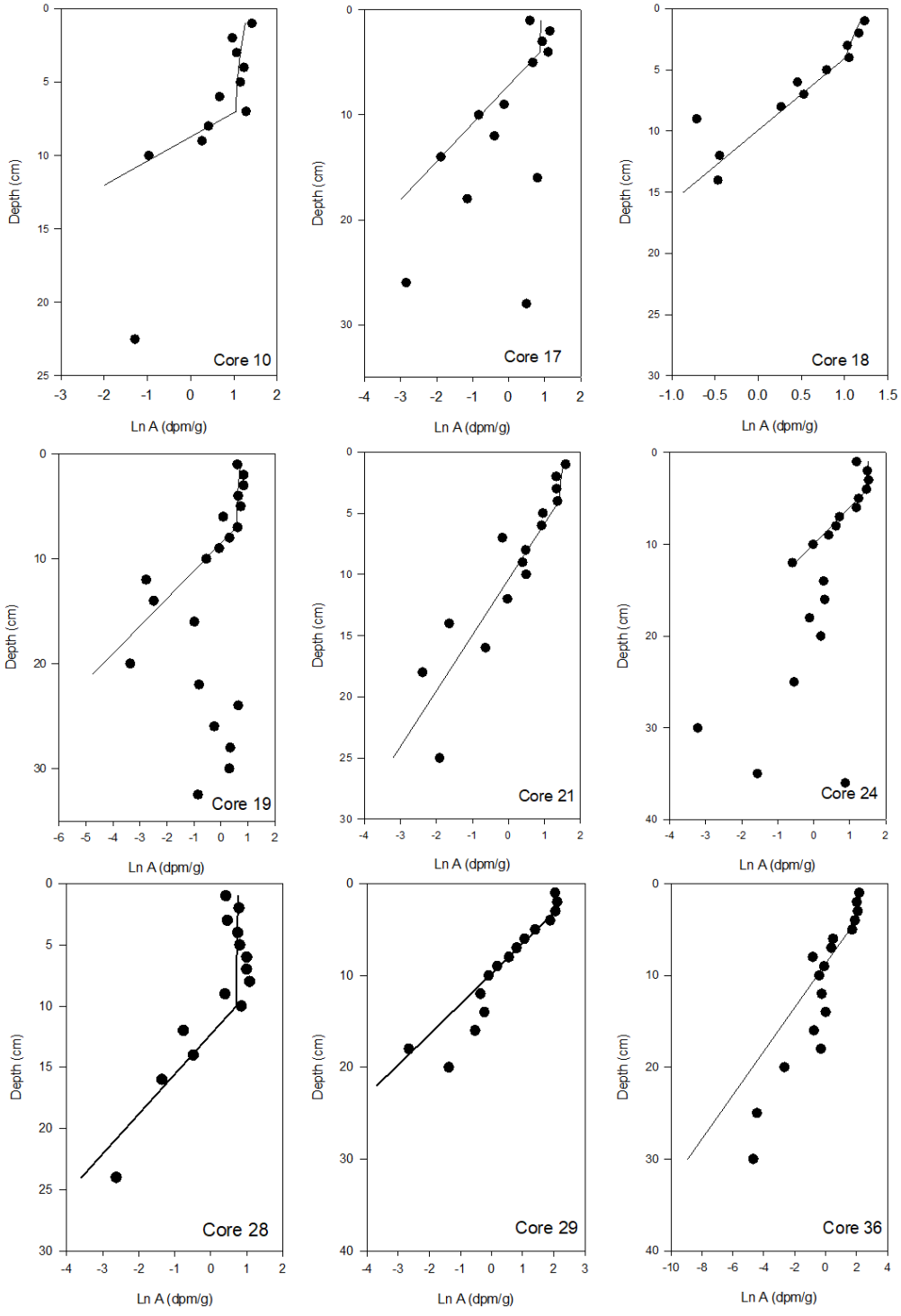
Depth (cm)
Ln A (dpm/g)
Core 10
Core 17
Core 18
Core 19
Core 21
Core 24
Core 28
Core 29
Core 36

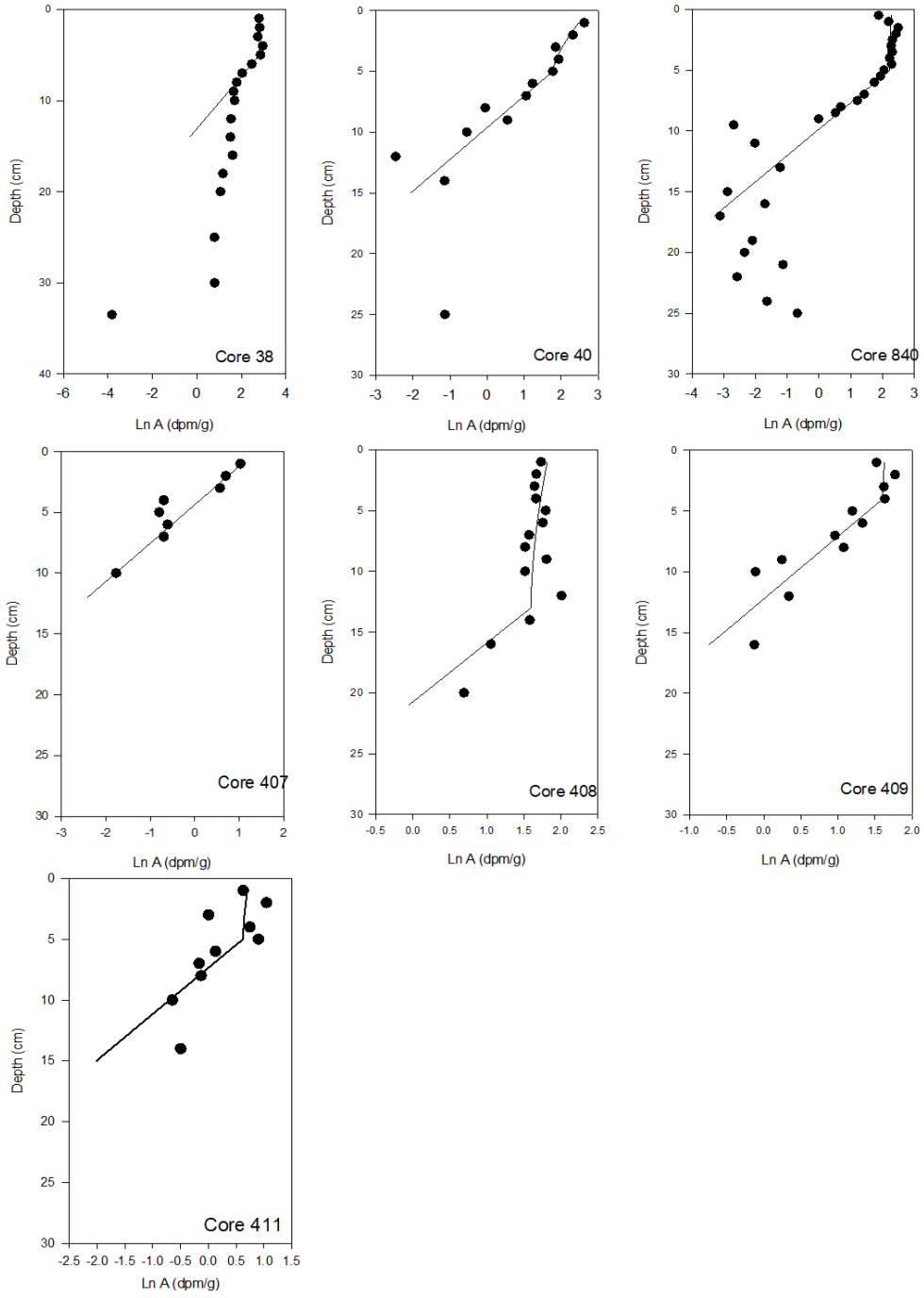

Figure 4-17: Fits of the two-layer advective-diffusive model to measured excess ^{210}Pb profiles in the cores.

Chapter 5 Discussion

Distribution of depositional basins across Hudson Bay

Based on review of more than 50,000 km of geophysical survey lines, unconsolidated deposits cover a minority of the seafloor across Hudson Bay. Sediment deposits are scattered throughout western Hudson Bay but are much sparser in that region generally than in eastern Hudson Bay. The difference between the type of deposits in the west and east does not appear to have anything to do with water depth, apart from none of the deposits being found shallower than 50 m water depth. One exception is the band of deposits east of the Belcher Islands, which is largely sheltered from the overall circulation of the bay (Hülse & Bentley, 2012).

The goal of reviewing the available geophysical data was to try to determine where modern sedimentation is taking place and, to a lesser extent, to aid in choosing coring locations for the 2018 Amundsen cruise. Due to the resolution of the 3.5kHz seismic data, it was not possible to distinguish between modern sedimentation and postglacial deposits. It also was not possible to determine distinct layers within most deposits similar to what Hougardy, 2014 and Josenhans, 1990 were able to determine using higher resolution Huntec data. The 3.5 kHz seismic data *did* allow for an overall view of the scope of sedimentation and give insight into spatial variation within Hudson Bay. The results of the new data analysis and the finding of sparse sedimentation throughout most of Hudson Bay largely agrees with the surficial sediment map produced by Josenhans *et al.* in 1988 (Figure 5-1) while also adding to this early work by expanding the analysis into areas closer to the coasts, where it was thought deposits would be present, as well as east of the Belcher Islands.

The findings of the subbottom analysis largely agree with the findings of Josenhans *et al.* 1988 that most of the seabed likely is comprised of glacial till. The till has been estimated at between 0 and 10 m thick. Because Josenhans *et al.* 1988 used Huntec data instead of 3.5 kHz seismic data, they were able to detect sediment in the central area of Hudson Bay, whereas with the 3.5 kHz data, we find little to no sedimentation in those areas. If you sample that central Hudson Bay area with a box corer there would be some muddy sediment

recovered (see discussion of sediment core results below) but this material does not represent significant modern sedimentation. The majority of the deposits located from the examined seismic data in this study lie in areas in the western and eastern sides of the bay that are previously mapped as either a mixture of glaciomarine sediment and modern sediment or glacial till and modern sediment (Josenhans *et al.* 1988). We also located many deposits in eastern Hudson Bay in areas previously mapped as bedrock. It is possible that these were missed due to Josenhans *et al.* (1988) using 3.5kHz data to laterally extrapolate the sediment deposits where they overlapped Huntec and sidescan data, making it possible that localized deposits were overlooked. The subbottom analysis in this study cannot be used to differentiate between modern sedimentation and glacial and post-glacial sedimentation but can be used to locate areas of high sedimentation vs low to virtually no sedimentation.

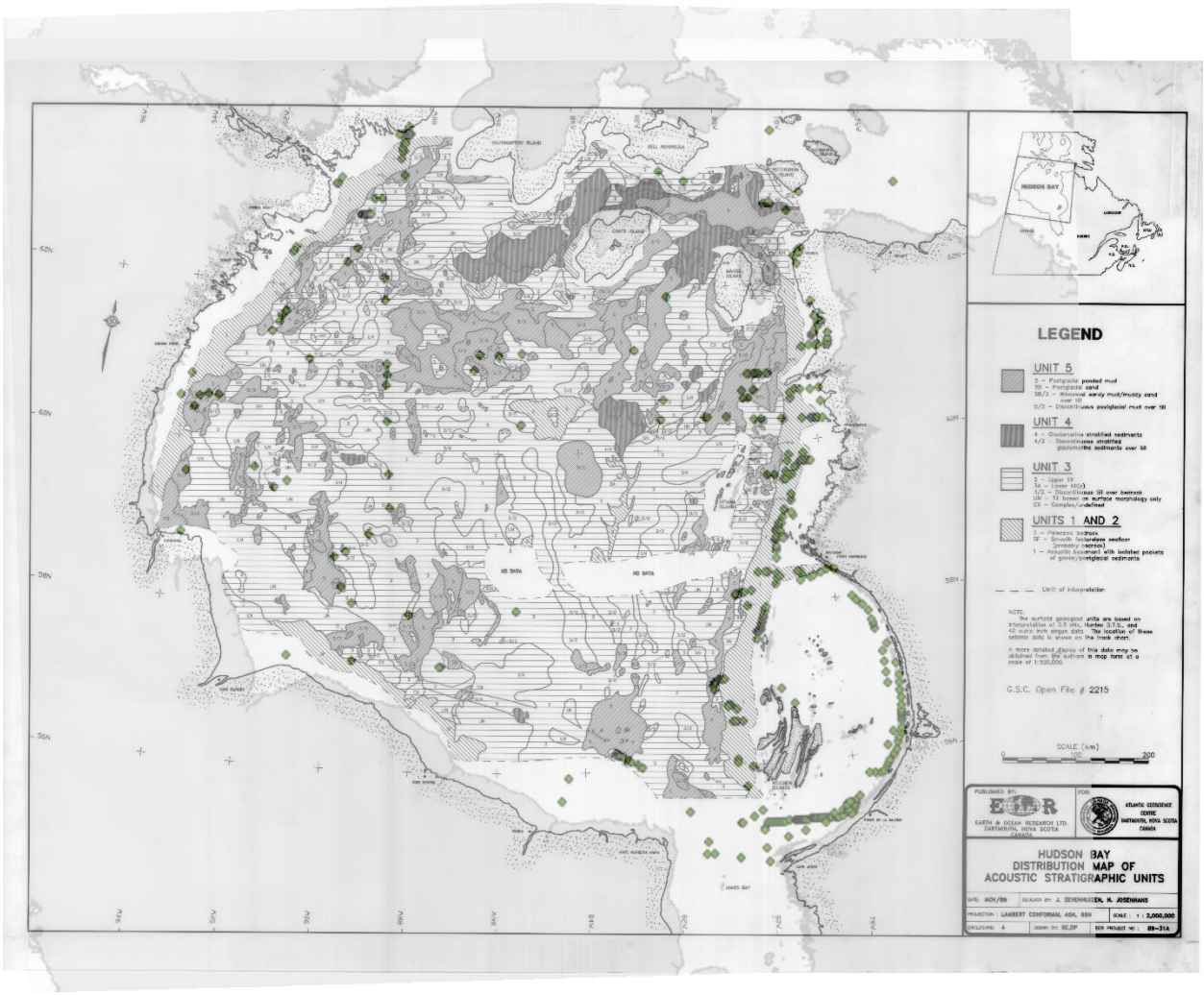

Figure 5-1: Sediment deposits identified from subbottom data overlying Zevenhuizen and Josenhans (1990) stratigraphic unit map

Sedimentation in Hudson Bay appears to follow spatial patterns that reflect a combination of geological, fluvial, and oceanographic processes. Figure 4-3 showed that the bulk of the sediment deposits in the eastern portion of Hudson Bay lay along or very near the geologic contact between the Precambrian crystalline bedrock and Paleozoic carbonate bedrock. The contact here appears to be irregular allowing for sediment to be deposited in the valleys of the contact (Grant, 1969). Throughout the bay, sedimentation also occurs at the bases of the

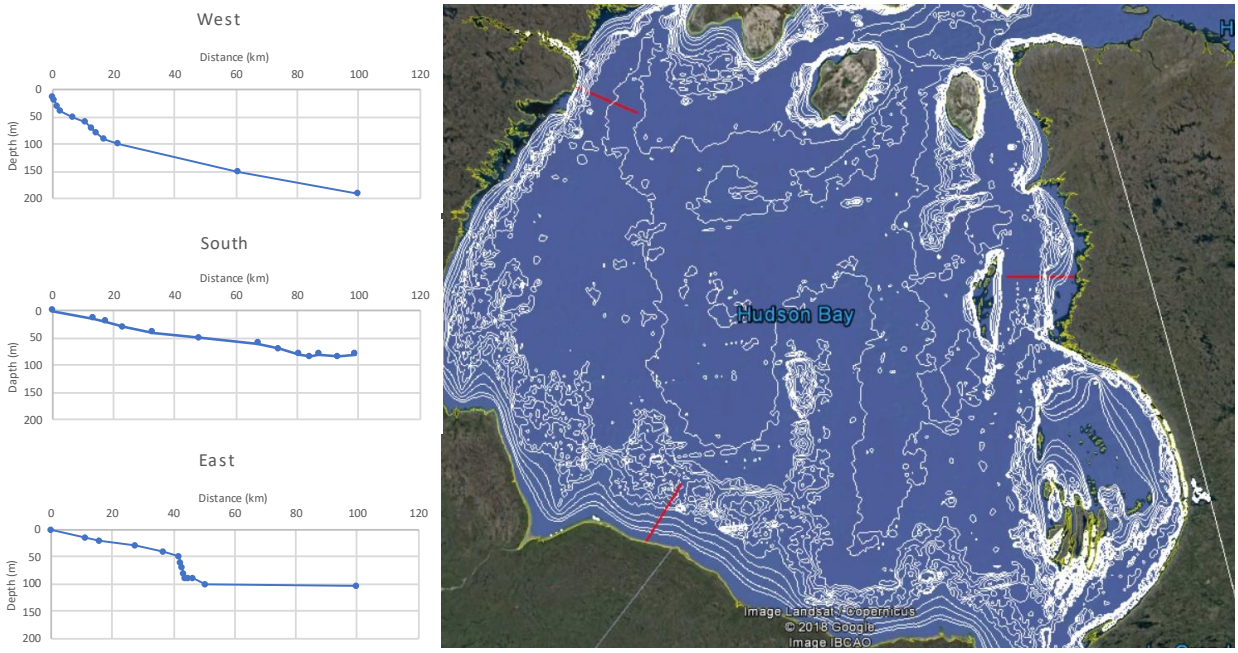

Figure 5-2 Cross sections of the slope gradients in Hudson Bay

slopes on both the west and east sides of the bay (Figure 5-2). Complex bedrock topography including discontinuous ridges and troughs previously have been identified as important components of the setting for thick sediment deposits along the southeast Hudson Bay coast (Gonthier et al., 1993; Hülse & Bentley, 2012).

Sedimentation is also affected by bottom currents and resuspension (Duboc et al., 2017; Thibodeau et al., 2017). Bottom currents in Hudson Bay simulated by the NEMO ocean model (courtesy Paul Myers, University of Alberta, and see also Ridenour et al., 2019, 2020) are shown in Figure 5-3. The bottom currents differ markedly from the surface currents, which include a fast-flowing, northward coastal current along the eastern shore of Hudson Bay (cf., Saucier et al., 2014). The bottom currents are strongest along the shallow coastal areas of the bay such as the southwest area between the Nelson River and the entrance to James Bay. Sediments that get resuspended along the western shore would tend to be moved south-southwestward while those that get resuspended along the southwest shore between the Nelson River and entrance to James Bay would tend to be moved southeastward (Figure 5-3). The bottom current directions are more variable around the entrance to James Bay and along the eastern shore. The bottom currents are almost negligible in the central, deeper portions of

the bay. The distribution of fast bottom currents in shallow coastal areas correlates well with the scarcity of deposits in water depths less than 50 m but does not explain the absence of sediment in central Hudson Bay.

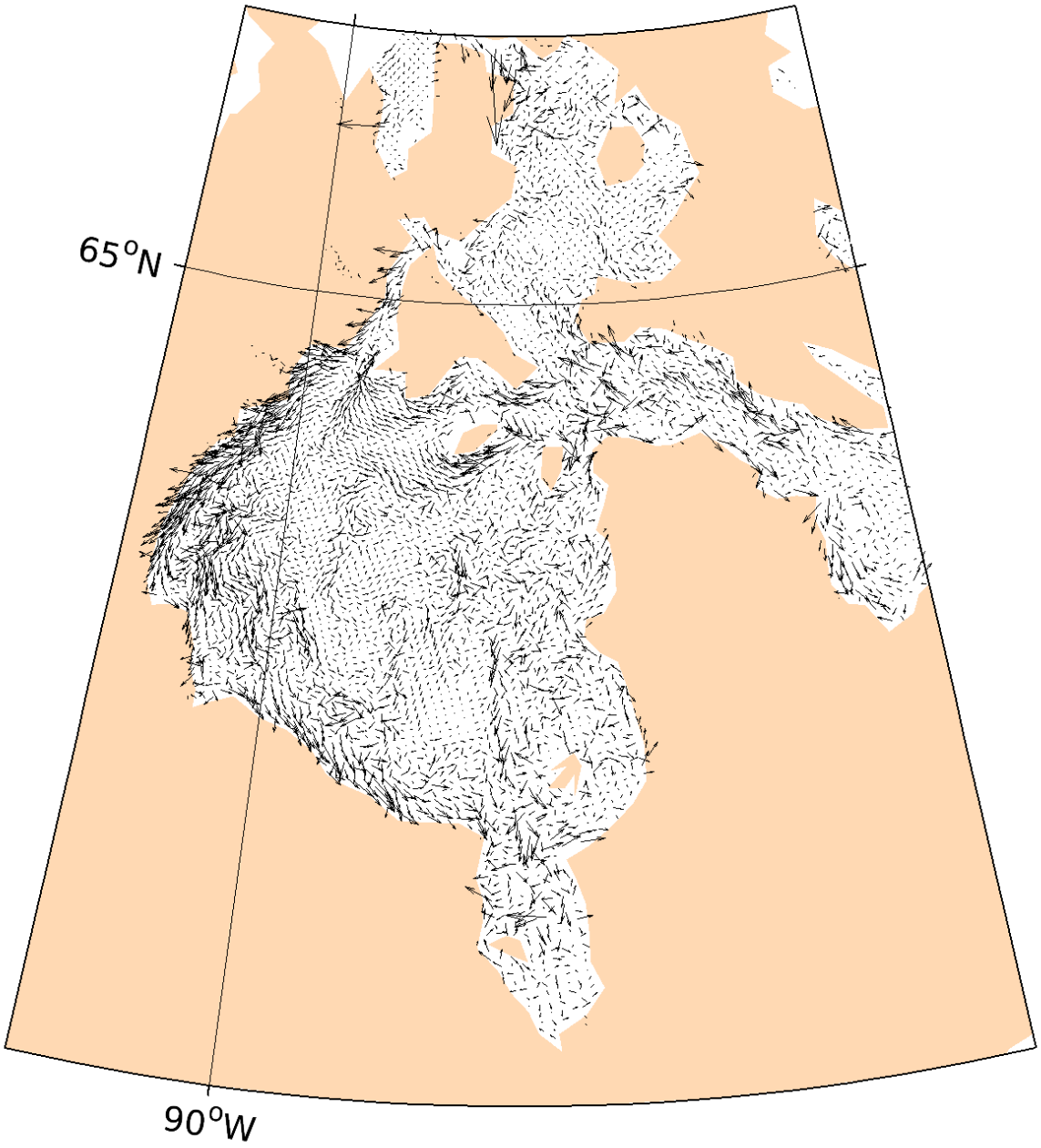

Figure 5-3: Bottom currents in Hudson Bay simulated by the NEMO ocean model (Figure courtesy of Paul Myers, University of Alberta).

Sediment core properties and sedimentation parameters in Hudson Bay

Northwestern Hudson Bay Cores

The cores from the northwestern portion of Hudson Bay are typified by porosity profiles that decrease with depth to approximately 10 cm and then sporadically increase and decrease through to the bottom of the core, with the exception of 28 which decreases with depth. All four cores have low ^{210}Pb inventories and, with the exception of one slice in core 17, have no ^{137}Cs present. This absence of ^{137}Cs indicates that the sediment source for this area is largely marine since ^{137}Cs is largely sourced from riverine input (Oughton et al., 1997). The low ^{210}Pb inventories are not expected and likely reflect dilution of the $^{210}Pb_{ex}$ flux by ^{210}Pb -poor coarse-grained sediment. There is a large amount of primary production in this area due to the polynya that covers the region during the winter (Sibert et al., 2011) and high spring primary production (Matthes et al., 2021). Typically, intense primary production would increase the amount of ^{210}Pb sorbed onto particles and deposited to the seafloor. Here, since the sediment is primarily sand sized particles in this area, it may be that *only* organic matter from marine primary production is delivering a flux of $^{210}Pb_{ex}$ to the seafloor (coarse-grained sediments having a negligible initial concentration because of their low surface area). Organic matter is degraded with depth as it settles, leading to often only 1%-2% of the surface export reaching the seabed, which does not represent a very large flux, even if it does carry a high initial activity of $^{210}Pb_{ex}$. It is well documented that an important control on ^{210}Pb deposition to sediments is scavenging by organic matter especially algal material (Kuzyk et al. 2013). Although the %OC is not high in the cores from the NW, if you were to normalize the %OC to the non-sand fraction, it would be really quite high. It is likely that the %OC is so high in NW Hudson Bay due to the polynya during the winter months allowing for a lot of primary production to take place (Sibert et al., 2011). The C/N ratios in this area (<10) indicate that the OC in these cores is largely marine derived. It is likely however, that the inventories of ^{210}Pb in these cores is still relatively low due to there not being enough biological activity to promote more accumulation than horizontal export of the ^{210}Pb to elsewhere in the Bay (Thibodeau *et al.*, 2007). The organic matter reaching the seabed may not accumulate permanently in this location but rather undergo resuspension and transport, in view of the

relatively high bottom currents along the northwest coast. Sibert et al. (2011) also proposed based on a biogeochemical ocean model that most of the organic matter produced in the polynya is transported to other regions of Hudson Bay before reaching the seafloor.

Core 19 also has the presence of what appears to be Dubawnt Group sediment starting at 20 cm depth. Similar sediment was found by previous workers (Haberzettl et al., 2010) in a core in central Hudson Bay as well as one in Hudson Strait. Both of these previously studied cores only had this sediment present at depths greater than 100 cm in the core, which could further indicate that the northwestern area of Hudson Bay has a low sedimentation rate overall and/or is net erosional in places.

Southern Hudson Bay Cores

The cores in southern Hudson Bay west of the entrance to James Bay are quite variable in their physical and chemical profiles, which is to be expected with the subbottom profiles showing very sporadic deposition. Core 32 is the only core that shows significant gravel sized particles as well as being the only core with a reversed porosity profile. Since the grain size is so large throughout this core, there is almost no ^{210}Pb present in the core. This core was obtained from a water depth of only 34 m in an area that had an abundance of sediment laden ice (Barber et al., 2021). We suspect that the coarse-grained sediment represents ice rafted debris perhaps picked up by ice when it became grounded and froze to the bottom in an intertidal setting.

Cores 36 and 38 both have a higher than average ^{210}Pb inventory and relatively low ^{137}Cs inventory. When modelled, both of these cores appear to have steady-state sedimentation that has been interrupted briefly by a depositional event. It is likely that these cores came from an area near where a slump took place and the sediment resuspended by the slump produced a rapidly deposited layer in a setting that was otherwise characterized by steady-state sedimentation. This interpretation is plausible considering the proximity of the cores to the base of Midbay Bank, which has a high-grade slope (Figure 5-4). Sediment transported by bottom currents towards the southeast along the southwest shore of Hudson Bay may accumulate along the top of the bank and eventually over steepen the slope, leading to a

submarine landslide. Midbay Bank has had scarce study despite it being an important bathymetric feature of offshore Hudson Bay.

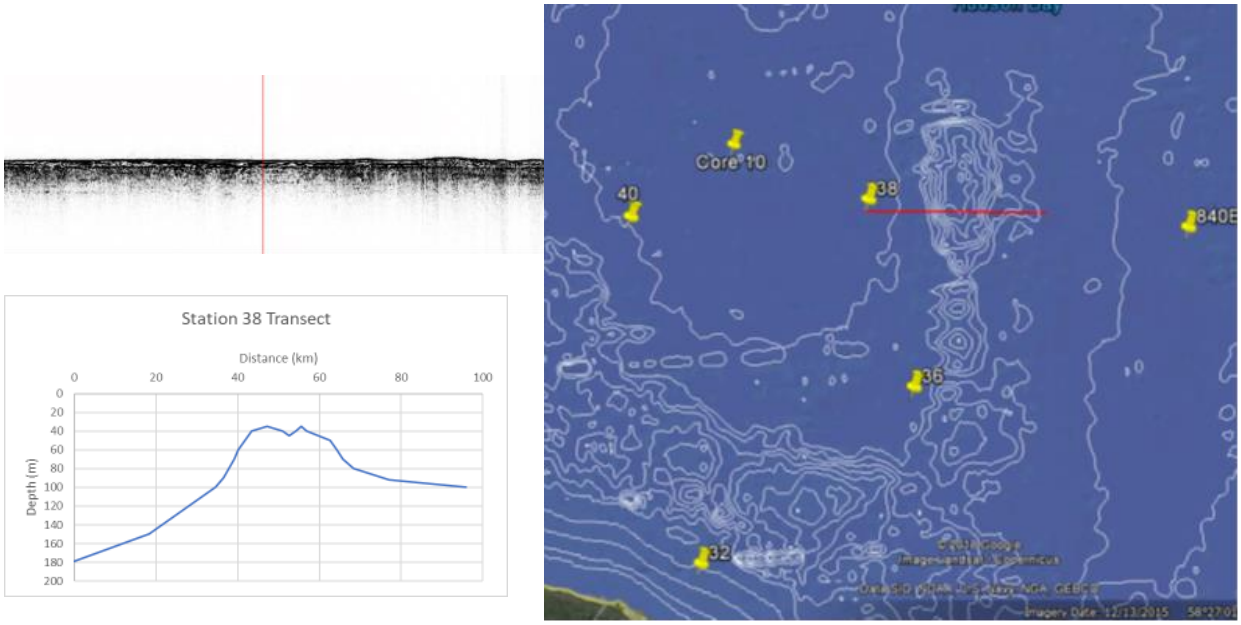

Figure 5-4 Cross section of the Midbay Bank and its proximity to cores 36 and 38. Top left: Subbottom image where core 38 was taken. Bottom left: Cross section of Midbay Bank (red line) Right: Map showing location of core 38

Eastern Hudson Bay Cores

Cores on the eastern side of Hudson Bay are typified by high ^{210}Pb inventories and comparatively high ^{137}Cs inventories. There are also many more deposits identifiable in the subbottom data in eastern Hudson Bay. The larger radioisotope *and* sediment supply could be due to the accumulation of pack ice and the final ice melt in the spring taking place in the southeastern part of Hudson Bay (Hochheim & Barber, 2014) allowing for material that underwent suspension freezing into the ice to be deposited. This could also be due to the abundance of riverine input in southern Hudson Bay and James Bay and along the eastern coast of Hudson Bay (Déry et al., 2005). Not only is river discharge higher in the southern part of the bay but the southern rivers and especially those draining the Hudson Bay Lowlands and the clay belt of northern Ontario and Quebec (Dresser, 1913) probably carry higher suspended sediment loads compared to rivers discharging along the west coast. Finally,

bottom currents will promote eastward transport of sediments that undergo resuspension along the southwest coast of Hudson Bay (Figure 5-3).

Cores 405 and 407 give us a unique look at the difference between deposition on the east vs the west side of the entrance to James Bay. Core 407 on the western side of the mouth has ^{210}Pb present in a normal decreasing-with-depth trend but it is a relatively low amount of ^{210}Pb, considering the proximity to the Winisk River as well as being a theoretical site where resuspended material from along the southern shore would be deposited. Core 405 has very high levels of ^{210}Pb compared to any other core collected for this thesis, with the excess Pb not reaching background levels by the bottom of the core. There is also ^{137}Cs through to the bottom of the core indicating that this is likely all modern sedimentation as well as sourced from riverine input (Appleby, 2001). There is possibly also additional ^{210}Pb being deposited here from resuspended material from the south that has bypassed James Bay. The site of core 405 represents an important depo-centre for modern sediment in Hudson Bay that warrants further investigation.

Cores 411, 409, and 408 comprise a transect from the mouth of the Winisk River heading northeast into the Winisk Trough. The cores show higher ^{210}Pb and ^{137}Cs inventories closer to the river mouth decreasing out into the trough. It is surprising to see higher inventories here than elsewhere near the coast considering the sparse number of deposits in the south, but this is likely due to the shelter of Winisk Trough and Midbay Bank to the west allowing for the sediment to be deposited with less effect from wave-based resuspension and ice-rafting.

Basin-wide correlations of core results

Overall, there is a lack of correlation between grain size and water depth which further indicates that the dominant influence on sedimentation are local factors. There is also a weak inverse correlation between sedimentation rate and water depth. A positive correlation between surface porosity and water depth shows a reduction in sediment settling processes further down core (below the SML). There is also a moderate to strong correlation between surface OC% and water depth as well as surface TN% and water depth. This suggests that water depth has more control over OC and TN than local depositional controls.

Comparison with other published cores

The cores from this study in addition to previously published data allow for a near complete coverage of the bay with the exception of the northeast section of the bay near the entrance to Hudson Strait. An overall trend from low ^{210}Pb and ^{137}Cs in the northwest to the southeast is visible in Figures 5-5 and 5-6, respectively. Among the most striking results is that eight of the new cores obtained from northwest and southwest Hudson Bay had zero ^{137}Cs (Figure 4-14) and twenty of the cores in the combined data set have a ^{137}Cs inventory below 2.0 dpm/cm^2 (Figure 4-16). ^{137}Cs binds to clay sized particles in terrestrial and freshwater environments primarily (Foster et al., 2006; Kuzyk et al., 2013; Smith & Ellis, 1982), which is in part due to less competition with Na^+ and K^+ ions which are more abundant in saltwater environments (Foster et al., 2006). ^{137}Cs enters Hudson Bay primarily through the river discharge and erosion of terrestrial soils (Foster et al., 2006; Kuzyk et al., 2013). There is a weak correlation between the latitude and ^{137}Cs inventories indicating that more ^{137}Cs is found in the southern part of Hudson Bay. This is to be expected because there is a higher amount of river discharge in the southern portion of the bay compared to the northern half of the bay (Déry et al., 2005). Furthermore, ^{137}Cs deposition associated with atmospheric weapons testing in the 1950s and 1960s varied with latitude – decreasing northward in Canada (Barrie et al., 1992; Walling & He, 2000).

One important factor in the very low ^{137}Cs in the new data set is that the sediment texture in northwest and southwest Hudson Bay, where most of the new cores were collected, is mostly comprised of silt sized particles with the exceptions of 10, 17, 18, 19 which are predominantly sand, and 32, which has a significant amount of pebbles in the surface sample. The proportion of clay-size particles that would be expected to carry ^{137}Cs originally deposited on land is very low in the northwest and southwest regions. Particle size distributions also explain in part the lack of spatial pattern in the ^{210}Pb inventories (Figure 4-9) because ^{210}Pb adsorbs onto silt and clay sized particles (Kuzyk et al., 2015). This however does not account for a higher ^{210}Pb inventory than expected in the sand-dominated sediments in the northwest portion of the bay (Figure 4-15). As described previously, we expect that marine primary production delivers a high initial ^{210}Pb flux to the seafloor in northwest Hudson Bay, but the sand dilutes this input.

One way of exploring the processes involved in sedimentation (e.g., particle scavenging, river sediment supply, lateral sediment transport and focusing) is to plot ^{210}Pb inventories vs. ^{137}Cs inventories for sediment cores (Figure 5-7; see Kuzyk et al. 2013). For the data examined here, core 38 in south-central offshore Hudson Bay really stands out with exceptionally high excess ^{210}Pb inventory relative to its ^{137}Cs inventory. This is partly because of the offshore location of this core, which causes low ^{137}Cs inventory because of low riverine ^{137}Cs supply, and also partially due to the core's proximity to the steep slope of Midbay Bank. Core 38 as well as core 36 to a lesser degree, appear to have been influenced by a slump which, through scavenging, may have added more ^{210}Pb to the sediments that otherwise would not have been deposited in those locations. Conversely, core 408 has a high inventory of ^{137}Cs (Figure 4-18) and a very low inventory of ^{210}Pb. This is likely due to core 408's proximity to the Winisk River assuming ^{137}Cs supply in this area largely comes from riverine input (Smith and Ellis, 1982). Core 405 has large inventories of both ^{137}Cs and ^{210}Pb. This is likely due to the large input of sediment into James Bay from southern rivers and possibly reflects sediment influxes from events such as La Grande River reservoir flooding (1979) and/or the decline of eelgrass meadows in east James Bay (1980s-1990s). The core indicates that sediments from James Bay are being deposited at the mouth of the bay. As well, a potential secondary source of sediment to the core 405 site that may originate in Hudson Bay is release of ice rafted material (Barber et al., 2021).

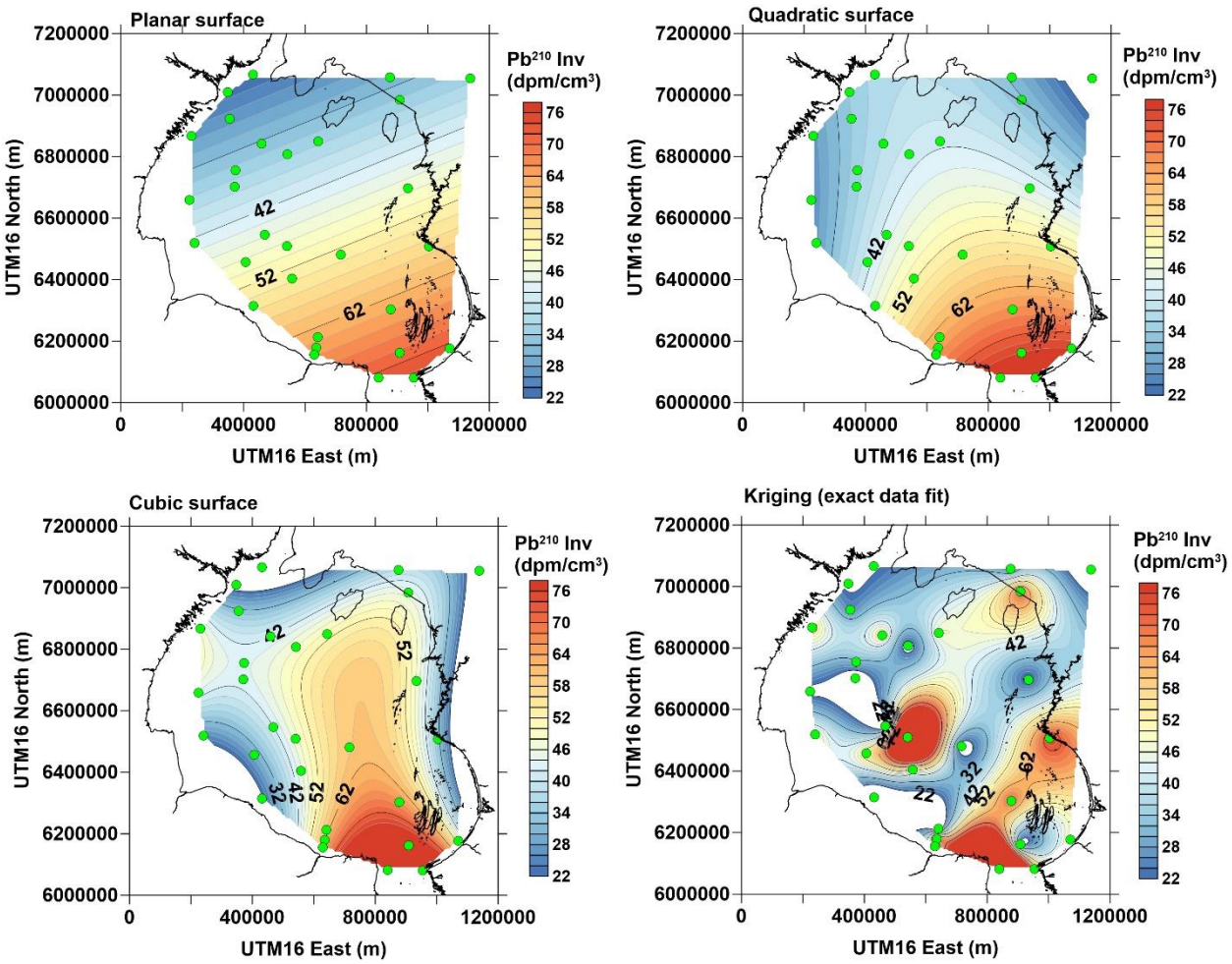

Figure 5-5: Spatial trends of ^{210}Pb in Hudson Bay based on the observed inventories and various smoothing methods. Courtesy of Dr. Ian Ferguson at the University of Manitoba.

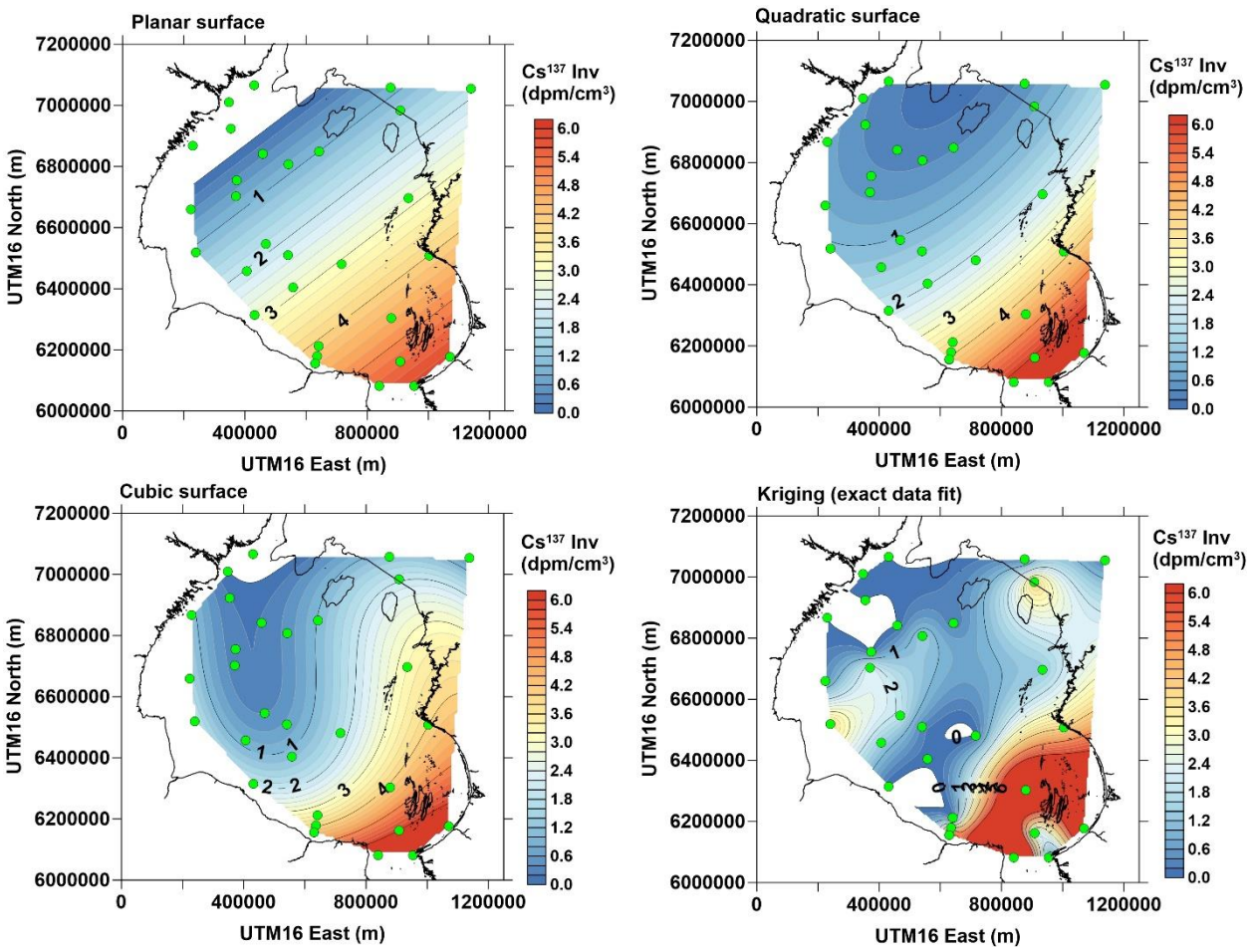

Figure 5-6: Spatial trends of ^{137}Cs in Hudson Bay based on the observed inventories and various smoothing methods. Courtesy of Dr. Ian Ferguson at the University of Manitoba.

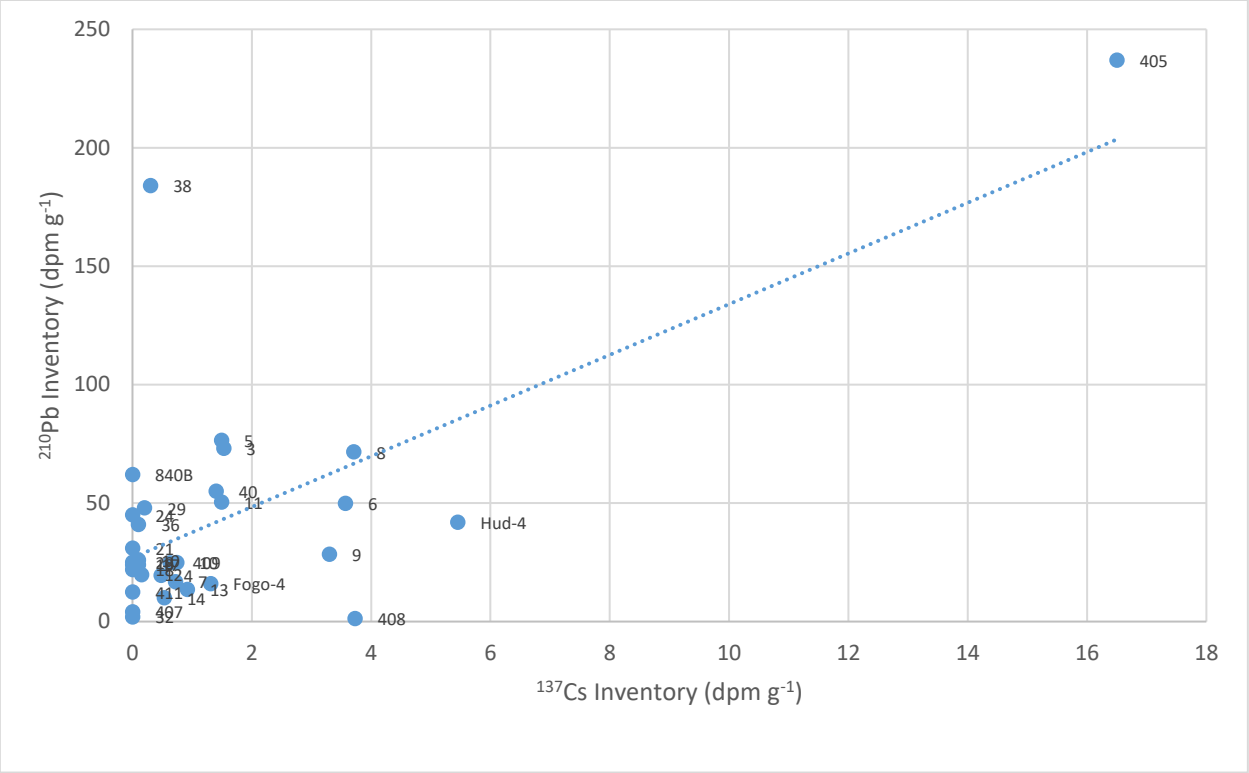

Figure 5-7: Excess ^{210}Pb inventories vs ^{137}Cs inventories. This figure includes inventories for new cores as well as previously published cores. ^{137}Cs data were adjusted to 1963.

Chapter 6 Conclusion

Bay-wide subbottom images indicate that most of the sediment deposition in Hudson Bay occurs along the west and especially east coasts at a water depth greater than 50 m. This is due to coastal currents making deposition temporary in shallow water, cyclonic (counterclockwise) circulation moving sediments generally eastward after resuspension, and the ability for sediment to settle permanently in topographic lows on the seafloor. The presence of a north-south oriented band of deposits along the east coast appears to coincide with the geologic contact between the Paleozoic limestone bedrock and the Precambrian crystalline bedrock. The scarcer deposits along the west coast appear to coincide with the geologic contact between Silurian and Devonian limestone formations. The bulk of sedimentation sites on both the western and eastern coasts also appear at the bottom of the slopes. Sedimentation along the southern coast of the bay west of the entrance to James Bay is scarce and limited to topographic lows due to the low-grade slope and sediment being moved by currents and ice. Modern sedimentation is also limited in the center of the bay likely due to low supply, with the sediment that gets resuspended along the bay's shorelines largely being kept closer to the coasts as it circulates, based on surficial and bottom currents.

Sediment cores collected for this thesis show that there is low ^{210}Pb accumulation in the northwest and southern portions of Hudson Bay west of the entrance to James Bay and higher ^{210}Pb in the east and at the outflow from James Bay. The cores also show that there is little to no ^{137}Cs accumulation in the northwest portion of the bay. Based on ^{210}Pb, ^{137}Cs, particle size data, and carbon and nitrogen data, sediment in the northwestern portion of Hudson Bay is not accumulating on the seafloor at a rapid rate despite higher biological activity that leads to relatively high %OC in the sediments after accounting for the diluting effects of sand. Inputs of sand-sized material presumably dilutes OC concentrations and ^{210}Pb inventories in this region. Sediment in the southern portion of Hudson Bay is largely being resuspended and laterally transported with currents, or ice rafted to the southeastern/eastern portion of the bay. The area east of the Belcher Islands is largely sheltered allowing for a large amount of sedimentation in the area. Sediment on the eastern side of Hudson Bay seems to be both

locally deposited sediment as well as some of the resuspended sediment from the southern portion of the bay.

Future work would benefit from additional subbottom data in a higher resolution, such as Huntec, to allow for a more in-depth study of the sediment deposits and whether the modern sediment is new, postglacial or paraglacial. Areas of interest include the entrance to James Bay and Midbay Bank. More sediment cores to cover any still existing gaps in the data, such as areas in the Winisk Trough, as well as more cores in the center of Hudson Bay, would be useful to help flesh out the constraints on deposition within the deeper areas of Hudson Bay. It is not possible at the present time to improve upon the estimate of the sediment sink as proposed in earlier work. There is much spatial variation in sediment accumulation rates at both regional and local scales. However, when considering the results for the larger data set of cores examined here and the larger geophysical data set compared to Josenhans, it can be concluded that the sediment sink was not grossly over- or underestimated in previous work, despite the gaps in the data. It would appear that, at most, 15% of the seafloor is presently accumulating sediments, as previously proposed, and that sedimentation rates vary from negligible values in places up to values of 0.15 cm yr^{-1} at other locations. There are also exceptional sites like the one identified at the entrance to James Bay where sedimentation rates are very high. There are no geophysical data for that site due to James Bay being largely too shallow for the CCGS Amundsen, which should be remedied in future work. Coring again in exceptional locations, with a gravity corer or piston corer would also be suggested to determine where the excess ^{210}Pb reaches background allowing for a more accurate calculation of the sedimentation rate. The addition of this coring work will aid in the potential for a future, more comprehensive sediment budget. The geophysical data will allow for the most optimal coring sites to be chosen for future work. This work can also now aid in a further understanding of the mercury and carbon cycles within the bay, as well as help create a comprehensive budget.

Chapter 7 References

Andrews, J. T., & Tedesco, K. (1992). Detrital carbonate-rich sediments, northwestern Labrador Sea: implications for ice-sheet dynamics and iceberg rafting (Heinrich) events in the North Atlantic. *Geology*, *20*(12), 1087–1090. https://doi.org/10.1130/0091-7613(1992)020<1087:DCRSNL>2.3.CO;2

Appleby, P. G. (2001). Chronostratigraphic techniques in recent sediments: tracking environmental change using lake sediments. *Basin Analysis, Coring, and Chronological Techniques*, *1*, 171–203.

Appleby, P. G., & Oldfield, F. (1992). Application of lead-210 to sedimentation studies. In *Uranium-series disequilibrium: applications to earth, marine, and environmental sciences* (2nd ed., pp. 729–784).

Barber, D. G., Harasyn, M. L., Babb, D. G., Capelle, D., McCullough, G., Dalman, L. A., Matthes, L. C., Ehn, J. K., Kirillov, S., Kuzyk, Z., Basu, A., Fayak, M., Schembri, S., Papkyriakou, T., Ahmed, M. M. M., Else, B., Guéguen, C., Meilleur, C., Dmitrenko, I., … Sydor, K. (2021). Sediment-laden sea ice in southern Hudson Bay: Entrainment, transport, and biogeochemical implications. *Elementa*, *9*(1), 1–20. https://doi.org/10.1525/elementa.2020.00108

Barrie, L. A., Gregor, D., Hargrave, B., Lake, R., Muir, D., Shearer, R., Tracey, B., & Bidleman, T. (1992). Arctic contaminants: sources, occurrence and pathways. *Science of the Total Environment, The*, *122*(1–2), 1–74. https://doi.org/10.1016/0048-9697(92)90245-N

Capelle, D. W., Kuzyk, Z. Z. A., Papakyriakou, T., Guéguen, C., Miller, L. A., & Macdonald, R. W. (2020). Effect of terrestrial organic matter on ocean acidification and CO2 flux in an Arctic shelf sea. *Progress in Oceanography*, *185*(June 2019). https://doi.org/10.1016/j.pocean.2020.102319

Carmack, E. C., Yamamoto-Kawai, M., Haine, T. W. N., Bacon, S., Bluhm, B. A., Lique, C., Melling, H., Polyakov, I. V., Straneo, F., Timmermans, M. L., & Williams, W. J. (2016). Freshwater and its role in the Arctic Marine System: Sources, disposition, storage, export,

and physical and biogeochemical consequences in the Arctic and global oceans. *Journal of Geophysical Research G: Biogeosciences*, *121*(3), 675–717. https://doi.org/10.1002/2015JG003140

Cooper, L. W., & Grebmeier, J. M. (2018). Deposition patterns on the Chukchi shelf using radionuclide inventories in relation to surface sediment characteristics. *Deep-Sea Research Part II: Topical Studies in Oceanography*, *152*(January), 48–66. https://doi.org/10.1016/j.dsr2.2018.01.009

Cumming, L. M. (1968). Rivers of the Hudson Bay Lowlands. In P. J. Hood (Ed.), *Earth Science Symposium on Hudson Bay* (pp. 144–168). Geological Survey of Canada.

Cutshall, N. H., Larsen, I. L., & Olsen, C. R. (1983). Direct analysis of 210Pb in sediment samples: Self-absorption corrections. *Nuclear Instruments and Methods In Physics Research*, *206*(1–2), 309–312. https://doi.org/10.1016/0167-5087(83)91273-5

De Haas, H., Boer, W., & Van Weering, T. C. E. (1997). Recent sedimentation and organic carbon burial in a shelf sea: The North Sea. *Marine Geology*, *144*(1–3), 131–146. https://doi.org/10.1016/S0025-3227(97)00082-0

de Haas, H., Weering, T. C. E. Van, & Stigter, H. De. (2002). Organic carbon in shelf seas : sinks or sources , processes and products. *Continental Shelf Research*, *22*, 691–717.

de Melo, M. L., Gérardin, M.-L., Fink-Mercier, C., & del Giorgio, P. A. (n.d.). Biogeochemistry Patterns in riverine carbon , nutrient and suspended solids export to the Eastern James Bay : links to climate , hydrology and landscape. *Biogeochemistry*, 1–57.

Déry, S. J., Stieglitz, M., McKenna, E. C., & Wood, E. F. (2005). Characteristics and trends of river discharge into Hudson, James, and Ungava Bays, 1964-2000. *Journal of Climate*, *18*(14), 2540–2557. https://doi.org/10.1175/JCLI3440.1

Donaldson, J. A. (1986). Precambrain Geology. In *Canadian Inland Seas* (pp. 1–16).

Dresser, J. A. (1913). The Clay Belt of Northern Ontario and Quebec. *Journal of Geography*, *11*, 250–255. https://doi.org/10.1080/00221341308985818

Duboc, Q., St-Onge, G., & Lajeunesse, P. (2017). Sediment records of the influence of river damming on the dynamics of the Nelson and Churchill Rivers, western Hudson Bay, Canada, during the last centuries. *Holocene*, *27*(5), 712–725. https://doi.org/10.1177/0959683616670465

Foster, I. D. L., Mighall, T. M., Proffitt, H., Walling, D. E., & Owens, P. N. (2006). Post-depositional137Cs mobility in the sediments of three shallow coastal lagoons, SW England. *Journal of Paleolimnology*, *35*(4), 881–895. https://doi.org/10.1007/s10933-005-6187-6

Gagnon, A. S., & Gough, W. A. (2005). Trends in the dates of ice freeze-up and breakup over Hudson Bay, Canada. *Arctic*, *58*(4), 370–382. https://doi.org/10.1007/s10584-005-1815-8

Godin, P., Macdonald, R. W., Kuzyk, Z. Z. A., Goñi, M. A., & Stern, G. A. (2017). Organic matter compositions of rivers draining into Hudson Bay: Present-day trends and potential as recorders of future climate change. *Journal of Geophysical Research: Biogeosciences*, *122*(7), 1848–1869. https://doi.org/10.1002/2016JG003569

Goharrokhi, M., McCullough, G. K., Owens, P. N., & Lobb, D. A. (2021). Sedimentation dynamics within a large shallow lake and its role in sediment transport in a continental-scale watershed. *Journal of Great Lakes Research*, *47*(3), 725–740. https://doi.org/10.1016/j.jglr.2021.03.022

Gonthier, N., D'Anglejan, B., & Josenhans, H. W. (1993). Seismo-stratigraphy and sedimentology of holcene sediments off grande riviere de la baleine, southeastern Hudson Bay, Quebec. *Geographie Physique et Quaternaire*, *47*(2), 147–166.

Grant, A. C. (1969). Some aspects of the bedrock geology of Hudson Bay as interpreted from continuous seismic reflection profiles. In P. J. Hood (Ed.), *Earth Science Symposium on Hudson Bay* (pp. 136–143). Geological Survey of Canada.

Haberzettl, T., St-onge, G., & Lajeunesse, P. (2010). Multi-proxy records of environmental changes in Hudson Bay and Strait since the fi nal outburst fl ood of Lake Agassiz – Ojibway. *Marine Geology*, *271*(1–2), 93–105. https://doi.org/10.1016/j.margeo.2010.01.014

Hare, A., Stern, G. A., Macdonald, R. W., Kuzyk, Z. Z., & Wang, F. (2008). Contemporary and

preindustrial mass budgets of mercury in the Hudson Bay Marine System: The role of sediment recycling. *Science of the Total Environment*, *406*(1–2), 190–204. https://doi.org/10.1016/j.scitotenv.2008.07.033

Henderson, P. (1989). *Provenance and depositional facies of surficial sediments in Hudson Bay, a glaciated epeiric sea*. University of Ottawa.

Hequette, A., Tremblay, P., & Hill, P. R. (1999). Nearshore erosion by combined ice scouring and near-bottom currents in eastern Hudson Bay, Canada. *Marine Geology*, *158*, 253–266.

Hochheim, K. P., & Barber, D. G. (2014). An Update on the Ice Climatology of the Hudson Bay System. *Arctic, Antarctic, and Alpine Research*, *46*(1), 66–83. https://doi.org/10.1657/1938-4246-46.1.66

Hougardy, D. D. (2014). *The Geologic History of Lake of the Woods, Minnesota, Reconstructed Using Seismic-Reflection Imaging and Sediment Core Analysis*.

Hülse, P., & Bentley, S. J. (2012). A210Pb sediment budget and granulometric record of sediment fluxes in a subarctic deltaic system: The Great Whale River, Canada. *Estuarine, Coastal and Shelf Science*, *109*, 41–52. https://doi.org/10.1016/j.ecss.2012.05.019

Josenhans, H., Balzer, S., Henderson, P., Nielson, E., Thorliefson, H., & Zevenhuizen, J. (1988). Preliminary seismostratigraphic and geomorphic interpretations of the Quaternary sediments of Hudson Bay. In *Current Research Part B: Eastern and Atlantic Canada* (pp. 271–286). Geological Survey of Canada.

Josenhans, H. W., & Zevenhuizen, J. (1990). Dynamics of the Laurentide Ice Sheet in Hudson Bay, Canada. *Marine Geology*, *92*(1–2), 1–26. https://doi.org/10.1016/0025-3227(90)90024-E

Kamula, C. Michelle, Macdonald, R. W., & Kuzyk, Z. Z. A. (2020). Sediment and particulate organic carbon budgets of a subarctic estuarine fjard: Lake Melville, Labrador. *Marine Geology*, *424*(February), 106154. https://doi.org/10.1016/j.margeo.2020.106154

Kamula, C.M., Kuzyk, Z. Z. A., Lobb, D. A., & Macdonald, R. W. (2017). Sources and accumulation of sediment and particulate organic carbon in a subarctic fjard

estuary:210Pb,137Cs, and δ13C records from lake melville, labrador. *Canadian Journal of Earth Sciences*, *54*(9), 993–1006. https://doi.org/10.1139/cjes-2016-0167

Kuzyk, Z. Z. A., Gobeil, C., & Macdonald, R. W. (2013). 210Pb and 137Cs in margin sediments of the Arctic Ocean: Controls on boundary scavenging. *Global Biogeochemical Cycles*, *27*(2), 422–439. https://doi.org/10.1002/gbc.20041

Kuzyk, Z. Z. A., Goñi, M. A., Stern, G. A., & Macdonald, R. W. (2008). Sources, pathways and sinks of particulate organic matter in Hudson Bay: Evidence from lignin distributions. *Marine Chemistry*, *112*(3–4), 215–229. https://doi.org/10.1016/j.marchem.2008.08.001

Kuzyk, Z. Z. A., Macdonald, R. W., & Johannessen, S. C. (2015). Calculating rates and dates and interpreting contaminant profiles in biomixed sediments. In J. M. Blais (Ed.), *Environmental Contaminants* (pp. 61–87). Springer Science+Business. https://doi.org/10.1007/978-94-017-9541-8_4

Kuzyk, Z. Z. A., Macdonald, R. W., Johannessen, S. C., Gobeil, C., & Stern, G. A. (2009). Towards a sediment and organic carbon budget for Hudson Bay. *Marine Geology*, *264*(3–4), 190–208. https://doi.org/10.1016/j.margeo.2009.05.006

Lajeunesse, P., & St-Onge, G. (2008). The subglacial origin of the Lake Agassiz-Ojibway final outburst flood. *Nature Geoscience*, *1*, 184–188.

Landy, J. C., Ehn, J. K., Babb, D. G., Thériault, N., & Barber, D. G. (2017). Sea ice thickness in the Eastern Canadian Arctic: Hudson Bay Complex & Baffin Bay. *Remote Sensing of Environment*, *200*(August), 281–294. https://doi.org/10.1016/j.rse.2017.08.019

Lavoie, C., Allard, M., & Hill, P. R. (2002). Holocene deltaic sedimentation along an emerging coast: Nastapoka River delta, eastern Hudson Bay, Quebec. *Canadian Journal of Earth Sciences*, *39*(4), 505–518. https://doi.org/10.1139/e01-079

Leivuori, M., & Niemistö, L. (1995). Sedimentation of trace metals in the Gulf of Bothnia. *Chemosphere*, *31*(8), 3839–3856. https://doi.org/10.1016/0045-6535(95)00257-9

Mackenzie, F. T., Lerman, A., & Ver, L. M. B. (1988). Role of the continental margin in the global carbon balance during the past three centuries. *Geology*, *26*(5), 423–426.

Maclean, B., Vilks, G., & Deonarine, B. (1992). Depositional environments and history of late Quaternary sediments in Hudson Strait and Ungava Bay: further evidence from seismic and biostratigraphic data. *Geographie Physique et Quaternaire*, *46*(3), 311–329. https://doi.org/10.7202/032917ar

Matthes, L. C., Ehn, J. K., Dalman, L. A., Babb, D. G., Peeken, I., Harasyn, M., Barber, D. G., & Mundy, C. J. (2021). *Environmental drivers of spring primary production in Hudson Bay*. 1–25.

Murray, A. S., Marten, R., Johnston, A., & Martin, P. (1987). Analysis for naturally occuring radionuclides at environmental concentrations by gamma spectrometry. *Journal of Radioanalytical and Nuclear Chemistry*, *115*(2), 263–288.

Nicolas, M. P. B., & Armstrong, D. K. (2017). *Update on Paleozoicstratigraphic correlations in theHudson Bay Lowland, northeasternManitoba and northernOntario*. *1*(1), 133–147. http://www2.gov.mb.ca/itm-cat/web/freedownloads.html,

Norris, A. W. (1986). Review of Hudson Platform Stratigraphy and Biostratigraphy. In *Canadian Inland Seas* (pp. 17–42).

Norris, A. W., & Sanford, B. V. (1968). No Titl. In P. J. Hood (Ed.), *Earth Science Symposium on Hudson Bay* (pp. 169–205). Geological Survey of Canada.

Oughton, D. H., Borretzen, P., Salbu, B., & Tronstad, E. (1997). Mobilisation of 137Cs and 90Sr from sediments: potential sources to arctic waters. *The Science of the Total Environment*, *202*, 155–165.

Pehrsson, S. J., Berman, R. G., Eglington, B., & Rainbird, R. (2013). Two Neoarchean supercontinents revisited: The case for a Rae family of cratons. *Precambrian Research*, *232*(October 2021), 27–43. https://doi.org/10.1016/j.precamres.2013.02.005

Pelletier, B. R. (1968). Submarine physiography, bottom sediments, and models of sediment transport in Hudson Bay. In P. J. Hood (Ed.), *Earth Science Symposium on Hudson Bay* (Issues 68–53, pp. 100–135). Geological Survey of Canada. https://doi.org/10.4095/102950

Pelletier, B. R. (1986). Seafloor Morphology and Sediments. In *Canadian Inland Seas* (pp. 143–

162).

Piper, D. J. W. (1991). Seabed geology of the Canadian eastern continental shelf. *Continental Shelf Research*, *11*(8–10), 1013–1035. https://doi.org/10.1016/0278-4343(91)90089-O

Ridenour, N. A., Hu, X., Sydor, K., Myers, P. G., & Barber, D. G. (2019). Revisiting the Circulation of Hudson Bay: Evidence for a Seasonal Pattern. *Geophysical Research Letters*, *46*(7), 3891–3899. https://doi.org/10.1029/2019GL082344

Saucier, F. J., Senneville, S., Prinsenberg, S., Roy, F., Smith, G., Gachon, P., Caya, D., & Laprise, R. (2004). Modelling the sea ice-ocean seasonal cycle in Hudson Bay, Foxe Basin and Hudson Strait, Canada. *Climate Dynamics*, *23*(3–4), 303–326. https://doi.org/10.1007/s00382-004-0445-6

Shilts, W. W. (1982). Quaternary evolution of the Hudson/ James Bay region. *Naturaliste Canadien*, *109*(3), 309–332.

Shilts, W. W. (1986). Glaciation of the Hudson Bay Region. In *Canadian Inland Seas* (pp. 55–78).

Sibert, V., Zakardjian, B., Gosselin, M., Starr, M., Senneville, S., & LeClainche, Y. (2011). 3D Bio-Physical Model of the Sympagic and Planktonic Productions in the Hudson Bay System. *Journal of Marine Systems*, *88*(3), 401–422. https://doi.org/10.1016/j.jmarsys.2011.03.014

Smith, J. N. (2001). *Why should we believe 210 Pb sediment geochronologies ? 55*, 121–123.

Smith, J. N. and E. K. M. (1982). Transport mechanism for Pb-210, Cs-137 and Pu fallout radionuclides through fluvial-marine settings. *Geochimica et Cosmocimica Acta*, *46*, 941–954.

Stainton, T. M. (2019). *An Initial Investigation into the Sources and Transport of Particulate Organic Matter in the Nelson River System , Manitoba*. University of Manitoba.

Stein, R., & Macdonald, R. W. (2004). Organic carbon budget: Arctic Ocean vs. global ocean. In R. Stein & R. W. Macdonald (Eds.), *The Organic Carbon Cycle in the Arctic Ocean* (pp.

315–322). Springer, Berlin.

Suteerasak, T., Elming, S. Å., Possnert, G., Ingri, J., & Widerlund, A. (2017). Deposition rates and14C apparent ages of Holocene sediments in the Bothnian Bay of the Gulf of Bothnia using paleomagnetic dating as a reference. *Marine Geology*, *383*, 1–13. https://doi.org/10.1016/j.margeo.2016.10.009

Syvitski, J. P. M., Peckham, S. D., Hilberman, R., & Mulder, T. (2003). Predicting the terrestrial flux of sediment to the global ocean: A planetary perspective. *Sedimentary Geology*, *162*(1–2), 5–24. https://doi.org/10.1016/S0037-0738(03)00232-X

Thibodeau, B., Migon, C., Dufour, A., Poirier, A., Mari, X., Ghaleb, B., & Legendre, L. (2017). Low sedimentary accumulation of lead caused by weak downward export of organic matter in Hudson Bay, northern Canada. *Biogeochemistry*, *136*(3), 279–291. https://doi.org/10.1007/s10533-017-0395-9

Todd, B. J., Lewis, C. F. M., Nielsen, E., Thorleifson, L. H., Bezys, R. K., & Weber, W. (1998). Lake Winnipeg: Geological setting and sediment seismostratigraphy. *Journal of Paleolimnology*, *19*(3), 215–243. https://doi.org/10.1023/A:1007997024412

Verardo, D. J., Froelich, P. N., & McIntyre, A. (1990). Determination of organic carbon and nitrogen in marine sediments using the Carlo Erba NA-1500 Analyzer. *Deep-Sea Research*, *37*, 57–165.

Walling, D., & He, Q. (2000). *The Global Distribution of Bomb-Derived 137Cs Reference Inventories*.

Whitehouse, P. L., Allen, M. B., & Milne, G. A. (2007). Glacial isostatic adjustment as a control on coastal processes: An example from the Siberian Arctic. *Geology*, *35*(8), 747–750. https://doi.org/10.1130/G23437A.1

Wright, S. M., Howard, B. J., Strand, P., Nylén, T., & Sickel, M. A. K. (1999). Prediction of 137Cs deposition from atmospheric nuclear weapons tests within the Arctic. *Environmental Pollution*, *104*(1), 131–143. https://doi.org/10.1016/S0269-7491(98)00140-7

Zaborska, A., Nietelski, J. W., Carroll, J., Papucci, C., & Pempkowiak, J. (2010). Sources and

distributions of 137Cs, 238Pu, 239,240Pu radionuclides in the north-western Barents Sea. *Journal of Environmental Radioactivity*, *101*, 323–331.

Zevenhuizen, J & Josenhans, H., 1990. Digital Maps of Surficial Geology of Hudson Bay Geological Survey of Canada, Open File 2215, 1990, 5 sheets, https://doi.org/10.4095/128157

Appendix 1: Table of Sediment Deposits from Geophysical Data

OBJECTID	Cruise	Date	Time	Longitude	Latitude	EndLong	EndLat	Top Depth (m)	Bottom Depth (m)	Thickness (m)	Length (km)
1	2004	242	12:20:00 PM	-83.6868	56.16942	-83.67253	56.16503	87.53	92.03	4.5	1.008849
2	2004	242	12:34:51 PM	-83.6073	56.14486	-83.60222	56.14322	78.59	80.39	1.8	0.366883
3	2004	242	12:37:23 PM	-83.5973	56.1417	-83.59058	-56.13958	77.16	79.67	2.51	0.481502
4	2004	242	12:42:17 PM	-83.5751	56.13478	-83.55874	56.12974	75.01	77.16	2.15	1.156511
5	2004	242	12:45:40 PM	-83.5539	56.1283	-83.54842	56.12663	75.36	78.59	3.23	0.392359
6	2004	242	12:48:32 PM	-83.543	56.12494	-83.52613	56.11973	75.72	81.46	5.74	1.198249
7	2004	242	12:52:40 PM	-83.5158	56.11653	-83.51093	56.115	73.93	77.52	3.59	0.348886
8	2004	242	12:54:32 PM	-83.509	56.1144	-83.50113	-56.11193	73.57	80.03	6.46	0.564476
9	2004	242	12:57:04 PM	-83.4944	56.10988	-83.48814	-56.10794	73.21	75.72	2.51	0.443054
10	2004	242	1:06:59 PM	-83.4533	56.0974	-83.42615	-56.08965	75.01	81.82	6.81	1.895506
11	2004	242	1:16:18 PM	-83.3953	56.08104	-83.26482	-56.04402	74.49	84.04	9.55	9.0881
12	2004	242	1:43:00 PM	-83.2535	56.04072	-83.129	-56.00404	67.67	72.22	4.55	8.745589
13	2004	242	2:16:24 PM	-83.1171	56.00062	-83.07281	-55.98851	61.13	64.64	3.51	3.066076

							-	55.9641			3.94726
14	2004	242	2:28:08 PM	-83.0416	55.9797	82.9846	1	58.79	64.25	5.46	5
					55.9546	-	55.9513				0.77909
15	2004	242	2:43:14 PM	-82.952	1	82.9409	4	59.57	62.69	3.12	6
						-	57.4102				1.04279
16	2004	241	10:38:48 PM	-87.7988	57.4144	87.7832	4	67.18	73.6	6.42	5
					55.1907	-	55.1843				4.17373
17	2004	243	12:03:53 AM	-80.5933	1	80.5285	9	90.13	96.88	6.75	4
					55.1773	-	55.1784				2.48295
18	2004	243	2:22:02 AM	-79.9379	3	79.8989	1	132.24	144.55	12.31	9
					55.1791	-	55.1796				1.30000
19	2004	243	2:34:49 AM	-79.8722	8	79.8517	2	129.78	143.32	13.54	9
					55.1801	-	55.1808				2.54778
20	2004	243	2:47:44 AM	-79.8176	1	79.7775	3	145.78	158.1	12.32	2
					55.1815	-	55.1846				4.69804
21	2004	243	3:07:10 AM	-79.757	5	79.6832	8	156.87	170.41	13.54	9
					55.1848	-	55.1860				1.96556
22	2004	243	3:20:16 AM	-79.6798	1	79.6489	1	158.1	171.64	13.54	2
					55.1890	-	55.1897				1.12707
23	2004	243	3:40:17AM	-79.5678	5	79.5501	6	110.5	114.36	3.86	5
					55.1902	-	55.1922				
24	2004	243	3:50:56 AM	-79.5386	1	79.4775	8	131.32	145.98	14.66	3.88504
					55.1944	-	55.1964				3.56857
25	2004	243	4:18:00 AM	-79.4106	3	79.3545	9	115.9	129.78	13.88	8
					55.1972	-	55.2060				10.1226
26	2004	243	5:04:20 AM	-79.2446	2	79.0859	7	143.49	157.43	13.94	2
					55.2073	-	55.2136				11.3500
27	2004	243	5:45:11 AM	-79.0712	2	78.8927	6	183.91	211.79	27.88	3
					55.2143	-	55.2172				5.80708
28	2004	243	6:31:30 AM	-78.8654	9	78.7739	8	122.59	142.1	19.51	1
					55.2173	-	55.2177				1.01208
29	2004	243	6:51:19 AM	-78.7716	4	78.7557	2	127.91	141.5	13.59	7

					55.2181	-78.6789					3.69567
30	2004	243	7:01:56 AM	-78.7372	6		55.2194	135.9	146.3	10.4	3
					55.2200	-					
31	2004	243	7:18:05 AM	-78.6554	2	78.6241	55.22	158.29	167.08	8.79	1.98787
					55.2199	-	55.2198				2.38716
32	2004	243	7:26:51 AM	-78.6179	8	78.5802	5	162.08	168.78	6.7	8
					55.2197	-	55.2203				2.99774
33	2004	243	7:37:18 AM	-78.5739	9	78.5267	2	153.39	156.27	2.88	3
					55.2232	-	55.2240				1.47113
34	2004	243	8:10:44 AM	-78.4078	5	78.3846	6	109.02	114.32	5.3	5
					55.2247	-					1.62370
35	2004	243	8:21:48 AM	-78.3654	9	78.3399	55.2258	106.9	116.44	9.54	2
					55.2298	-	55.2324				4.22768
36	2004	243	8:47:35 AM	-78.2467	3	78.1802	9	125.99	146.06	20.07	6
					55.2355	-	55.2766				15.8726
37	2004	243	9:24:40 AM	-78.082	5	77.8421	4	66.81	101.08	34.27	1
					55.2802	-	55.2824				0.27996
38	2004	243	10:36:03 AM	-77.8303	2	77.8282	2	46.26	77.78	31.52	4
					55.2837	-	55.3391				6.43071
39	2004	246	8:18:44 PM	-77.8284	8	77.7988	1	68.32	97.12	28.8	4
					55.3467	-	55.3507				
40	2004	246	10:00:34 PM	-77.7957	8	77.7941	6	67.38	73.13	5.75	0.45346
					55.3568	-	55.3913				
41	2004	246	10:16:04 PM	-77.7917	8	77.7778	3	76.78	104.11	27.33	3.92955
						-	55.4127				2.04215
42	2004	246	10:20:56 PM	-77.7761	55.3948	77.7693	4	62.8	80.6	17.8	5
					55.4173	-	55.4271				1.09484
43	2004	246	10:27:32 PM	-77.7642	7	77.7654	9	65.98	74.88	8.9	3
					55.4322	-	55.4360				0.42156
44	2004	246	10:30:29 PM	-77.764	5	77.7633	1	61.53	72.34	10.81	1
					55.4377	-	55.4453				0.86013
45	2004	246	10:32:24 PM	-77.7629	4	77.7608	8	65.98	80.6	14.62	5

					55.4972		55.5367				5.60380
46	2004	246	11:08:57 PM	-77.6892	3	-77.634	5	142.53	170.23	27.7	5
					55.5630	-	55.5906				3.79024
47	2004	246	11:36:03 PM	-77.6034	5	77.5679	2	140.12	159.44	19.32	1
					55.6009	-	55.6556				7.76399
48	2004	246	11:49:47 PM	-77.5541	1	77.4772	2	172.33	188.43	16.1	2
					55.6855	-	55.7000				
49	2004	247	12:21:10 AM	-77.4358	7	77.4166	7	190.47	201.91	11.44	2.01079
					55.7283		55.8010				14.8806
50	2004	247	12:36:50 AM	-77.3837	9	-77.184	8	188.25	206.84	18.59	7
					55.8011	-	55.8010				
51	2004	247	1:47:19 AM	-77.196	5	77.1816	9	96.59	103.02	6.43	0.90017
					55.8010	-					
52	2004	247	1:55:51 AM	-77.1721	2	77.0868	55.8016	88.86	98	9.14	5.32994
					55.8025	-	55.8057				
53	2004	247	2:20:47 AM	-77.0819	9	77.0769	9	50.8	58.18	7.38	0.47387
					55.8154	-	55.8154				
54	2004	247	2:27:30 AM	-77.0644	7	77.0644	7	70.21	83.34	13.13	0
						-	55.8202				0.50556
55	2004	247	2:27:56 AM	-77.0632	55.8165	77.0587	9	51.72	60.89	9.17	7
					55.8222	-	55.8255				0.44459
56	2004	247	2:30:19 AM	-77.0564	1	77.0526	8	59.48	71.46	11.98	6
					55.8265						4.64154
57	2004	247	2:38:43 AM	-77.0516	2	-77.013	55.8622	48.78	56.76	7.98	6
					55.8630		55.9122				6.42994
58	2004	247	3:04:32 AM	-77.0121	2	-76.958	5	99.13	117.97	18.84	8
					55.9167	-	55.9328				2.12488
59	2004	247	3:16:37 AM	-76.9528	7	76.9343	1	121.94	147.72	25.78	5
					55.9422	-	55.9978				7.17704
60	2004	247	3:32:40 AM	-76.9234	8	76.8646	1	85.58	102.69	17.11	3
					56.0780	-	56.0691				5.02603
61	2004	247	4:12:54 AM	-76.8575	5	76.7781	6	121.95	175.44	53.49	3

							-	56.0813				1.34812
62	2004	247	4:19:26 AM	-76.7747	56.0719	76.7611	4	38.51	43.86	5.35	5
					56.0864	-	56.1467				
63	2004	247	4:33:19 AM	-76.7531	9	76.6858	2	120.49	157.42	36.93	7.88974
					56.1958	-	56.2284				3.86010
64	2004	247	5:03:36 AM	-76.6911	3	76.6699	9	143.28	156.78	13.5	3
					56.2378	-	56.2500				1.46627
65	2004	247	5:09:47 AM	-76.6634	6	76.6545	7	110.69	119.47	8.78	5
					56.2532	-	56.2867				3.98877
66	2004	247	5:18:28 AM	-76.6521	5	76.6288	1	150.78	178.44	27.66	2
					56.2923	-	56.2978				0.65787
67	2004	247	5:23:23 AM	-76.6251	3	76.6214	8	51.51	65.1	13.59	6
					56.3064	-	56.3500				5.17322
68	2004	247	5:34:32 AM	-76.6159	8	76.5865	7	113.56	123.73	10.17	8
					56.3551	-	56.3628				0.85511
69	2004	247	5:38:55 AM	-76.5834	8	76.5821	4	87.67	91.37	3.7	9
						-	56.4231				6.55111
70	2004	247	5:48:57 AM	-76.5819	56.3642	76.5809	2	106.16	115.41	9.25	6
					56.4374	-	56.4547				1.92089
71	2004	247	5:59:08 AM	-76.581	8	76.5812	5	80.33	91.28	10.95	5
					56.4596	-	56.4888				3.24854
72	2004	247	6:10:44 AM	-76.5813	5	76.5809	6	96.75	108.61	11.86	3
					56.4929	-	56.5031				1.12978
73	2004	247	6:12:42 AM	-76.5807	8	76.5804	4	63.91	80.33	16.42	9
					56.5061	-	56.5390				
74	2004	247	6:23:17 AM	-76.5801	3	76.5685	6	70.3	104.96	34.66	3.72939
					56.5526		56.5602				0.92755
75	2004	248	12:30:28 AM	-76.5717	8	-76.578	5	72.74	87.72	14.98	3
					56.5751	-	56.5832				0.89681
76	2004	248	12:37:28 AM	-76.5829	6	76.5828	3	53.49	64.18	10.69	9
					56.5910		56.6363				
77	2004	248	12:53:09 AM	-76.5828	2	-76.582	9	59.91	75.95	16.04	5.04524

					56.6460	-76.5843	56.6759				3.32721
78	2004	248	12:58:21 AM	-76.5822	5		5	60.78	102.01	41.23	3
					56.6857	-76.5864					1.34055
79	2004	248	1:11:37 AM	-76.5857	5		56.6978	69.53	84.51	14.98	6
					56.7434		56.8085				7.23809
80	2004	248	1:35:03 AM	-76.5826	4	-76.582	3	79.16	98.42	19.26	2
					56.8117	-76.5958	56.8563				5.02596
81	2004	248	1:45:53 AM	-76.582	9		5	55.46	68.77	13.31	7
					56.8605	-76.6027	56.8814				2.35094
82	2004	248	2:04:11 AM	-76.5968	8		8	90.57	98.12	7.55	3
					56.9269	-76.6146	57.0958				18.7777
83	2004	248	2:49:40 AM	-76.6196	8		3	88.42	122.74	34.32	9
					57.1485	-76.7036	57.3224				19.8458
84	2004	248	3:48:29 AM	-76.6297	1		4	121.95	150.83	28.88	6
					57.3280	-76.7292	57.3776				
85	2004	248	4:53:22 AM	-76.7059	3		3	143.34	175.44	32.1	5.6898
					57.3812	-76.8172	57.4423				8.52823
86	2004	248	5:12:10 AM	-76.7311	5		2	132.65	160.46	27.81	2
					57.4443	-76.8442	57.4489				1.19293
87	2004	248	5:35:35 AM	-76.8262	9		7	108.04	119.81	11.77	3
					57.4574	-76.9383	57.4719				4.18659
88	2004	248	5:51:43 AM	-76.8737	7		6	96.28	113.39	17.11	2
						-77.1892					4.58884
89	2004	248	7:36:41 AM	-77.1595	57.6552		57.6933	100.56	108.04	7.48	3
					57.7148	-77.2125	57.7245				1.15990
90	2004	248	7:50:53 AM	-77.2056	1		7	95.21	100.56	5.35	5
					57.7379	-77.2349	57.7560				2.15688
91	2004	248	7:59:41 AM	-77.2219	2		3	105.9	114.46	8.56	5
					57.7622	-77.2634	57.7968				4.09092
92	2004	248	8:09:05 AM	-77.2396	9		1	124.09	139.07	14.98	7
					57.8564	-77.3222	57.8875				3.66735
93	2004	248	8:32:29 AM	-77.3013	9		3	115.53	127.3	11.77	3

						-					9.15087
94	2004	248	8:48:46 AM	-77.3261	57.8931	77.4272	57.9555	123.02	140.14	17.12	7
					57.9605	-	57.9691				
95	2004	248	9:11:26 AM	-77.4388	3	77.4583	2	125.16	133.72	8.56	1.49647
					57.9703	-	57.9860				2.75782
96	2004	248	9:20:02 AM	-77.4612	9	77.4974	8	129.44	146.55	17.11	8
					57.9880	-					1.34156
97	2004	248	9:24:34 AM	-77.5019	3	77.5195	57.9957	124.09	138	13.91	9
						-	58.0384				2.27669
98	2004	248	9:46:26 AM	-77.5878	58.0258	77.6182	6	118.74	128.37	9.63	8
					58.0540		58.0977				7.79995
99	2004	248	9:57:19 AM	-77.6572	4	-77.761	6	128.37	139.07	10.7	8
					58.4120	-	58.4370				3.53097
100	2004	248	1:19:00 PM	-78.1492	7	78.1117	5	46	60.98	14.98	6
					62.8687	-					15.8265
101	2004	237	1:21:21 AM	-76.1943	4	76.5062	62.8743	354.45	361.72	7.27	8
					62.8166	-	62.7495				24.9905
102	2004	237	6:08:40 AM	-78.5767	2	79.0457	3	401.23	418.95	17.72	4
					61.0650	-	61.0411				6.23850
103	2004	238	12:54:41 AM	-86.1772	6	86.2821	6	235.67	242.12	6.45	8
					60.9170	-	60.9012				2.89829
104	2004	238	2:31:43 AM	-86.7582	2	86.8008	3	213.13	217.96	4.83	4
					59.6909	-	59.6695				
105	2004	238	1:42:36 PM	-91.4506	7	91.5277	4	131.76	135.32	3.56	4.93926
					59.6024	-	59.5929				2.20862
106	2004	238	2:23:15 PM	-91.7717	4	91.8061	2	123.21	124.64	1.43	4
					55.3296	-					4.53868
107	2005	273	6:58:31 PM	-78.1289	3	78.0578	55.3239	120.88	135.86	14.98	9
						-	55.3030				
108	2005	273	7:18:03 PM	-78.0107	55.3138	77.9595	4	79.16	93.07	13.91	3.45202
					55.2972	-	55.2841				2.52761
109	2005	273	7:27:43 PM	-77.936	4	77.9034	9	86.65	105.9	19.25	6

					57.5456	-	57.5269				2.10950
110	2005	283	5:02:33 PM	-91.6244	9	91.6295	2	57.77	67.39	9.62	1
					55.3019		55.3135				
111	2005	274	12:45:17 PM	-77.9645	8	-78.012	2	77.02	93.07	16.05	3.27432
					55.3243	-	55.3600				4.85853
112	2005	274	1:10:18 PM	-78.0565	1	78.1006	8	124.09	139.07	14.98	7
					56.7199	-	56.7124				0.83574
113	2005	279	4:45:34 AM	-80.8077	3	80.8062	6	195.33	206.86	11.53	5
					56.9405		56.9863				6.37986
114	2005	279	7:20:57 AM	-81.1306	3	-81.194	3	149.61	153.78	4.17	3
					58.2886		58.4129				19.2333
115	2005	284	8:42:30 AM	-90.3963	6	-90.167	3	144.84	150.44	5.6	4
					62.1730	-	62.1594				2.91520
116	2005	270	12:31:57 PM	-78.8521	8	78.8041	9	183.6	191.12	7.52	9
					55.3878	-	55.4074				9.37751
117	2005	274	3:13:35 PM	-78.0708	4	77.9263	6	116.6	132.65	16.05	6
							55.4102				1.15884
118	2005	274	3:22:57 PM	-77.913	55.4084	-77.895	9	105.9	120.88	14.98	9
					62.1174	-	62.1202				0.61102
119	2005	270	4:32:56 PM	-78.7982	5	78.7882	9	182.53	192.19	9.66	4
					55.4097	-	55.3827				3.08603
120	2005	274	7:00:43 PM	-77.9239	8	77.9353	9	133.72	144.41	10.69	8
					55.3389	-	55.3178				2.36021
121	2005	274	7:25:00 PM	-77.9539	3	77.9585	6	95.21	112.32	17.11	2
					55.3043		55.2903				2.72494
122	2005	274	7:40:11 PM	-77.9373	4	-77.902	5	87.72	114.46	26.74	6
					56.0125	-	55.6802				38.5121
123	2005	280	5:12:43 PM	-84.7002	2	84.8741	2	92.05	94.65	2.6	1
					55.2837	-	55.2954				2.61776
124	2005	274	7:55:11 PM	-77.9063	5	77.9421	6	87.72	110.18	22.46	3
					55.3009	-	55.3053				1.18366
125	2005	274	8:05:59 PM	-77.9694	7	77.9865	4	78.09	93.07	14.98	3

					55.5680	-					13.7193
126	2005	280	7:43:07 PM	-84.9341	5	84.9914	55.449	33.16	44.93	11.77	6
					55.3062	-	55.2894				4.17766
127	2005	274	8:21:26 PM	-77.9623	3	77.9033	1	86.65	115.53	28.88	3
					55.2950	-	55.2984				3.70315
128	2005	274	10:09:44 PM	-77.8545	6	77.9127	8	88.79	119.81	31.02	8
					55.3175	-	55.3407				2.66683
129	2005	274	10:54:22 PM	-77.9368	6	77.9475	6	81.3	90.93	9.63	6
					55.3892	-	55.4018				
130	2005	274	11:14:30 PM	-77.9711	1	77.9745	4	116.6	127.3	10.7	1.41991
					55.4407	-	55.4225				2.87524
131	2005	275	3:01:26 AM	-77.84	5	77.8723	2	130.77	146.92	16.15	6
						-	55.3812				5.37907
132	2005	275	3:39:58 AM	-77.9327	55.3982	78.0125	9	124.31	137.23	12.92	4
					55.3446	-	55.2345				14.1887
133	2005	275	4:50:09 AM	-78.2022	9	78.3155	9	125.71	138.23	12.52	5
					55.1864	-	55.1266				19.9658
134	2005	275	5:41:36 AM	-78.3902	1	78.6866	6	151.9	186.06	34.16	5
						-	55.0539				
135	2005	275	7:06:34 AM	-78.877	55.0923	79.0477	5	141.56	159.92	18.36	11.6763
					55.0097	-	54.9605				16.8774
136	2005	275	8:18:36 AM	-79.289	1	79.5393	4	103.63	110.97	7.34	6
					54.8920	-	54.7501				26.0560
137	2005	275	9:58:25 AM	-79.8305	5	80.1542	2	123.21	140.34	17.13	8
					54.6339	-					0.14154
138	2005	275	11:57:16 AM	-79.8603	1	79.8586	54.6331	50.69	57.48	6.79	6
					57.3928	-	57.3582				3.89249
139	2005	273	3:34:01 AM	-77.0254	1	77.0149	6	91.8	103.07	11.27	8
					57.2575	-	57.2262				3.56122
140	2005	273	4:14:19 AM	-76.9891	1	76.9759	9	90.19	99.85	9.66	5
					57.1743	-	57.0474				14.3101
141	2005	273	4:51:51 AM	-76.9572	1	76.9171	7	104.68	115.96	11.28	9

142	2005	273	5:28:27 AM	-76.8916	56.9814 4	-76.8871	56.9709 1	103.07	107.91	4.84	1.20228
143	2005	273	6:19:05 AM	-76.8369	56.8520 1	-76.8491	56.2771 2	127.23	148.17	20.94	63.9293 9
144	2005	273	11:46:43 AM	-76.8918	56.2230 2	-76.957	56.1327 4	162.66	181.99	19.33	10.8205 9
145	2005	275	4:19:39 PM	-80.3545	54.7007 3	-80.7342	54.7123 7	106.97	113.39	6.42	24.4237 6
146	2005	273	1:56:34 PM	-77.0001	56.0868 5	-77.6265	55.6140 1	175.55	188.43	12.88	65.5198 8
147	2005	273	4:14:37 PM	-77.7005	55.5561 7	-78.1075	55.3675 7	138.51	156.22	17.71	33.1365 2
148	2005	276	4:49:28 AM	-80.7307	54.7174 4	-81.4993	54.7704 6	60.98	68.46	7.48	49.6842 2
149	2005	276	10:16:12 AM	-81.5666	54.8419 7	-81.4795	54.6612 2	64.18	71.67	7.49	20.8609 2
150	2005	280	11:54:48 PM	-84.9521	55.5616 8	-84.9315	55.5635 6	34.5	46.6	12.1	1.31141 2
151	2005	281	1:47:48 AM	-84.7969	55.8153	-84.8005	55.9082 6	95	105.59	10.59	10.3391 6
152	2007	220	11:06:57 PM	-79.162	56.7341 2	-79.2246	56.7718 4	67.74	73.47	5.73	5.67257 5
153	2007	223	4:41:00 PM	-81.7352	54.8781 2	-81.8166	55.3926 3	40.12	44.29	4.17	57.4444 3
154	2007	230	4:39:16 AM	-94.1109	59.0199 2	-94.1175	59.1356 1	47.53	50.72	3.19	12.8704 1
155	2007	221	10:20:19 AM	-80.3115	55.3892 6	-80.2833	55.3264 8	98.33	106.7	8.37	7.20372 6
156	2007	221	10:28:55 AM	-80.298	55.3592 6	-80.2225	55.2366 2	96.24	102.51	6.27	14.4505 4
157	2007	223	5:20:22 PM	-81.8249	55.4393 2	-82.0835	55.5951 6	59.92	63.57	3.65	23.7783 5

							-	62.0575				1.06130
158	2007	234	10:02:18 AM	-92.4275	62.0515	92.4433	2	42.54	45.87	3.33	2
					62.7933	-	62.7941				0.09233
159	2007	235	10:40:23 AM	-92.0907	2	92.0912	2	33.61	39.08	5.47	4
					62.7953	-	62.7944				0.10569
160	2007	237	11:54:00 PM	-92.0944	1	92.0934	9	29.7	33.35	3.65	3
					63.2939	-	63.3267				6.83829
161	2007	238	10:26:15 AM	-90.5612	9	90.6771	1	52.94	57.85	4.91	8
					55.2369	-	55.2390				5.69776
162	2007	221	12:23:19 PM	-79.8645	2	79.7747	1	150.3	160.8	10.5	5
						-					2.24848
163	2007	221	12:53:22 PM	-79.6629	55.242	79.6275	55.2424	117.75	123	5.25	3
					55.2427	-	55.2434				2.84772
164	2007	221	1:06:07 PM	-79.6036	1	79.5587	8	175.5	188.1	12.6	5
					55.2437	-	55.2441				2.36604
165	2007	221	1:19:41 PM	-79.5406	3	79.5032	5	177.6	188.1	10.5	1
					55.2446		55.2452				2.96152
166	2007	221	1:30:53 PM	-79.4647	4	-79.418	9	121.95	133.5	11.55	7
					55.2467	-	55.2479				3.96232
167	2007	221	1:46:32 PM	-79.3631	4	79.3006	6	148.2	159.75	11.55	9
					55.2485	-	55.2494				4.91842
168	2007	221	2:25:54 PM	-79.1201	4	79.0425	4	142.95	155.55	12.6	2
					55.2501	-	55.2541				12.8330
169	2007	221	3:04:43 PM	-78.9801	2	78.7777	7	125.1	140.85	15.75	8
					55.2618	-	55.2962				11.5611
170	2007	221	3:51:38 PM	-78.6643	3	78.4921	8	149.25	161.85	12.6	1
					55.5981	-	55.7429				
171	2007	223	7:32:04 PM	-82.0923	7	82.9093	9	53.67	59.92	6.25	53.7008
					55.2972	-	55.3674				23.0219
172	2007	221	4:48:30 PM	-78.4871	6	78.1446	2	148.2	156.6	8.4	2
					55.3822	-	55.4063				8.76138
173	2007	221	5:23:16 PM	-78.0632	8	77.9311	1	104.1	115.65	11.55	7

					55.7929	-	55.7943				0.54120
174	2007	223	10:27:43 PM	-83.2239	1	83.2322	2	49.5	54.19	4.69	3
					55.8273	-	55.8699				16.3075
175	2007	223	11:43:24 PM	-83.4373	5	83.6873	9	65.65	73.47	7.82	8
						-	55.8814				0.79046
176	2007	224	12:14:48 AM	-83.7523	55.8797	83.7646	2	70.34	72.95	2.61	1
					55.8975	-	55.8975				
177	2007	224	12:46:21 AM	-83.8689	6	83.8689	6	83.37	90.66	7.29	0
					55.4133	-	55.3903				2.61565
178	2007	222	12:24:06 AM	-77.9348	1	77.9441	9	134.94	146.45	11.51	6
					55.3841	-	55.3763				0.88512
179	2007	222	12:57:37 AM	-77.9467	1	77.9498	6	80.55	88.91	8.36	1
					55.3389	-	55.3153				2.67083
180	2007	222	1:13:46 AM	-77.9638	4	77.9717	5	88.91	104.61	15.7	7
					55.9159	-					16.4876
181	2007	224	1:15:31 AM	-83.9774	3	84.2315	55.9576	82.07	87.54	5.47	8
					55.3093	-	55.2951				1.60593
182	2007	222	1:25:14 AM	-77.9738	2	77.9785	3	74.25	83.63	9.38	1
					55.2875	-	55.3026				5.81893
183	2007	222	1:33:29 AM	-77.9807	4	77.8927	3	89.88	151.11	61.23	7
					55.3061	-	55.2957				1.41161
184	2007	222	2:14:09 AM	-77.8823	5	77.8696	2	72.69	109.42	36.73	7
					56.0297	-	55.8400				21.1001
185	2007	224	5:41:03 AM	-84.7168	7	84.7103	5	96.24	100.42	4.18	1
					55.7396	-	55.7400				0.12001
186	2007	224	8:27:13 AM	-84.8351	8	84.8333	8	61.48	64.09	2.61	6
						-	55.3281				
187	2007	222	3:18:43 AM	-77.8606	55.3029	77.8152	8	92.23	177.16	84.93	4.02236
					55.3298	-					
188	2007	222	4:02:32 AM	-77.8162	3	77.8225	55.325	69.56	84.41	14.85	0.66743
					55.3234	-					2.84196
189	2007	222	4:12:59 AM	-77.8243	6	77.8512	55.303	82.07	108.64	26.57	5

					55.3000	-	55.3143				2.35535
190	2007	222	4:44:42 AM	-77.8568	9	77.8843	9	91.44	108.64	17.2	9
					55.3104	-	55.3067				0.50403
191	2007	222	6:54:53 AM	-77.8913	9	77.8869	4	66.43	79.72	13.29	2
					55.2957	-	55.2782				3.84056
192	2007	222	7:10:36 AM	-77.8728	1	77.9251	6	69.56	87.54	17.98	6
					55.2823	-	55.2957				1.76020
193	2007	222	8:03:49 AM	-77.9295	8	77.9444	4	79.72	96.92	17.2	3
					55.3181	-	55.3381				2.27194
194	2007	222	8:25:34 AM	-77.9648	5	77.9577	7	68	80.5	12.5	2
					55.3818	-	55.4058				
195	2007	222	9:10:23 AM	-77.9393	5	77.9311	3	129.74	139.12	9.38	2.71554
					55.4069	-	55.4082				0.66673
196	2007	222	11:02:01 AM	-77.9286	4	77.9389	3	133.89	149.59	15.7	8
					55.7401	-	55.6577				9.55708
197	2007	224	9:28:05 AM	-84.833	7	84.8762	2	56.79	59.92	3.13	1
						-	55.9018				8.76529
198	2007	225	4:52:24 PM	-84.7978	55.8244	84.8238	7	87.87	96.24	8.37	6
					57.5645	-	57.5681				1.83116
199	2007	226	12:20:33 AM	-91.4024	7	91.4324	3	33.87	36.99	3.12	2
					59.5547	-	59.5805				2.92740
200	2007	227	7:40:50 PM	-91.8074	1	91.8171	8	121.41	125.57	4.16	1
					59.6037		59.6216				2.03580
201	2007	227	7:53:14 PM	-91.827	6	-91.835	1	121.93	125.05	3.12	7
					59.6393	-	59.6637				2.78109
202	2007	227	8:02:56 PM	-91.8427	3	91.8531	8	119.84	123.49	3.65	9
					62.6399	-	62.6419				
203	2007	217	2:07:30 AM	-78.1339	2	78.2478	6	494.62	508.8	14.18	5.82537
					60.2120	-	60.1732				4.61858
204	2007	217	3:48:26 PM	-78.5944	3	78.5645	4	102.65	109.42	6.77	7
						-	60.0040				1.40282
205	2007	217	4:41:09 PM	-78.4484	60.0154	78.4374	5	90.14	97.44	7.3	6

							-	59.9988			0.01191
206	2007	217	5:28:14 PM	-78.4371	59.9988	78.4373	6	84.93	88.06	3.13	6
					60.0015		60.0032				0.57645
207	2007	217	6:32:52 PM	-78.4448	6	-78.435	7	87.54	92.75	5.21	6
					59.9943	-	60.0006				0.69992
208	2007	217	7:03:34 PM	-78.4317	1	78.4319	1	83.37	88.06	4.69	6
					60.0031	-	60.0116				0.95897
209	2007	217	7:08:37 PM	-78.4325	3	78.4346	9	88.06	92.75	4.69	9
					55.3973	-					6.87305
210	2007	222	2:16:25 PM	-77.9383	2	78.0388	55.3737	114.7	125.7	11	8
					55.3708		55.3637				
211	2007	222	2:35:14 PM	-78.0546	7	-78.093	3	105.27	113.91	8.64	2.55683
					55.3590	-	55.2442				17.2171
212	2007	222	3:15:57 PM	-78.118	6	78.3005	6	117.06	125.7	8.64	2
					55.1819	-	55.1083				25.9330
213	2007	222	4:22:58 PM	-78.3982	2	78.7855	7	150.83	174.4	23.57	7
					55.1003	-	54.9572				48.1041
214	2007	222	6:40:37 PM	-78.8313	8	79.5435	1	135.12	146.91	11.79	7
					54.9472	-	54.7668				
215	2007	222	7:51:38 PM	-79.5909	6	79.9661	5	110.98	119.58	8.6	31.2875
					54.6757	-	54.6739				0.20036
216	2007	222	10:05:02 PM	-79.9533	3	79.9538	5	62.01	78.16	16.15	3
					54.6746	-	54.6743				0.70476
217	2007	222	10:24:44 PM	-79.9527	3	79.9418	9	54.19	63.05	8.86	5
					54.6753	-					
218	2007	222	10:50:21 PM	-79.9421	8	79.9515	54.6756	53.67	60.44	6.77	0.60526
					54.6758	-					0.12085
219	2007	222	10:53:30 PM	-79.9553	1	79.9565	54.675	44.29	45.33	1.04	2
					54.6742	-	54.6734				0.08006
220	2007	222	11:27:03 PM	-79.9536	1	79.9535	9	62.53	83.37	20.84	3
							-	54.6792			0.75357
221	2007	222	11:46:58 PM	-79.9658	54.6798	79.9775	8	58.88	65.65	6.77	8

222	2007	222	11:55:04 PM	-79.9838	54.67966	-80.007	54.68261	66.17	72.95	6.78	1.526711
223	2007	226	2:57:27 AM	-91.5946	57.65822	-91.5977	57.65759	67.74	71.91	4.17	0.201301
224	2007	217	7:05:55 PM	-78.4319	59.99431	-78.4346	60.01183	87.02	91.18	4.16	1.953603
225	2007	217	7:11:37 PM	-78.4349	60.01501	-78.4378	60.01996	90.14	101.08	10.94	0.574872
226	2007	217	7:18:37 PM	-78.4318	60.01999	-78.4329	60.01611	87.02	91.71	4.69	0.434722
227	2007	217	7:24:50 PM	-78.4314	60.00837	-78.4241	60.00035	88.06	92.75	4.69	0.97819
228	2007	217	7:48:59 PM	-78.4562	60.01759	-78.4564	60.01227	87.54	93.79	6.25	0.598797
229	2007	217	7:52:08 PM	-78.4478	60.00991	-78.4331	60.00871	90.66	100.04	9.38	0.827275
230	2007	217	7:57:38 PM	-78.4141	60.00687	-78.4138	60.00702	85.19	91.44	6.25	0.02568
231	2007	217	8:16:48 PM	-78.4329	60.00947	-78.453	60.00965	91.44	100.04	8.6	1.115212
232	2007	217	8:39:12 PM	-78.459	60.01784	-78.4345	59.98851	92.23	95.35	3.12	3.533988
233	2007	217	9:03:55 PM	-78.4373	60.00169	-78.4425	60.01786	88.58	94.31	5.73	1.820584
234	2007	217	9:20:13 PM	-78.4656	60.01698	-78.4497	60.00049	90.66	95.87	5.21	2.036407
235	2007	218	11:29:20 AM	-78.6553	58.31666	-78.6615	58.31525	86.76	90.66	3.9	0.39433
236	2007	218	6:09:07 PM	-79.8046	58.03049	-79.8377	58.02115	142.85	149.4	6.55	2.208304
237	2007	218	8:19:56 PM	-79.8741	58.00348	-79.8781	58.00128	143.52	145.6	2.08	0.342619

238		2007	218	9:41:09 PM	-79.8683	57.98831	-79.8696	57.98546	142.48	146.12	3.64	0.326581
239		2007	218	10:25:07 PM	-79.836	58.02508	-79.8361	58.02056	141.41	150.05	8.64	0.502854
240		2007	218	11:59:42 PM	-79.8886	57.92538	-79.9434	57.78979	173.64	180.97	7.33	15.42245
241		2007	219		-79.9943	57.69801	-80.0124	57.66477	151.68	155.86	4.18	3.850665
242		2007	219	2:19:35 AM	-80.1236	57.41155	-80.1309	57.39018	52.37	57.06	4.69	2.416225
243		2007	219	2:56:09 AM	-80.1463	57.3437	-80.149	57.33559	51.58	55.49	3.91	0.915739
244		2007	219	7:12:50 AM	-79.5303	56.95908	-79.4651	56.91886	91.44	97.7	6.26	5.970691
245		2010	202	7:46:47 AM	-91.8423	59.60929	-91.8313	59.61218	131.26	135.28	4.02	0.698326
246		2010	204	12:55:05 PM	-91.853	57.40685	-91.7605	57.43706	44.23	54.36	10.13	6.473342
247		2010	208	11:42:44 AM	-91.9194	57.43437	-91.8034	57.46579	39.43	50.09	10.66	7.767911
248		2010	209	5:05:10 AM	-88.5536	57.65654	-88.552	57.65695	74.08	77.31	3.23	0.105751
249		2010	209	6:41:12 AM	-88.7364	57.43375	-88.7568	57.40398	68.45	74.89	6.44	3.527592
250		2010	210	1:06:49 AM	-85.2595	55.69055	-84.7042	56.01616	42.1	50.63	8.53	50.11676
251	78HudsonBay		209	1978-07-27T01:46	-88.8939	62.83044	-88.933	62.83021	210		6	1.983521
252	78HudsonBay		209	1978-07-27T02:16	-89.132	62.83136	-89.1724	62.832			10	2.052134
253	78HudsonBay		209	1978-07-27T10:07	-89.4675	62.66969	-89.2282	62.66979	205		7	12.21667

254	78HudsonBay	209	1978-07-27T13:52	-89.557	62.33537	-89.617	62.30166	180	5	4.862477
255	78HudsonBay	209	1978-07-27T14:58	-89.7935	62.18268	-89.8375	62.15281	170	4	4.030038
256	78HudsonBay	213	1978-08-02T16:22	-93.5843	60.71413	-93.491	60.71478	110	8	5.075322
257	78HudsonBay	213	1978-08-02T17:00	-93.351	60.71576	-93.2883	60.71558	120	4	3.412344
258	78HudsonBay	213	1978-08-02T17:52	-93.1626	60.71498	-93.037	60.71438	130	5	6.835825
259	78HudsonBay	214	1978-08-03T00:22	-91.7162	61.4163	91.6233	61.48175	155	3	8.795608
260	78HudsonBay	214	1978-08-03T01:13	-91.6148	61.4877	91.5172	61.55233	160	4	8.857093
261	78HudsonBay	214	1978-08-03T1:43	-91.4974	61.56533	91.4876	61.57183	160	6	0.891493
262	78HudsonBay	214	1978-08-03T01:15	-91.4679	61.58483	-91.458	61.59133	160	4	0.891023
263	78HudsonBay	214	1978-08-03T01:52	-91.4383	61.6043	91.4186	61.61733	165	5	1.782435
264	78HudsonBay	214	1978-08-03T02:10	-91.4087	61.62393	91.3596	61.65744	163	4	4.539616
265	78HudsonBay	214	1978-08-03T12:54	-90.0838	63.00583	90.0667	63.00587	140	3	0.866053
266	78HudsonBay	214	1978-08-03T12:57	-90.0495	63.00592	90.0323	63.00596	145	5	0.866449
267	78HudsonBay	214	1978-08-03T13:00	-90.0152	63.006	89.9981	63.00695	150	5	0.869075
268	77HudsonBay	213	1977-08-01T11:54	-89.9434	63.07927	89.9067	63.07922	130	3	1.848301
269	77HudsonBay	213	1977-08-01T15:57	-88.5082	63.07782	88.3518	63.07652	140	3	7.873532

270	77HudsonBay	217	1977-08-04T03:14	-88.9983	59.31121	-88.9991	59.28423	125	4	3.000556
271	77HudsonBay	219	1977-08-06T09:36	-85.8693	60.24451	-85.8193	60.24454	200	7	2.759467
272	77HudsonBay	219	1977-08-06T22:46	-80.9934	60.29132	-80.9383	60.29199	140	5	3.036013
273	77HudsonBay	220	1977-08-07T00:22	-80.7189	60.2907	-80.6307	60.28343	155	5	4.924819
274	77HudsonBay	220	1977-08-07T02:28	-80.0375	60.25375	-79.9218	60.25048	175	8	6.392612
275	77HudsonBay	220	1977-08-07T03:01	-79.8392	60.24815	-79.8226	60.24781	171	4	0.913077
276	77HudsonBay	220	1977-08-07T04:30	-79.345	60.24618	-79.2942	60.24613	149.6	5	2.801437
277	77HudsonBay	220	1977-08-07T06:00	-78.8703	60.24685	-78.7662	60.24688	116	12	5.741692
278	77HudsonBay	220	1977-08-07T06:33	-78.6245	60.24654	-78.6068	60.24652	110	6	0.977571
279	77HudsonBay	220	1977-08-07T06:42	-78.5891	60.24646	-78.5714	60.24642	90	10	0.977185
280	77HudsonBay	220	1977-08-07T06:51	-78.536	60.24633	-78.5183	60.24629	90	10	0.977578
281	77HudsonBay	220	1977-08-07T06:57	-78.5006	60.24625	-78.4829	60.24621	100	10	0.977194
282	77HudsonBay	220	1977-08-07T07:03	-78.4449	60.24642	-78.4044	60.24692	80	7	2.236681
283	77HudsonBay	220	1977-08-07T07:21	-78.3639	60.24742	-78.2828	60.24842	70	7	4.473576
284	77HudsonBay	220	1977-08-07T13:52	-80.1383	60.49183	-80.2134	60.49109	158	5	4.111707
285	77HudsonBay	220	1977-08-07T19:33	-82.2178	60.49771	-82.2357	60.49765	150	5	0.983109

286	77HudsonBay	222	1977-08-09T05:59	-93.7311	60.58035	-93.6622	60.58125	100	4	3.762905
287	77HudsonBay	222	1977-08-09T07:35	-93.1165	60.58457	-93.0287	60.58703	130	5	4.802863
288	77HudsonBay	223	1977-08-10T19:24	-80.437	60.5805	-79.8228	60.58154	150	7	33.54673
289	77HudsonBay	223	1977-08-10T23:03	-79.0035	60.58122	-78.8203	60.58181	120	4	10.00888
290	77HudsonBay	224	1977-08-11T00:06	-78.6737	60.58228	-78.5367	60.58141	140	13	7.482741
291	77HudsonBay	224	1977-08-11T00:59	-78.4097	60.60433	-78.4126	60.64433	70	5	4.450867
292	77HudsonBay	224	1977-08-11T01:45	-78.59	60.64754	-78.6449	60.64771	120	8	2.995788
293	77HudsonBay	224	1977-08-11T06:00	-79.693	60.828	-79.9686	60.83363	120	8	14.9508
294	77HudsonBay	224	1977-08-11T07:20	-80.0053	60.83387	-80.2616	60.83542	130	4	13.89263
295	77HudsonBay	226	1977-08-13T08:4	-90.8445	61.08056	-90.8092	61.08059	122	3	1.896579
296	77HudsonBay	226	1977-08-13T20:39	-86.7373	61.07567	-86.6462	61.077	200	5	4.901214
297	77HudsonBay	227	1977-08-14T18:30	-78.8156	61.07901	-78.7982	61.07925	80	5	0.932931
298	77HudsonBay	227	1977-08-14T19:03	-78.6071	61.08194	-78.3585	61.08517	80	3	13.37194
299	77HudsonBay	227	1977-08-14T20:06	-78.2359	61.08708	-78.1683	61.08858	85	10	3.638179
300	77HudsonBay	227	1977-08-14T20:21	-78.157	61.09187	-78.1568	61.11015	85	15	2.02721
301	77HudsonBay	227	1977-08-14T20:33	-78.1567	61.12832	-78.1565	61.14655	85	10	2.0271

302	77HudsonBay	227	1977-08-14T20:45	-78.1564	61.16477	-78.1563	61.17389	80		7	1.014216
303	77HudsonBay	227	1977-08-14T21:03	-78.1561	61.20122	-78.1568	61.21833	80		10	1.902805
304	77HudsonBay	231	1977-08-18T09:09	-78.4805	61.41068	-78.4621	61.41095	80		10	0.981495
305	77HudsonBay	231	1977-08-18T09:18	-78.4252	61.41135	-78.4068	61.41158	70		6	0.981124
306	77HudsonBay	231	1977-08-18T21:53	-82.0539	61.66504	-82.4713	61.66311	200		8	22.03301
307	77HudsonBay	239	1977-08-27T23:02	-79.6217	58.79834	-79.4785	58.79957	147		4	8.251074
308	78HudsonBay	218	1978-08-07T06:44	-88.6827	63.33771	-88.5809	63.33717	180		5	5.079478
309	78HudsonBay	226	1978-08-15T15:20	-80.0389	55.34402	-80.0303	55.33612	100		4	1.034465
310	78HudsonBay	226	1978-08-15T21:12	-79.9993	54.93577	-80.0013	54.9205	110		5	1.702338
311	78HudsonBay	227	1978-08-16T11:08	-80.1252	55.08013	-80.0106	55.0824	120		10	7.297707
312	2010	191	3:00:48	-80.1788	63.05364	-80.2015	62.95934	286.56	288.57	2.01	10.54802
313	2010	191	5:09:53	-80.1768	62.94855	-80.1669	62.94418	282.47	283.75	1.28	0.699898
314	2010	191	5:30:37	-80.0563	62.89452	-80.0321	62.88422	297.33	301.12	3.79	1.677893
315	2010	191	6:45:14	-79.8315	62.79697	-79.3035	62.70231	330.64	337.25	6.61	28.86714
316	2010	191	7:50:03	-79.1407	62.72893	-79.1077	62.73003	369.89	374.17	4.28	1.682389
317	2010	191	8:42:12	-79.435	62.67464	-79.4508	62.66276	330.37	336.81	6.44	1.547959

318	2010	191	10:37:45	-79.4954	62.64989	-79.5212	62.64569	322.32	324.47	2.15	1.398242
319	2010	191	13:07:05	-79.4431	62.53903	-79.3547	62.49214	166.87	178.8	11.93	6.911675
320	2010	191	13:24:52	-79.3402	62.48404	-79.1937	62.40179	154.94	169.85	14.91	11.84944
321	2010	191	14:52:00	-78.8113	62.17914	-78.7769	62.15919	178.8	187	8.2	2.849641
322	2010	191	19:36:16	-78.8272	61.61607	-78.8988	61.38018	133.78	139.32	5.54	26.50338
323	2010	191	21:33:17	-78.9481	61.19887	-78.9531	61.18221	120.27	123.63	3.36	1.872611
324	2010	191	22:04:26	-78.9782	61.09787	-79.0097	60.98334	119.08	124.14	5.06	12.84756
325	2010	191	22:36:03	-79.0109	60.97907	-79.0244	60.92955	119.44	123.78	4.34	5.554743
326	2010	191	23:47:17	-79.0438	60.69172	-79.0295	60.67687	130.95	132.65	1.7	1.825486
327	2010	191	23:57:39	-79.003	60.64878	-78.9465	60.59045	121.86	125.84	3.98	7.179603
328	2010	192	0:22:10	-78.9368	60.57986	-78.9002	60.53698	116.18	120.16	3.98	5.171652
329	2010	192	1:10:22	-78.8043	60.42567	-78.8198	60.42961	119.02	125.27	6.25	0.959979
330	78HudsonBay	240	1978-08-29T03:37	-87.8334	57.32843	-87.864	57.32823	100		5	1.836921
331	78HudsonBay	244	1978-09-02T07:18	-81.1928	56.99988	-81.1626	56.99895	240		10	429.0935
332	78HudsonBay	246	1978-09-04T21:40	-80.7302	56.53389	-80.7144	56.53391				0.971091
333	78HudsonBay	246	1978-09-04T22:01	-80.6193	56.53397	-80.6039	56.53389				0.946357

334	78HudsonBay	246	1978-09-04T22:34	-80.4491	56.53305	-80.4336	56.53297	0.948036
335	78HudsonBay	247	1978-09-05T02:46	-80.7558	56.74963	-80.8331	56.74967	4.712828
336	78HudsonBay	247	1978-09-05T08:47	-81.1522	57.01969	-80.9092	57.08286	16.28843
337	78HudsonBay	247	1978-09-05T15:14	-80.0823	57.58065	-80.0976	57.58076	0.909597
338	78HudsonBay	248	1978-09-06T11:06	-80.0842	57.66507	-79.9688	57.71975	9.165305
339	78HudsonBay	248	1978-09-06T11:54	-79.9601	57.73913	-79.9572	57.74555	0.737049
340	78HudsonBay	248	1978-09-06T12:03	-79.9503	57.75976	-79.9463	57.76752	0.895302
341	78HudsonBay	248	1978-09-06T12:12	-79.9382	57.78303	-79.9302	57.79855	1.789696
342	78HudsonBay	248	1978-09-06T12:30	-79.9141	57.82958	-79.9101	57.83734	0.894774
343	78HudsonBay	248	1978-09-06T12:45	-79.894	57.86837	-79.8704	57.91373	5.233118
344	78HudsonBay	248	1978-09-06T13:24	-79.8463	57.95967	-79.836	57.97935	2.271059
345	78HudsonBay	248	1978-09-06T15:03	-80.2703	58.00135	-80.2856	58.00137	0.901864
346	78HudsonBay	249	1978-09-07T04:13	-80.5862	58.13515	-80.1954	58.18813	23.66861
347	78HudsonBay	249	1978-09-07T05:22	-80.177	58.19041	-80.1403	58.19498	2.210827
348	78HudsonBay	249	1978-09-07T07:04	-79.5851	58.26723	-79.5136	58.27643	4.307487
349	78HudsonBay	249	1978-09-07T10:10	-78.4783	58.39421	-78.4421	58.39651	2.122389

350	78HudsonBay	249	1978-09-07T15:28	-78.9565	58.41357	-79.0478	58.41374	5.320206
351	78HudsonBay	249	1978-09-07T18:31	-79.7656	58.41527	-79.8313	58.41629	3.829572
352	78HudsonBay	249	1978-09-07T19:28	-80.0121	58.41689	-80.0249	58.41687	0.746888
353	78HudsonBay	251	1978-09-09T03:26	-89.9979	58.16709	-90.0138	58.16727	0.931504
354	78HudsonBay	252	1978-09-10T18:00	-90.3627	58.74853	-90.3477	58.74863	0.864046
355	78HudsonBay	253	1978-09-11T15:31	-88.5803	57.99872	-88.5672	57.99871	0.769698
356	78HudsonBay	254	1978-09-12T00:28	-85.9526	57.99621	-85.9369	57.99627	0.923938
357	78HudsonBay	254	1978-09-12T18:59	-80.5874	58.15067	-80.573	58.15147	0.849434
358	78HudsonBay	254	1978-09-12T19:32	-80.4261	58.15847	-80.3674	58.16127	3.460602
359	78HudsonBay	255	1978-09-13T00:12	-79.5473	58.39684	-79.5413	58.25967	15.25232
360	78HudsonBay	255	1978-09-13T01:24	-79.5402	58.56894	-79.5402	58.57639	0.828403
361	78HudsonBay	255	1978-09-13T02:06	-79.5398	58.67311	-79.5397	58.68051	0.822857
362	78HudsonBay	255	1978-09-13T02:18	-79.5395	58.70268	-79.5394	58.71008	0.822857
363	78HudsonBay	255	1978-09-13T02:27	-79.5393	58.72486	-79.5392	58.73225	0.821636
364	78HudsonBay	255	1978-09-13T02:54	-79.5385	58.79139	-79.5384	58.79877	0.820858
365	78HudsonBay	255	1978-09-13T3:00	-79.5383	58.80617	-79.5388	58.82942	2.585111

366	78HudsonBay	255	1978-09-13T03:42	-79.5407	58.91467	-79.541	58.93017	1.723523
367	78HudsonBay	255	1978-09-13T07:42	-79.3111	59.52893	-79.3074	59.53675	0.893811
368	78HudsonBay	255	1978-09-13T08:15	-79.2704	59.61479	-79.2667	59.62258	0.890939
369	78HudsonBay	255	1978-09-13T09:03	-79.2113	59.73979	-79.208	59.74792	0.922924
370	78HudsonBay	255	1978-09-13T09:33	-79.178	59.82104	-79.1747	59.82917	0.922911
371	78HudsonBay	255	1978-09-13T15:15	-78.8221	59.83421	-78.8054	59.83432	0.937118
372	78HudsonBay	255	1978-09-13T19:39	-78.992	59.67305	-79.0085	59.67291	0.922391
373	78HudsonBay	255	1978-09-13T19:45	-79.0249	59.67276	-79.0413	59.67262	0.9215
374	78HudsonBay	256	1978-09-14T02:07	-79.554	59.58467	-79.57	59.58467	0.898059
375	78HudsonBay	256	1978-09-14T02:40	-79.7295	59.58467	-79.7455	59.58467	0.898059
376	78HudsonBay	256	1978-09-14T06:01	-78.9051	59.75315	-78.8699	59.75305	1.972994
377	78HudsonBay	256	1978-09-14T06:22	-78.7818	59.75285	-78.7642	59.75275	0.986339
378	78HudsonBay	256	1978-09-14T06:31	-78.729	59.75265	-78.7113	59.75263	0.987183
379	78HudsonBay	256	1978-09-14T06:43	-78.6585	59.75245	-78.6409	59.75245	0.987193
380	78HudsonBay	256	1978-09-14T10:07	-79.1096	59.58475	-79.1257	59.58461	0.903691
381	78HudsonBay	256	1978-09-14T10:28	-79.2059	59.58413	-79.222	59.58403	0.903265

382	78HudsonBay	256	1978-09-14T11:02	-79.2577	59.53452	-79.2575	59.52905	0.608347
383	78HudsonBay	257	1978-09-15T00:35	-79.3259	59.16664	-79.3087	59.16652	0.978482
384	78HudsonBay	257	1978-09-15T13:30	-79.0994	59.08671	-79.114	59.08652	0.832703
385	78HudsonBay	257	1978-09-15T14:24	-79.3694	59.08417	-79.385	59.08408	0.886995
386	78HudsonBay	257	1978-09-15T20:19	-79.5296	58.91556	-79.4485	58.91627	4.655252
387	78HudsonBay	257	1978-09-15T22:12	-79.3248	58.83907	-79.457	58.83727	7.609167
388	78HudsonBay	257	1978-09-15T22:45	-79.5065	58.8365	-79.5396	58.83603	1.902528
389	78HudsonBay	258	1978-09-16T04:08	-79.4549	59.00332	-79.439	59.00338	0.910924
390	78HudsonBay	258	1978-09-16T04:20	-79.3913	59.00356	-79.3754	59.00361	0.910911
391	78HudsonBay	258	1978-09-16T05:56	-79.1362	59.13627	-79.1367	59.14469	0.936837
392	78HudsonBay	258	1978-09-16T06:44	-79.1324	59.27205	-79.1321	59.28054	0.944316
393	78HudsonBay	258	1978-09-16T07:14	-79.1301	59.354	-79.13	59.36186	0.873808
394	78HudsonBay	258	1978-09-16T14:52	-79.1218	60.48593	-79.1217	60.49296	0.781817
395	78HudsonBay	258	1978-09-16T15:19	-79.1211	60.54694	-79.121	60.55362	0.742694
396	78HudsonBay	258	1978-09-16T21:15	-78.537	61.19063	-78.2875	61.36307	23.35527
397	78HudsonBay	259	1978-09-17T07:44	-78.5287	61.58739	-78.5116	61.58694	0.904382

398	78HudsonBay	260	1978-09-18T02:15	-78.8752	62.00129	-78.8924	62.00122	0.89731
399	78HudsonBay	260	1978-09-18T04:30	-78.9402	62.08883	-78.9222	62.08898	0.93737 5
400	78HudsonBay	260	1978-09-18T07:57	-78.7709	62.16668	-78.789	62.16667	0.93975 1
401	78HudsonBay	260	1978-09-18T21:53	-79.0616	62.58774	-79.0773	62.58771	0.80655 4
402	78HudsonBay	261	1978-09-19T14:30	-79.6359	62.67142	-79.4681	62.67109	8.56616 2
403	78HudsonBay	262	1978:09-20T05:57	-79.6592	60.77376	-79.6932	60.77355	1.84342 6
404	78HudsonBay	262	1978:09-20T06:33	-79.8669	60.77238	-79.9016	60.77215	1.88620 6
405	78HudsonBay	262	1978:09-20T06:51	-79.9711	60.77168	-80.0058	60.77145	1.88667 5
406	78HudsonBay	262	1978-09-20T07:15	-80.1101	60.77116	-80.1623	60.77106	2.83266 7
407	78HudsonBay	267	1978-09-25T18:43	-91.1506	62.29673	-91.1415	62.30463	0.99721 9
408	78HudsonBay	267	1978-09-25T19:01	-91.0956	62.34423	-91.0859	62.35241	1.03872
409	78HudsonBay	269	1978-09-27T07:33	-88.4637	63.2613	-88.4594	63.26882	0.86348 3
410	78HudsonBay	269	1978-09-27T08:00	-88.4252	63.329	-88.353	63.44912	13.8314 3
411	78HudsonBay	269	1978-09-27T09:21	-88.2979	63.54493	-88.2934	63.5529	0.91298 1
412	78HudsonBay	270	1978-09-28T06:15	-88.2207	63.588	-88.2023	63.5881	0.91254
413	78HudsonBay	270	1978-09-28T10:47	-88.1857	63.5028	-88.4956	63.50428	15.3764 1

414	78HudsonBay	270	1978-09-28T17:33	-88.3296	63.41859	-88.3089	63.4186		1.026124

Appendix 2: Total Nitrogen vs Depth Plots

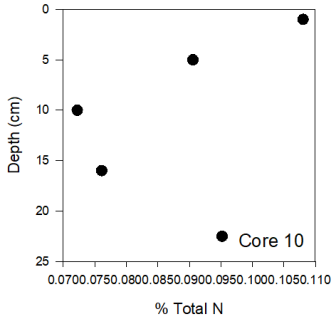

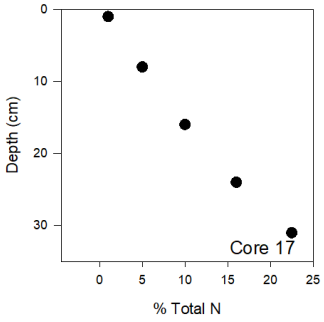

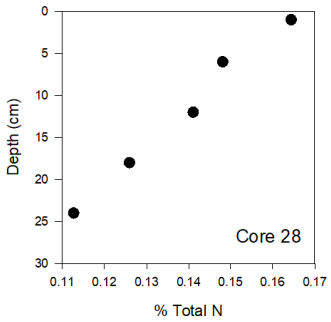

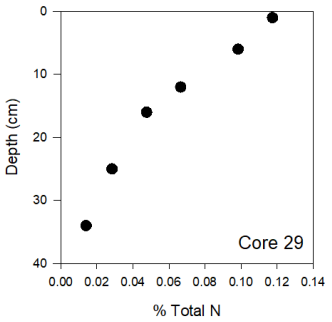

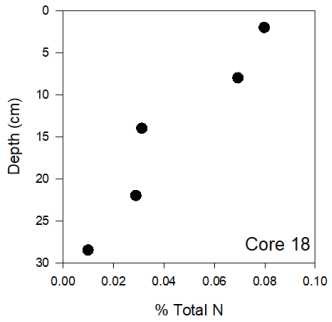

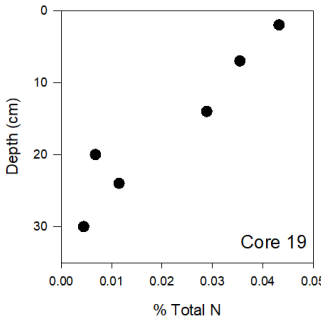

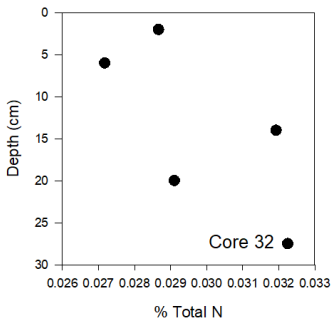

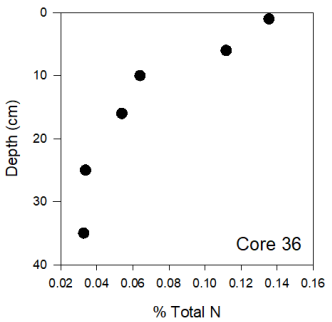

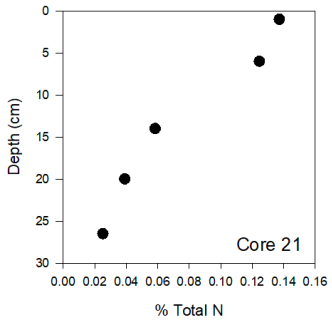

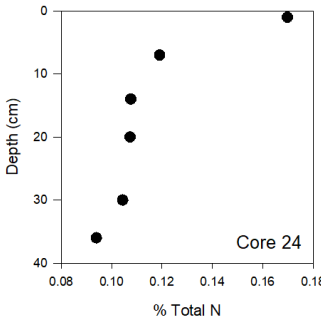

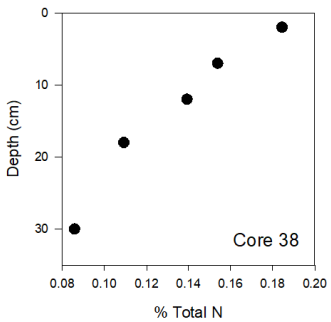

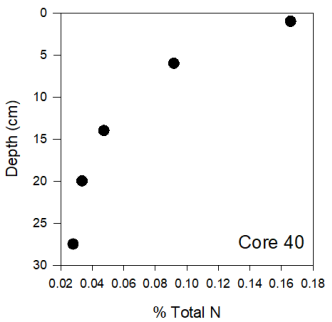

Appendix 3: Field Notes and Core Photographs

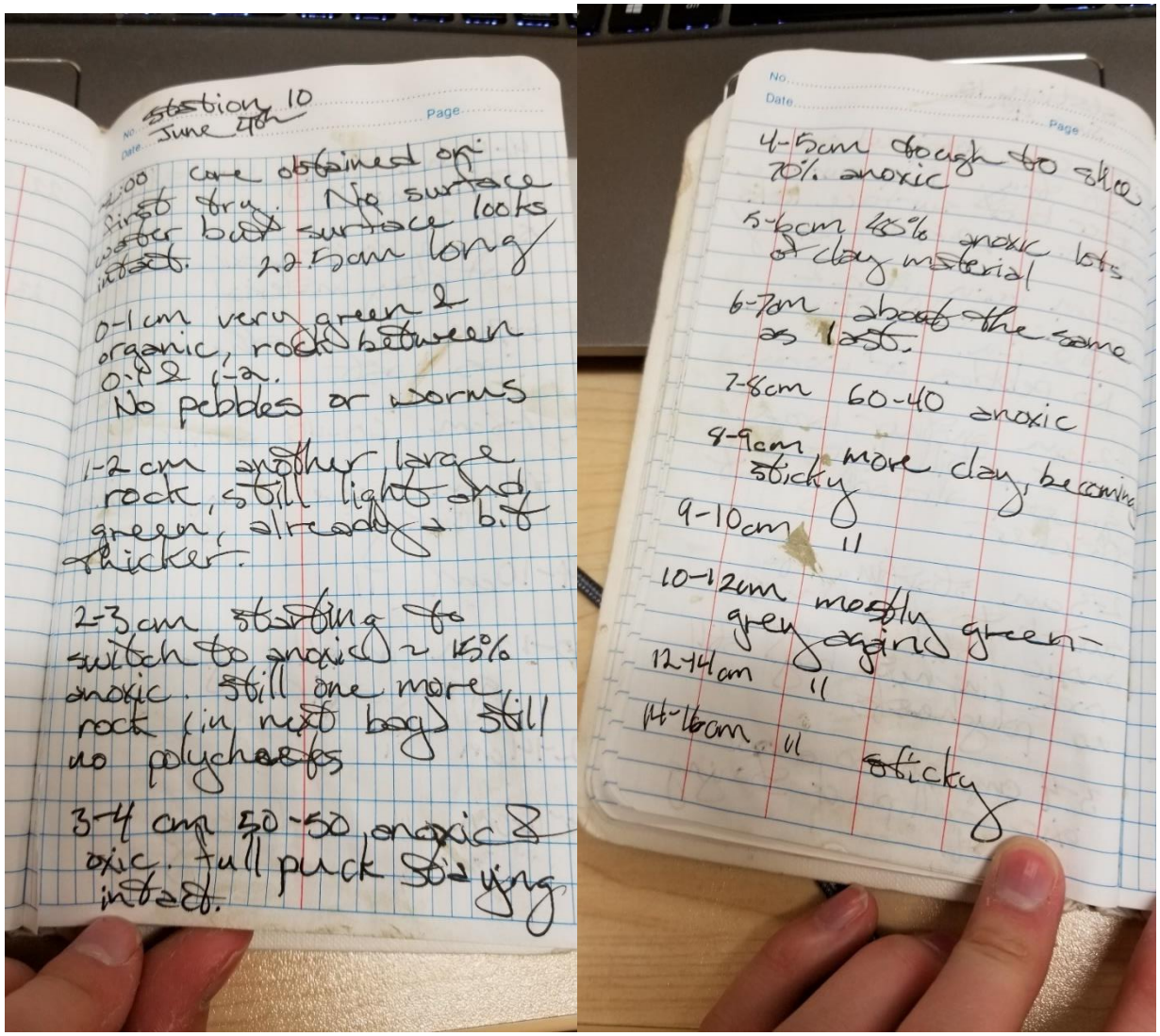
station 10
June 4th
12:00 core obtained on first try. No surface water but surface looks intact. 22.5cm long
0-1cm very green & organic, rock between 0.5 & 1cm.
No pebbles or worms
1-2cm another large rock, still light and green, already a bit thicker.
2-3cm starting to switch to anoxic ~ 15% anoxic. Still one more rock (in next bag) still no polychaetes
3-4cm 50-50 anoxic & oxic. Full puck starting instead.
4-5cm tough to slice 70% anoxic
5-6cm 45% anoxic lots of clay material
6-7cm about the same as last.
7-8cm 60-40 anoxic
8-9cm more clay, becoming sticky
9-10cm "
10-12cm mostly green-grey again
12-14cm "
14-16cm " sticky

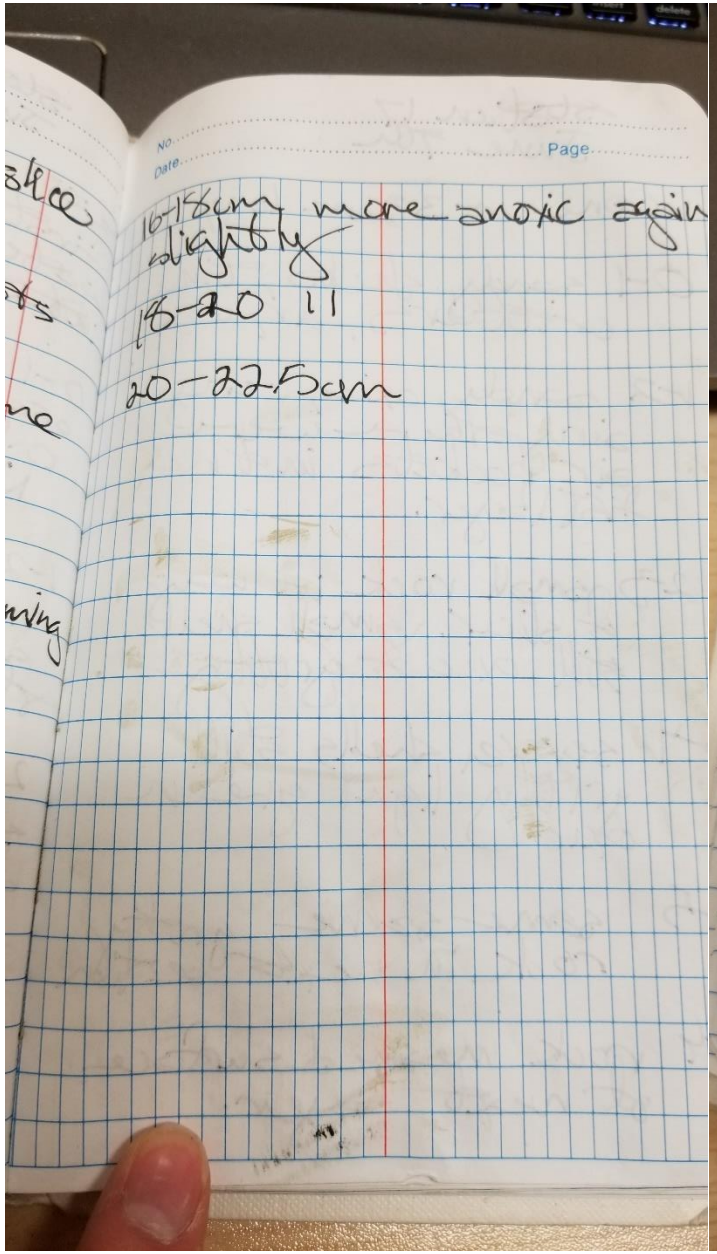

16-18cm more anoxic again slightly

18-20 ||

20-22.5cm

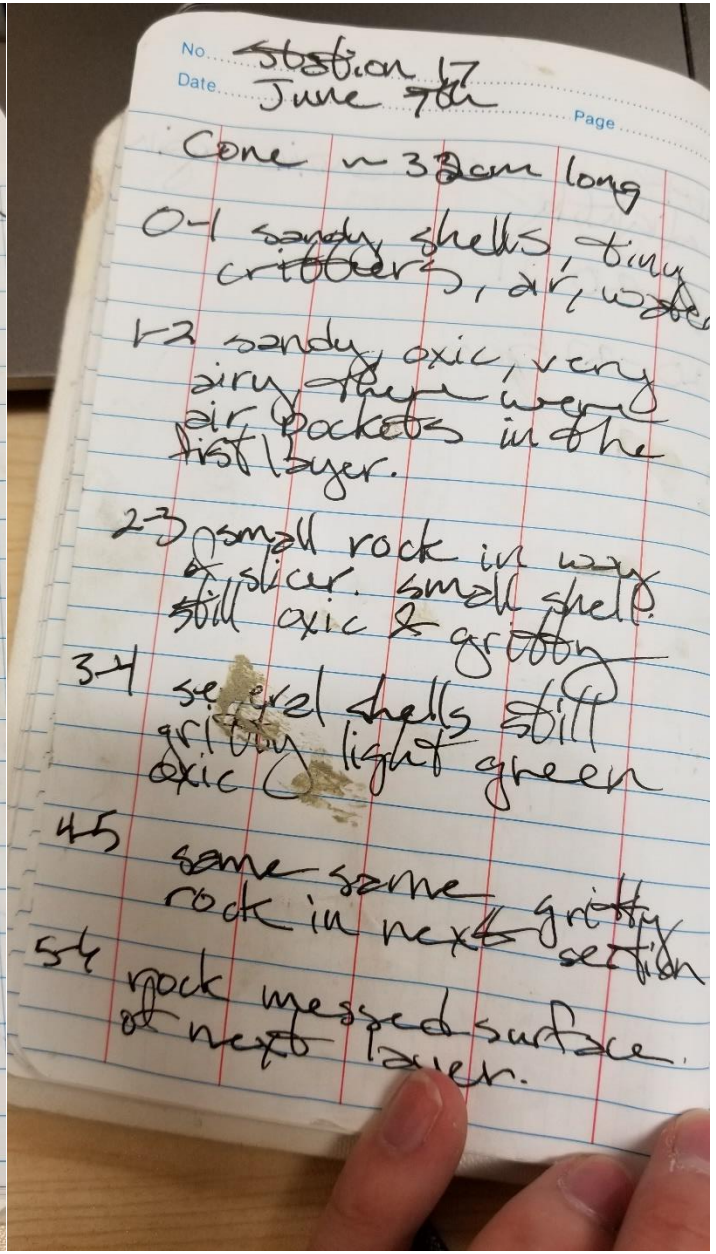

Station 17
June 7th

Cone ~ 32cm long

0-1 sandy shells, tiny critters, air, water

1-2 sandy oxic, very airy there were air pockets in the first layer.

2-3 small rock in way & slicer. small shell still oxic & gritty

3-4 several shells still gritty light green oxic

4-5 some some gritty rock in next section

5-4 rock messed surface of next layer.

still sandy sticking to slicer now.

6-7cm switch to 66% mud. still oxic

7-8 cm mostly mud, 1% anoxic 99% oxic 5% sand

8-9cm almost all mud now stickier still 97% oxic small patches of sand

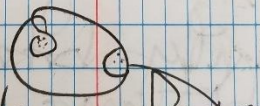

-air bubble of formally polychaete home

9-10cm ~~[illegible]~~ mud still a little gri through

10-12cm mud & sand 90% mud sand ~~[illegible]~~ spirsted throughout.

12-14cm still anoxic 20% - 25% sand

14-16cm 15% anoxic, mud stuck largely staying together.

16-18 almost all light green still light amounts of sand throughout core

18-20 slightly darker, likely a bit more anoxic. slow transition rather than clear layer

sand at bottom of layer.

Divided to the 2cm

sections do end because of changing layers.

20-22cm sandy on top muddy on bottom.

top 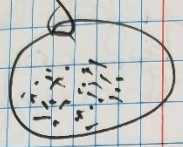 fairly sized grains. bdm

22-24cm slightly gritty mud all the way through still very oxic

24-26cm mostly mud. little bit of sand at bottom.

26-28cm

20% sand  little anoxic streak

27cm was sand

28-30cm mud slightly gritty. still mostly light green.

30-31 mud. slightly soupy might be due to box core draining through bottom.

Station 18
June 8th 2018
26.5cm

0-1cm large rock removed, in expense bare surface sandy mud, pebble rocks in wash of slicer. light green/brown.

1-2cm light green, slutty organics, gritty sandy mud.

2-3 same as last but stickier

3-4 slight anoxic streaks 10% shell, end of hole from big ass rock, puck nearly stays together

4-5 50% black 50% green start of black anox layer

5-6cm 60-70% black sticky mud still some grit but (less) slight smell(?)

6-7cm about the same as last. not so gritty significantly less sand than surface

7-8cm ~40% anoxic near end of anox? layer.

8-9cm base anoxic layer. patch of sand

0-10cm surface of slice is half mud half sand

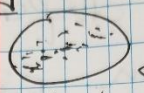

10-12 cm sand layer carried through to this layer.

12-14cm return to mostly mud

Start of another anoxic layer with some sand at 13cm

14-16 light green mud small grains of sand dispersed throughout tiny rock in bottom

16-18 same as last layer rode in the way of slicer. In this be

18-20cm looks yet the same. Light green grey dispersed sand.

20-22cm patch of anoxic at top. but otherwise still light grey green mud no anoxic smell or black streaks

22-24cm same as last two no anoxic

24-26cm small black streaks <5%

26-28.5cm slight black streaks 5%

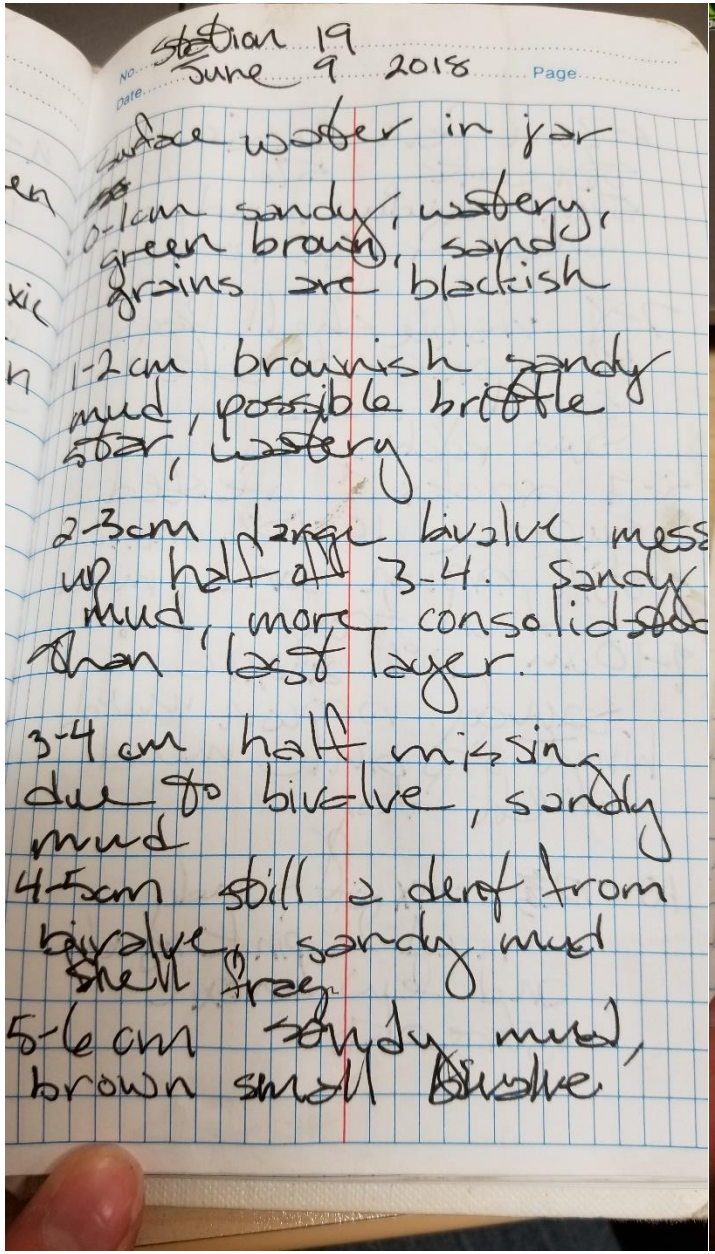
Station 19
June 9 2018
surface wobber in jar
0-1cm sandy, watery, green brown, sand grains are blackish
1-2cm brownish sandy mud, possible brittle star, watery
2-3cm large bivalve mess up half of 3-4. sandy mud, more consolidated than last layer.
3-4 cm half missing due to bivalve, sandy mud
4-5cm still a dent from bivalve, sandy mud shell frags
5-6 cm sandy mud, brown small bivalve

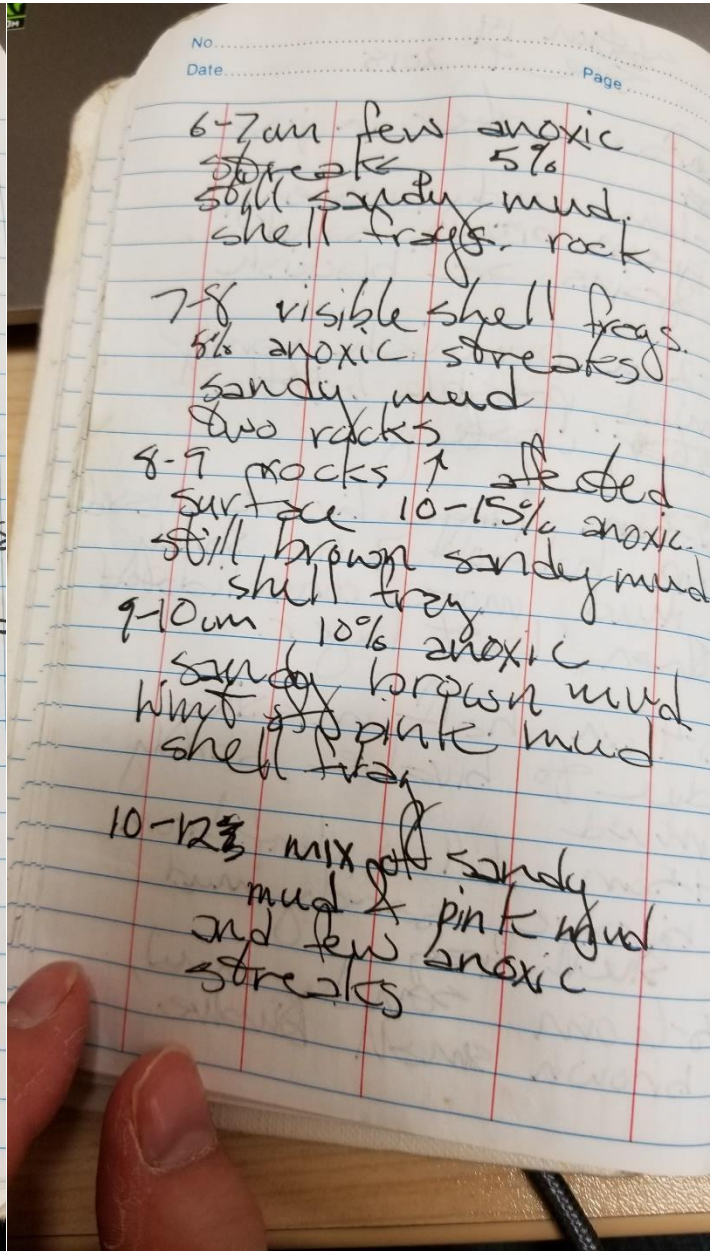
6-7cm few anoxic streaks 5%
still sandy mud. shell frags. rock
7-8 visible shell frags. 5% anoxic streaks sandy mud two rocks
8-9 rocks 1 affected surface 10-15% anoxic still brown sandy mud shell frag
9-10cm 10% anoxic sandy brown mud w/ pink mud shell frag
10-12cm mix of sandy mud & pink mud and few anoxic streaks

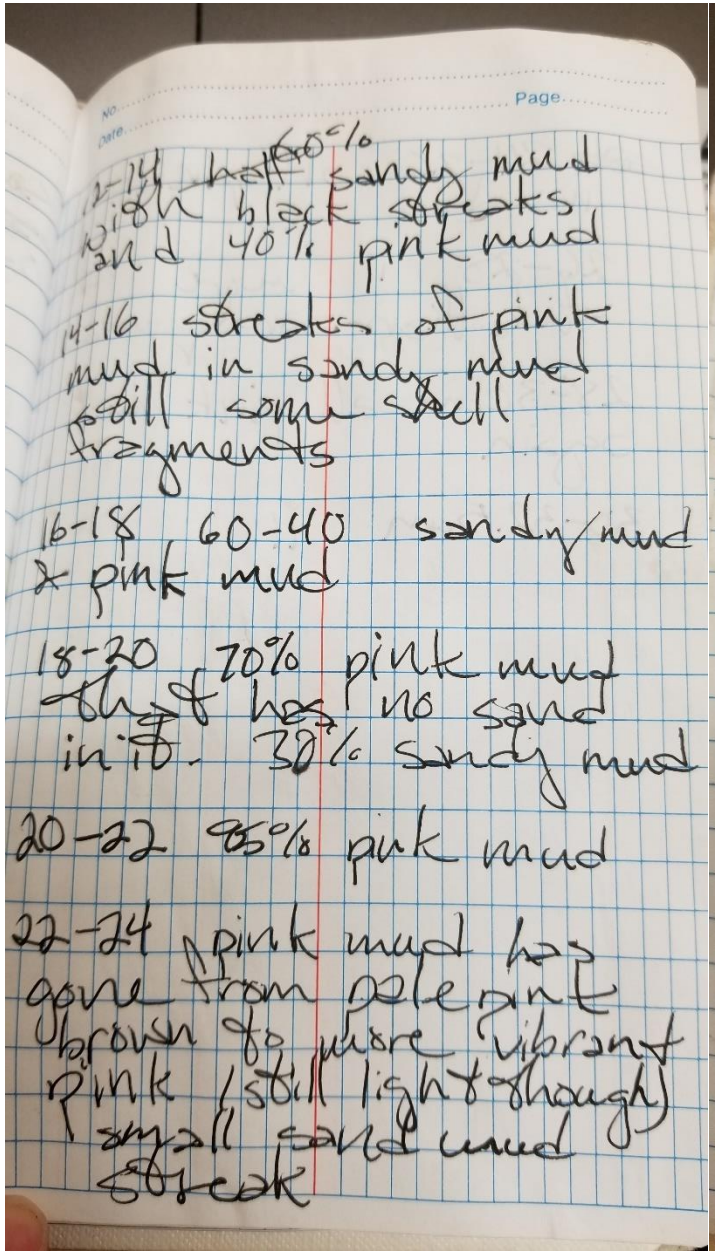

12-14 half 60% sandy mud with black streaks and 40% pink mud

14-16 streaks of pink mud in sandy mud still some shell fragments

16-18 60-40 sandy/mud & pink mud

18-20 70% pink mud that has no sand in it. 30% sandy mud

20-22 95% pink mud

22-24 pink mud has gone from pale pink brown to more vibrant pink / still light & though small sand mud streak

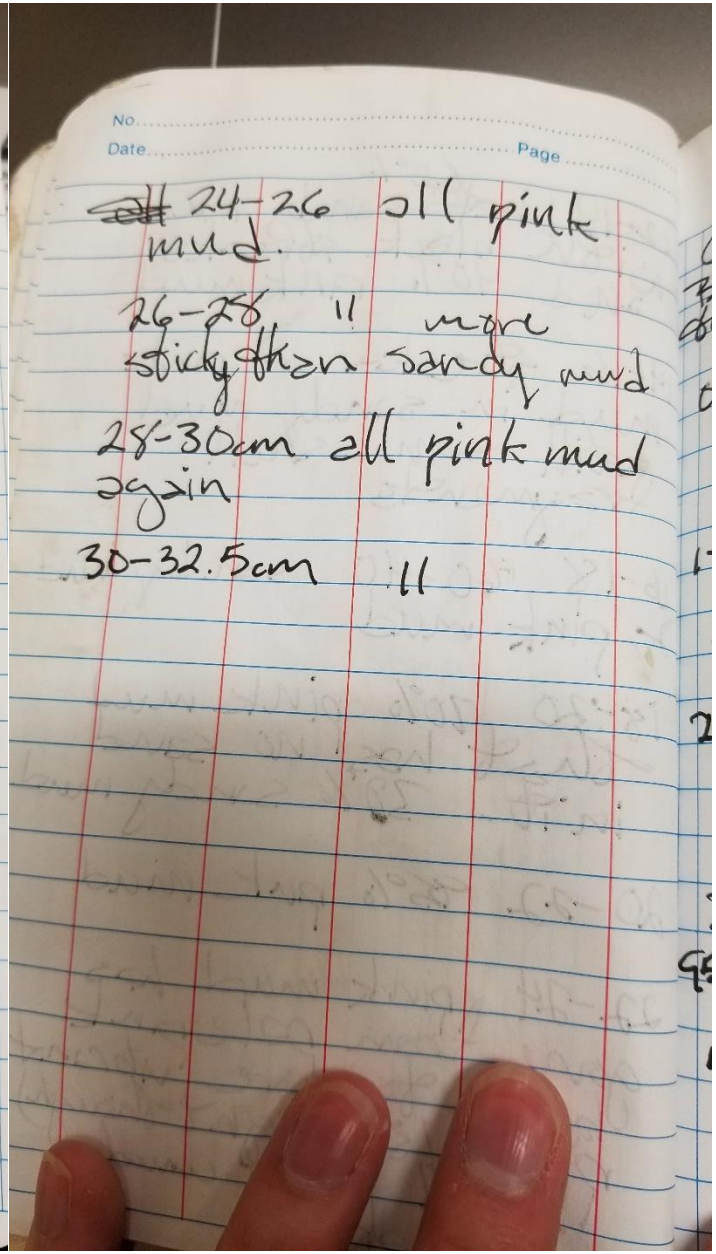

24-26 all pink mud.

26-28 " more sticky than sandy mud

28-30cm all pink mud again

30-32.5cm "

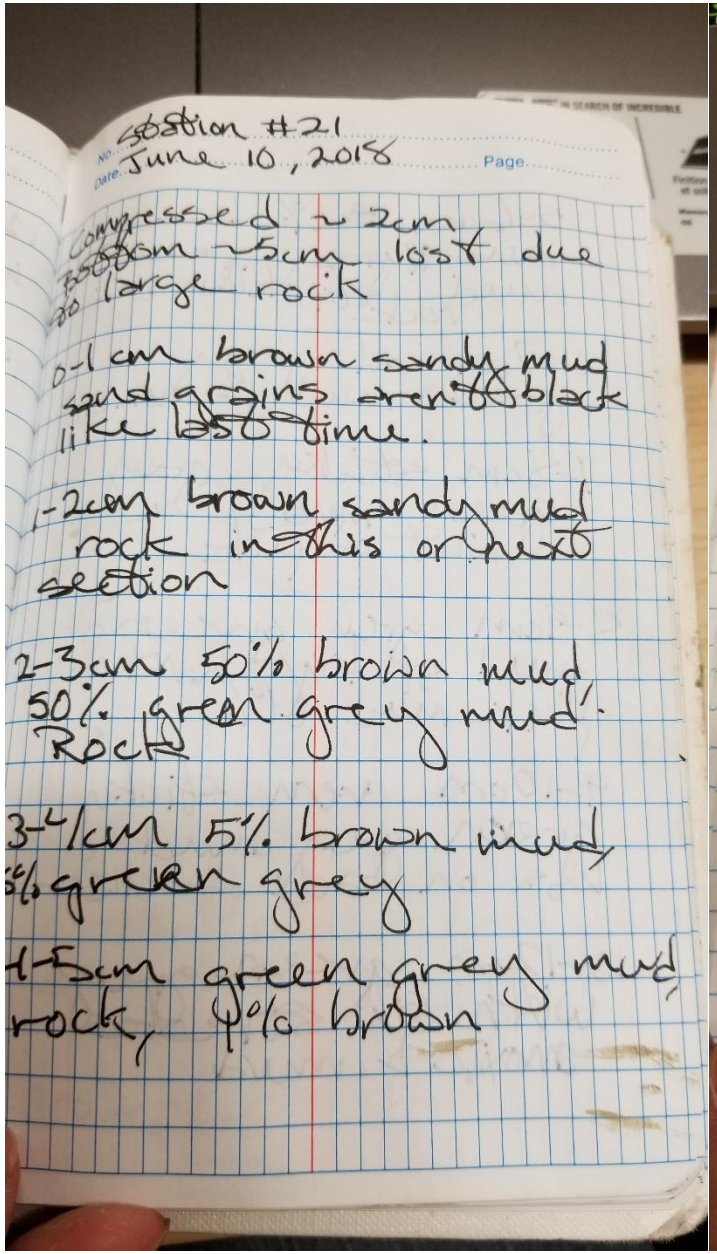

Station #21
Date June 10, 2018 Page

Compressed ~ 2cm
Bottom ~5cm lost due to large rock

0-1 cm brown sandy mud
sand grains are black
like last time.

1-2cm brown sandy mud
rock in this or next
section

2-3cm 50% brown mud
50% green grey mud
Rock

3-4cm 5% brown mud
5% green grey

4-5cm green grey mud
rock, 5% brown

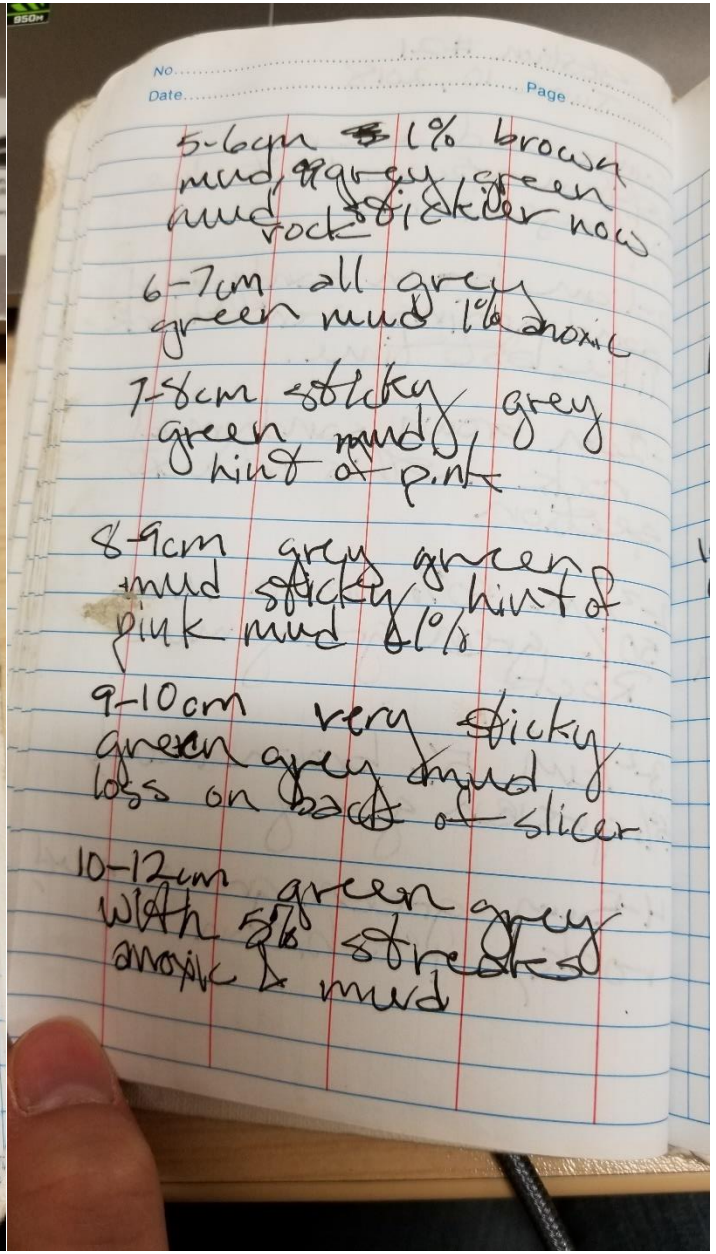

No.
Date Page

5-6cm 1% brown
mud, green grey
mud rock slicker now

6-7cm all grey
green mud 1% brown

7-8cm sticky grey
green mud
hint of pink

8-9cm grey green
mud sticky hint of
pink mud 1%

9-10cm very sticky
green grey mud
less on back of slicer

10-12cm green grey
with 5% streaks
brown mud

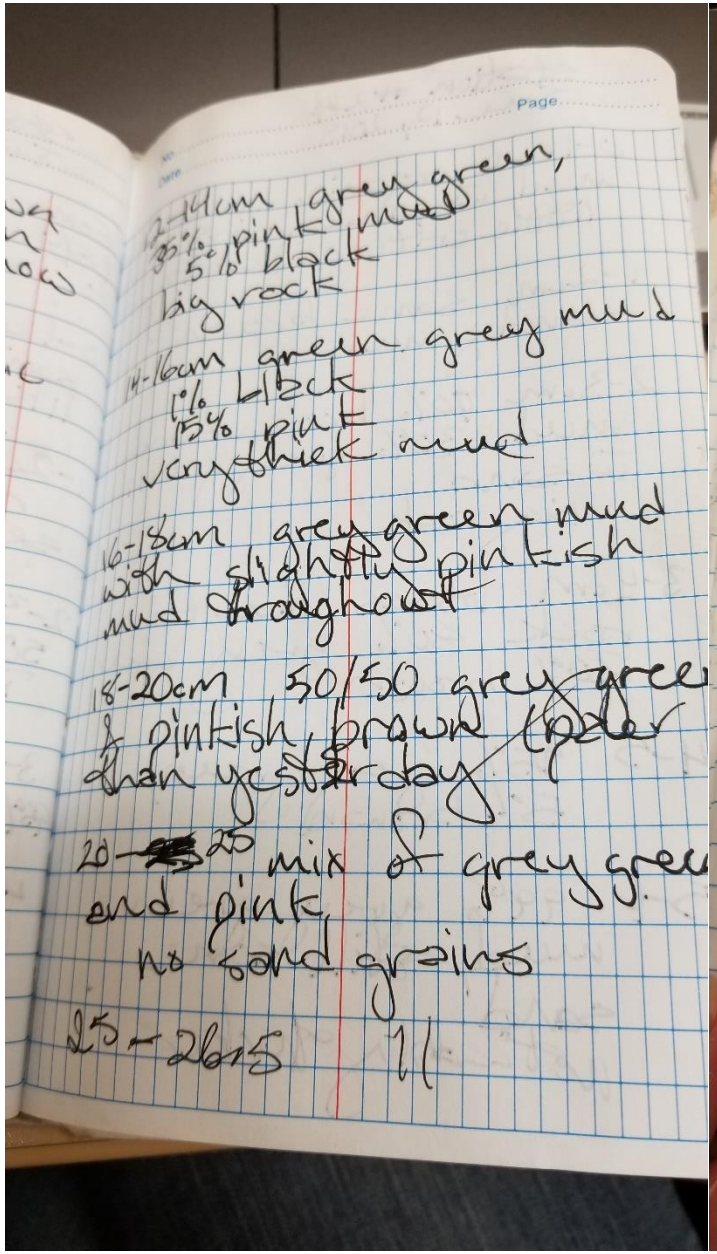

2-14cm grey green,
95% pink mud
5% black
big rock

14-16cm green grey mud
1% black
15% pink
very thick mud

16-18cm grey green mud
with slightly pinkish
mud throughout

18-20cm 50/50 grey green
& pinkish brown (softer
than yesterday)

20-25 mix of grey green
and pink
no sand grains

25-26.5 "

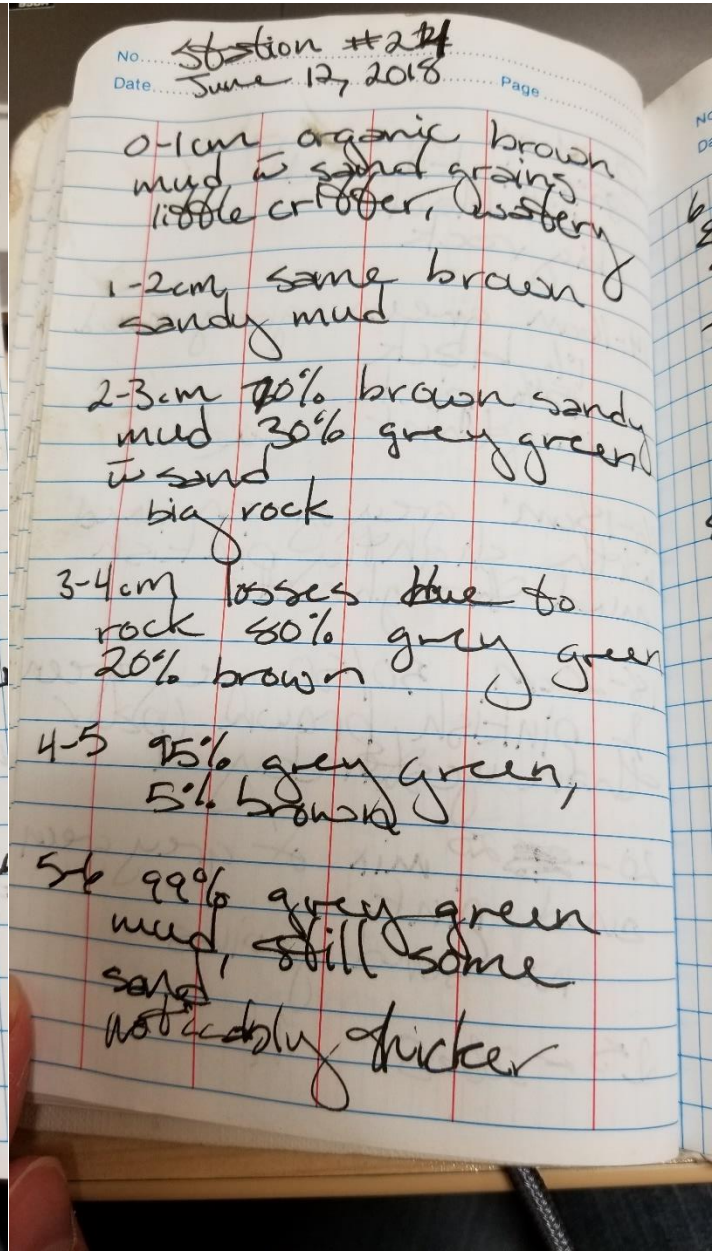

No. Station #24
Date June 17, 2018 Page

0-1cm organic brown
mud w sand grains
little critter, wiggly

1-2cm same brown
sandy mud

2-3cm 70% brown sandy
mud 30% grey green
w sand
big rock

3-4cm losses blue to
rock 80% grey green
20% brown

4-5 95% grey green,
5% brown

5+ 99% grey green
mud, still some
sand
noticably thicker

6-7 grey green mud. sticky some sand grains

7-8 very sticky grey green mud less sand. hint of brown mud

8-9 grey green mud w hint of brown some sand in streaks

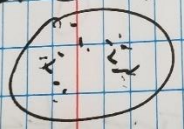

9-10cm same as 12-14 starting to stick together rather than to the slicer

10-12cm same as 12-14 hint of brown

12-14 same as 12-14

14-16 same grey green slightly sandy mud bit of kind of brown

16-18 same grey green slightly sandy mud

18-20 same grey green mud

20-25 streaks of slightly darker grey mud

25-30 all darker grey mud anoxic? no smell

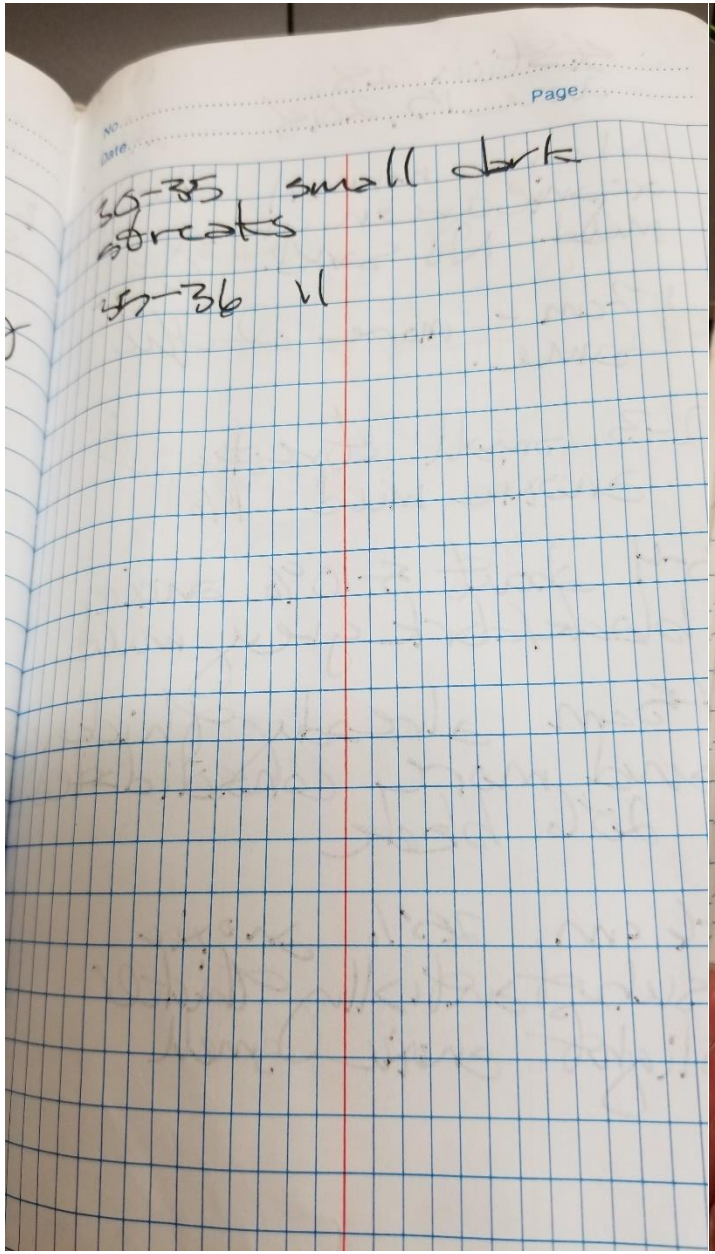

No. Page
Date

39-35 small dark
streaks

35-36 VL

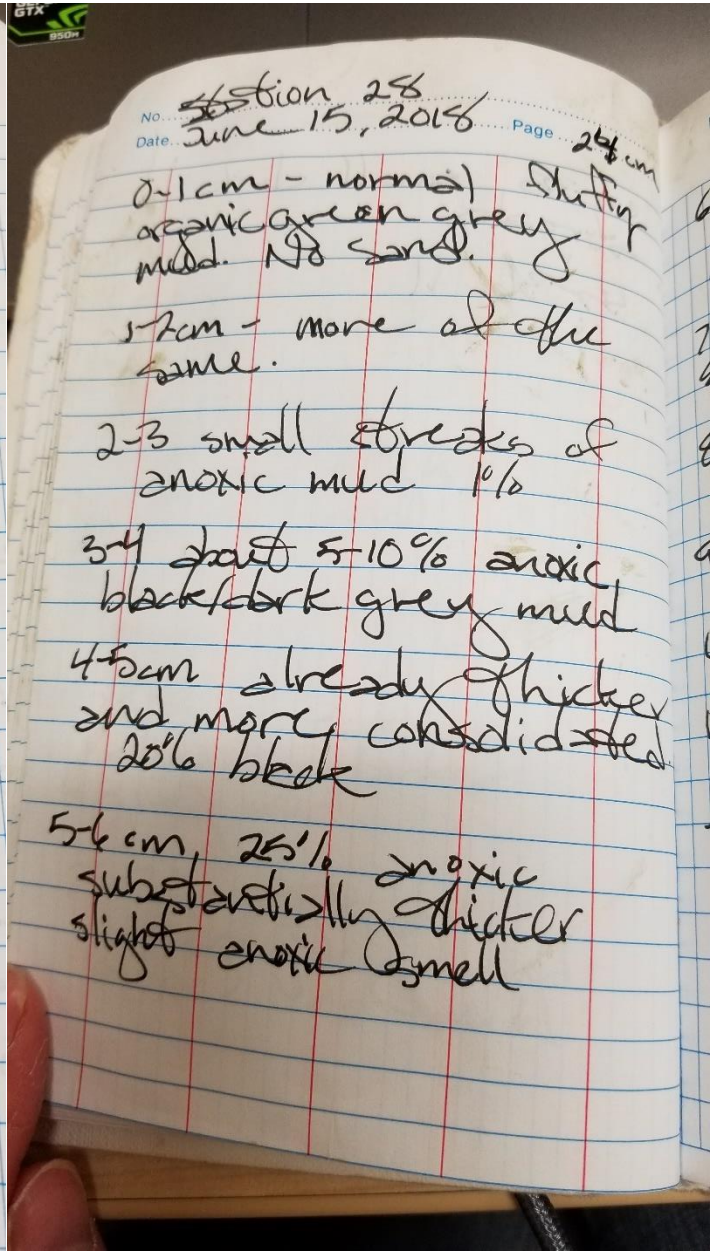

No. Section 28
Date June 15, 2016 Page 24 cm

0-1cm - normal fluffy
organic green grey
mud. No sand.

1-2cm - more of the
same.

2-3 small streaks of
anoxic mud 1%

3-4 about 5-10% anoxic
black/dark grey mud

4-5cm already thicker
and more consolidated
20% black

5-6 cm, 25% anoxic
substantially thicker
slight anoxic smell

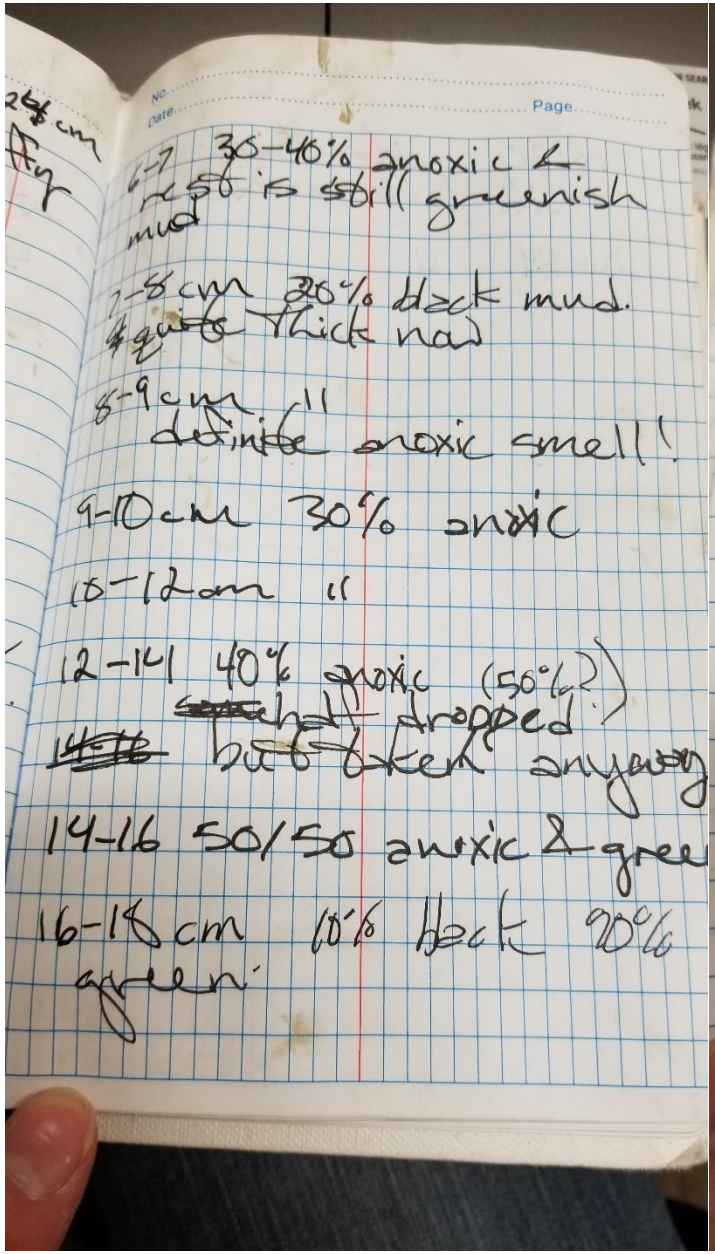

6-7 30-40% anoxic & rest is still greenish mud

7-8 cm 20% black mud. & quite thick mud

8-9 cm " definite anoxic smell!

9-10 cm 30% anoxic

10-12 cm "

12-14 40% anoxic (50%?) ~~sediment~~ half dropped ~~but~~ but taken anyway

14-16 50/50 anoxic & gree

16-18 cm 10% black 90% green

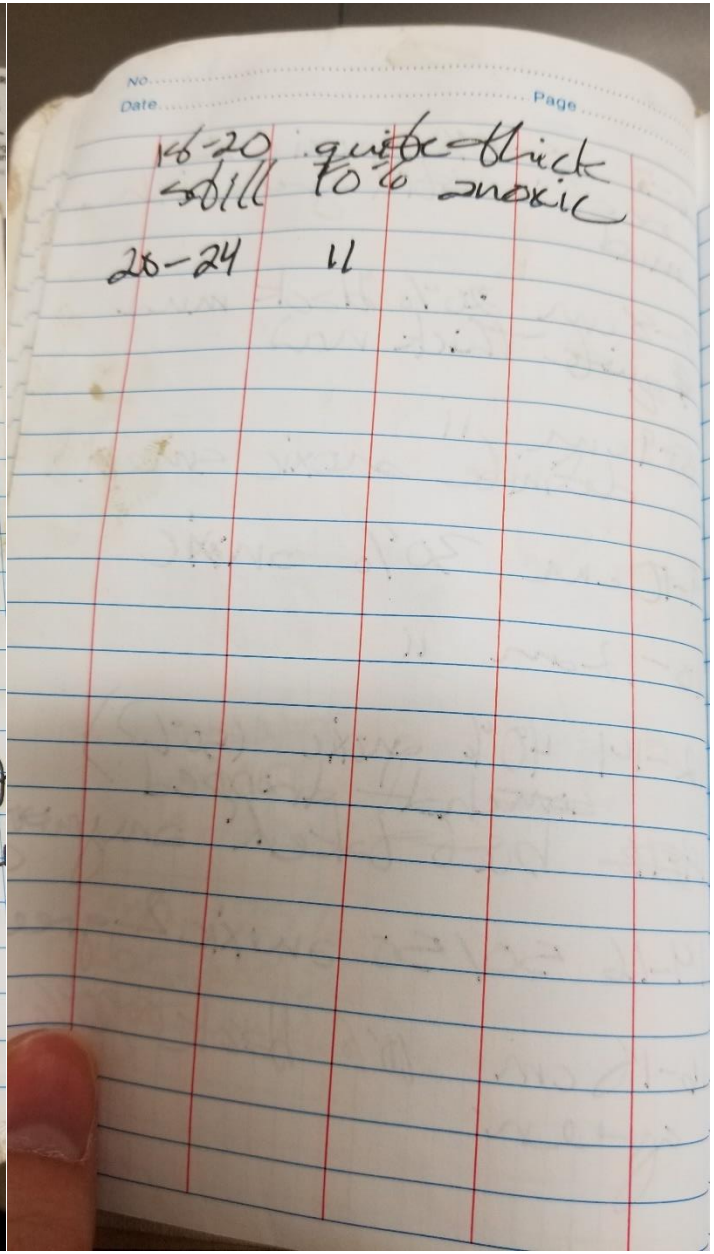

16-20 quite thick still 10% anoxic

20-24 "

Station 29
June 16, 2018

0-1 sandy yellow brown mud. Fluffy organics

1-2cm same brown sandy mud with 20% streaks of slightly reddish brown mud.

2-3 85% green grey sandy mud 15% brown (reddish) distinct smell, not quite the same as anoxic smell.

3-4 brown 10% 90% grey green sandy (mud/grain) (rocks @ 3-4

4-5 95% green grey sandy mud

5-6 " some air pockets in the sed

6-7cm all grey green sandy mud black streaked bases in next 2 layers thick now.

7-8 thick grey green mud 15% sandy

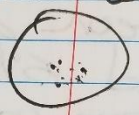

8-9 grey green mud 10% sand

9-10cm grey green mud 20% anoxic black streaks

10-12cm patches of sandy sed. 15%

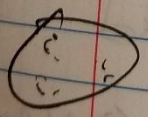

12-14cm
20% sand.

14-16 sandy mud 30% -40
grey green mud rest.
few black streaks
& medium sized rock

16-18cm patch of
gravel on left of section
60% sandy mud

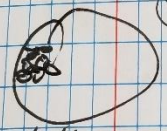

18-20 still a patch of
gravel but smaller particles
50% grey green mud

20-25 30% sandy 70%
mud

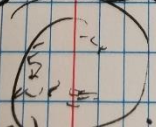

gravel mid way thro

25-30 sandy
35% sand
65% mud.
kind of pink mud
sandy layers throughout

30-34 hints of reddish
brown mud (different
from top 30% sandy
-turn 2000 colour
more near bottom
(80%)

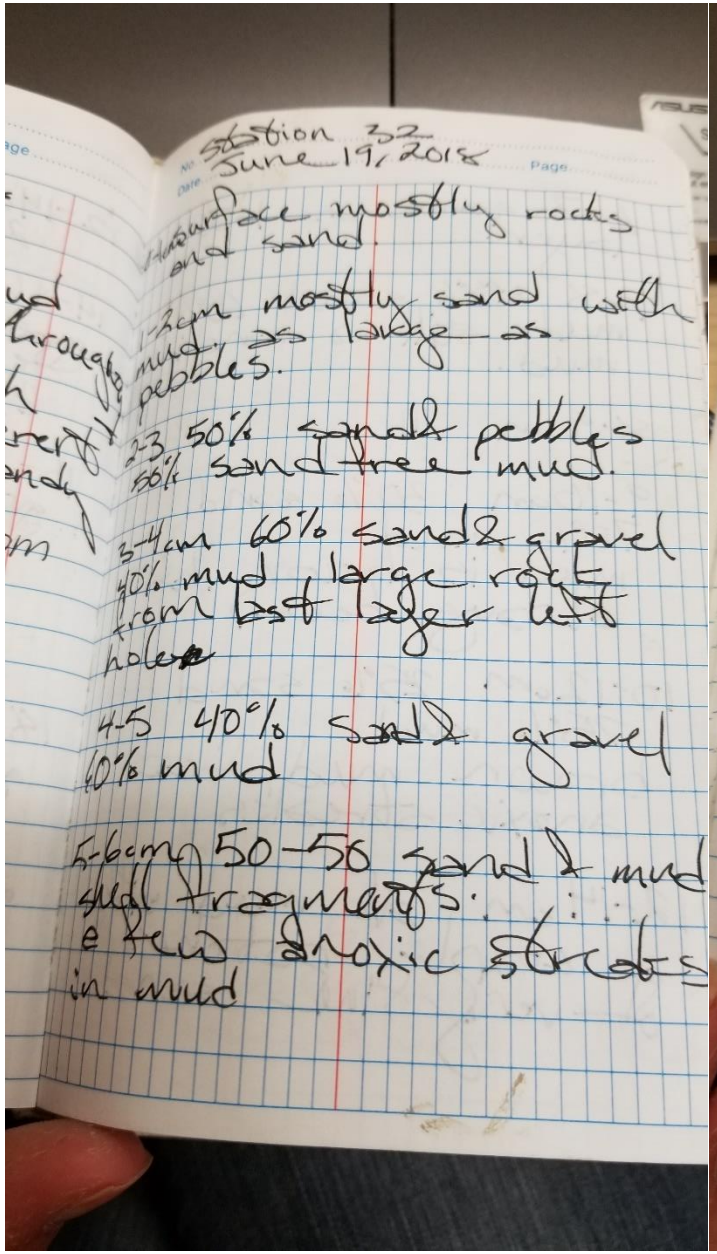

Station 32
June 19, 2018

Subsurface mostly rocks and sand.

1-2cm mostly sand with mud. as large as pebbles.

2-3 50% sand& pebbles 50% sand free mud.

3-4cm 60% sand & gravel 40% mud large rock from last layer left holes

4-5 40% sand & gravel 40% mud

5-6cm 50-50 sand & mud mud fragments. a few anoxic streaks in mud

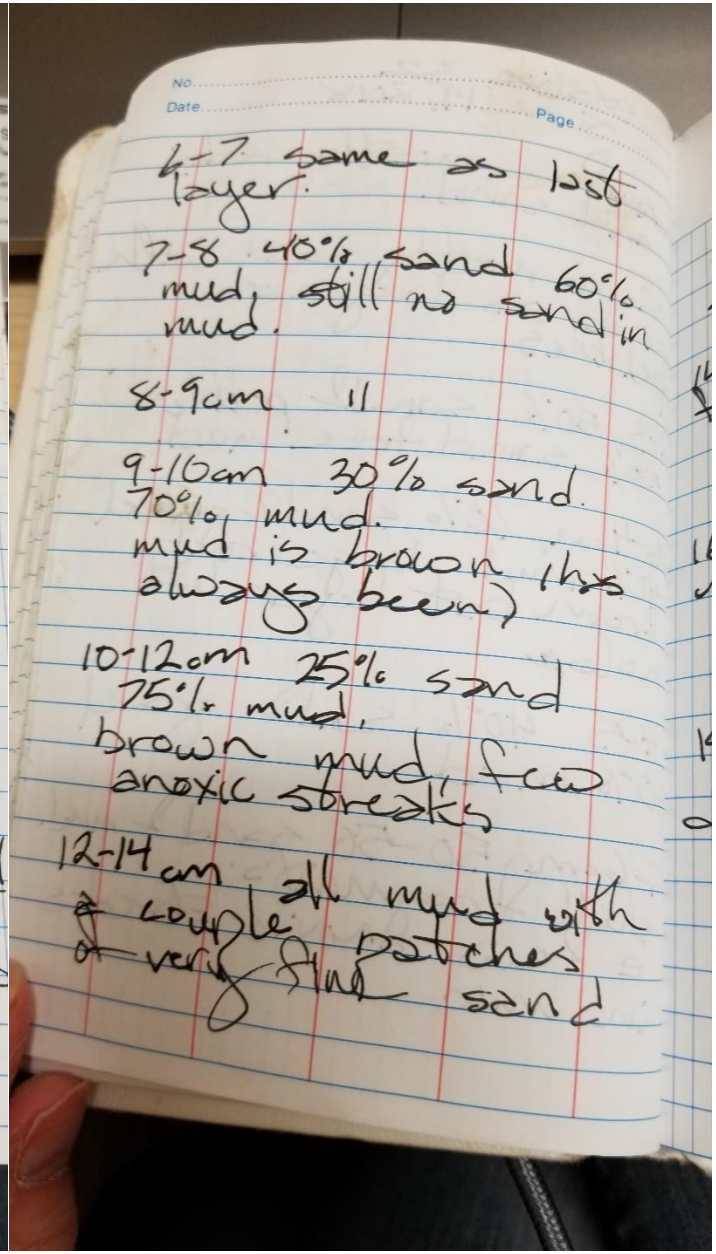

6-7 same as last layer.

7-8 40% sand 60% mud, still no sand in mud.

8-9cm "

9-10cm 30% sand 70% mud. mud is brown (has always been)

10-12cm 25% sand 75% mud. brown mud, few anoxic streaks

12-14cm all mud with a couple patches of very fine sand

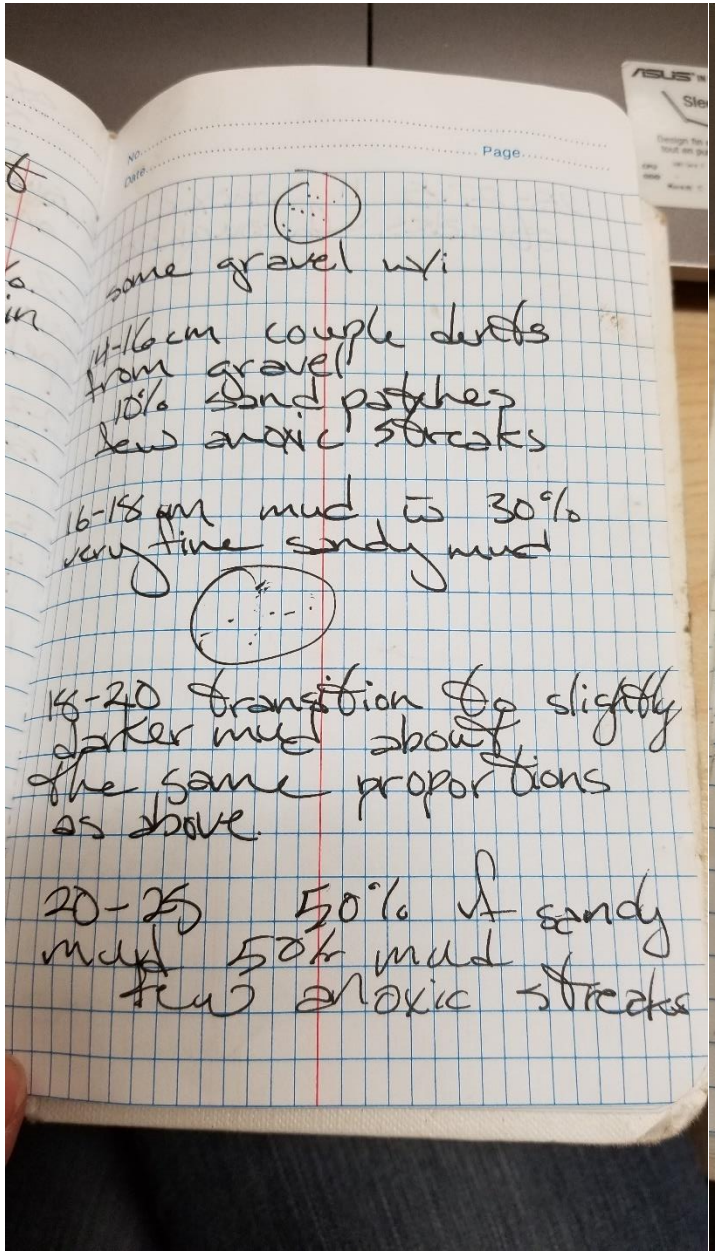

some gravel w/i

14-16cm couple dents from gravel
10% sand patches
few anoxic streaks

16-18 cm mud w 30% very fine sandy mud

18-20 transition to slightly darker mud about the same proportions as above.

20-25 50% of sandy mud 50% mud
few anoxic streaks

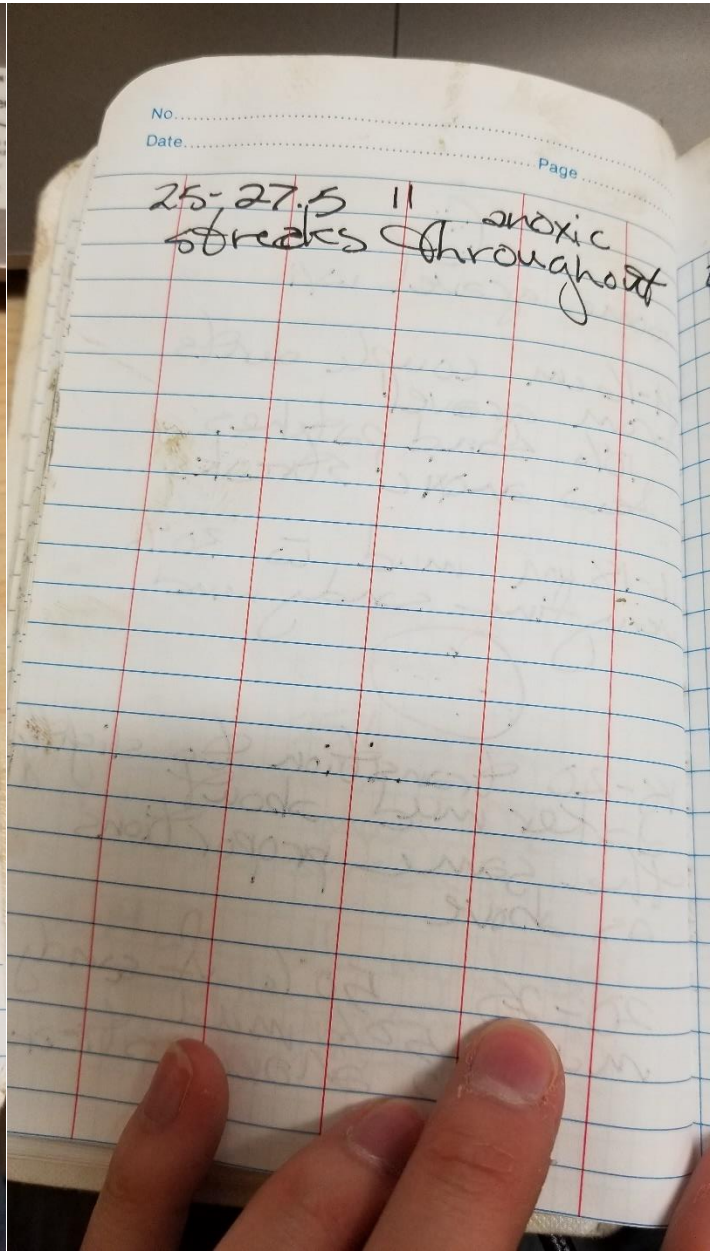

25-27.5 II anoxic streaks throughout

Station 36
June 22, 2018

0-1cm little bit of surface water fluffy organics. Brittle star little sandy

1-2cm Brown mud. Intermixed medium sand grains

2-3 half sand brown mud, half grey green mud.

3-4 green grey mud with thin streaks of brown mud. slightly sandy

4-5 grey green mud, sandier than last layer

5-6 streaks & sandy grey green in grey green mud.

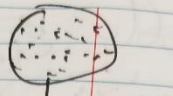

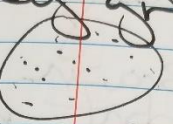

6-7 substantially thicker than first two layers same as last layer

7-8 hole in center but nothing in it. weird. same as last layer

8-9 grey green mud. streaks of darker grey. Hint of [illegible] mud

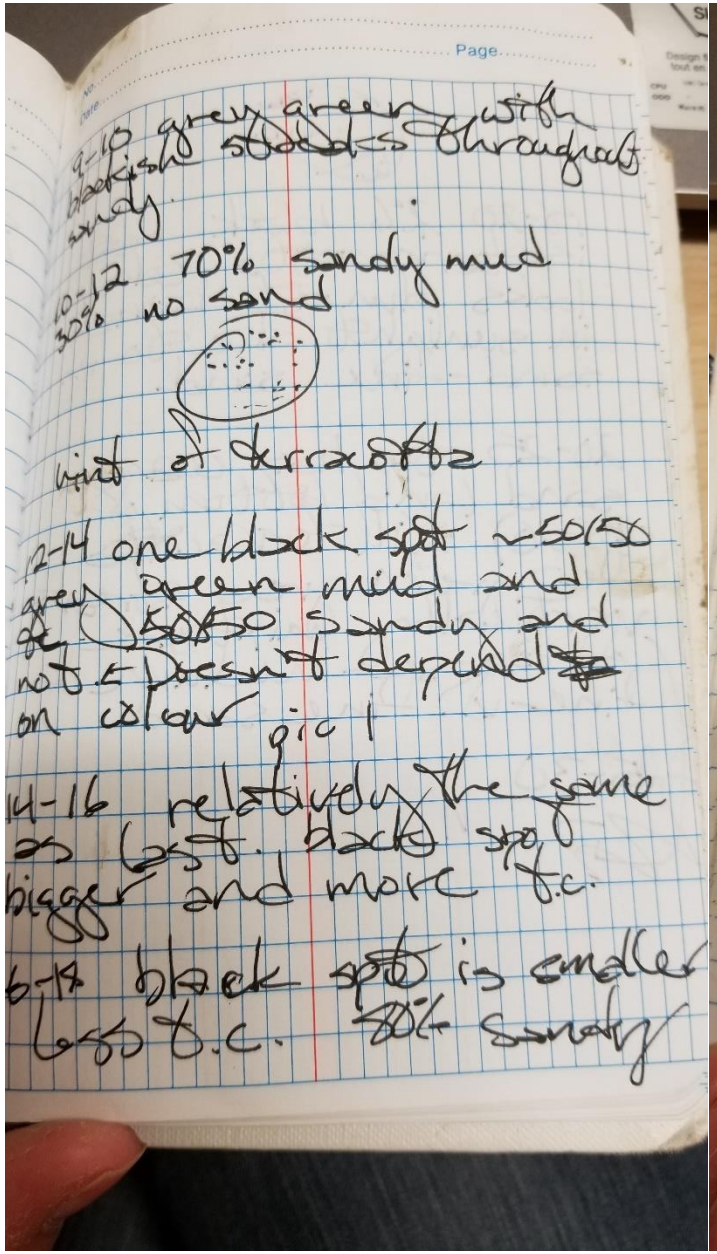

0-10 grey green with blackish shades throughout sandy.

10-12 70% sandy mud 30% no sand

hint of terracotta

12-14 one black spot ~50/50 grey green mud and ~50/50 sand and not. Doesn't depend on colour pic 1

14-16 relatively the same as last. black spot bigger and more t.c.

16-18 black spot is smaller less t.c. 80% sandy

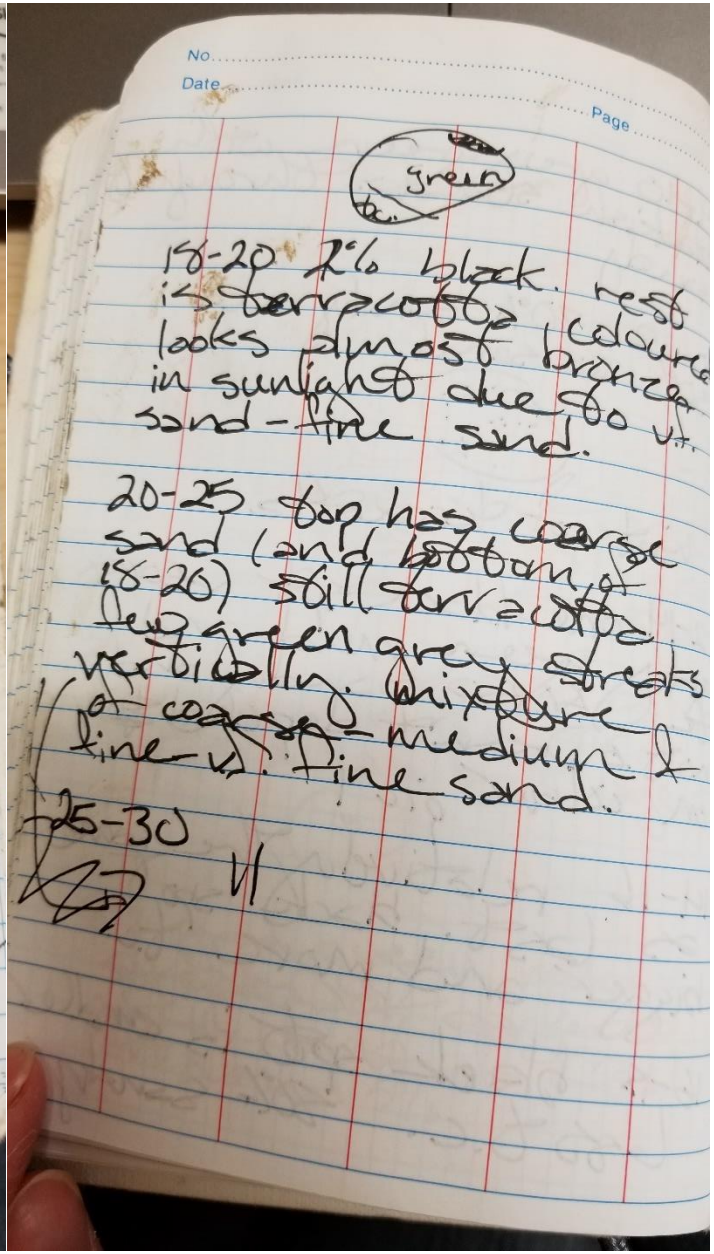

18-20 2% black. rest is terracotta colour looks almost bronze in sunlight due to v.f. sand - fine sand.

20-25 top has coarse sand (and bottom of 18-20) still terracotta few green grey streaks vertically. mixture of coarse, medium & fine vs. fine sand.

25-30

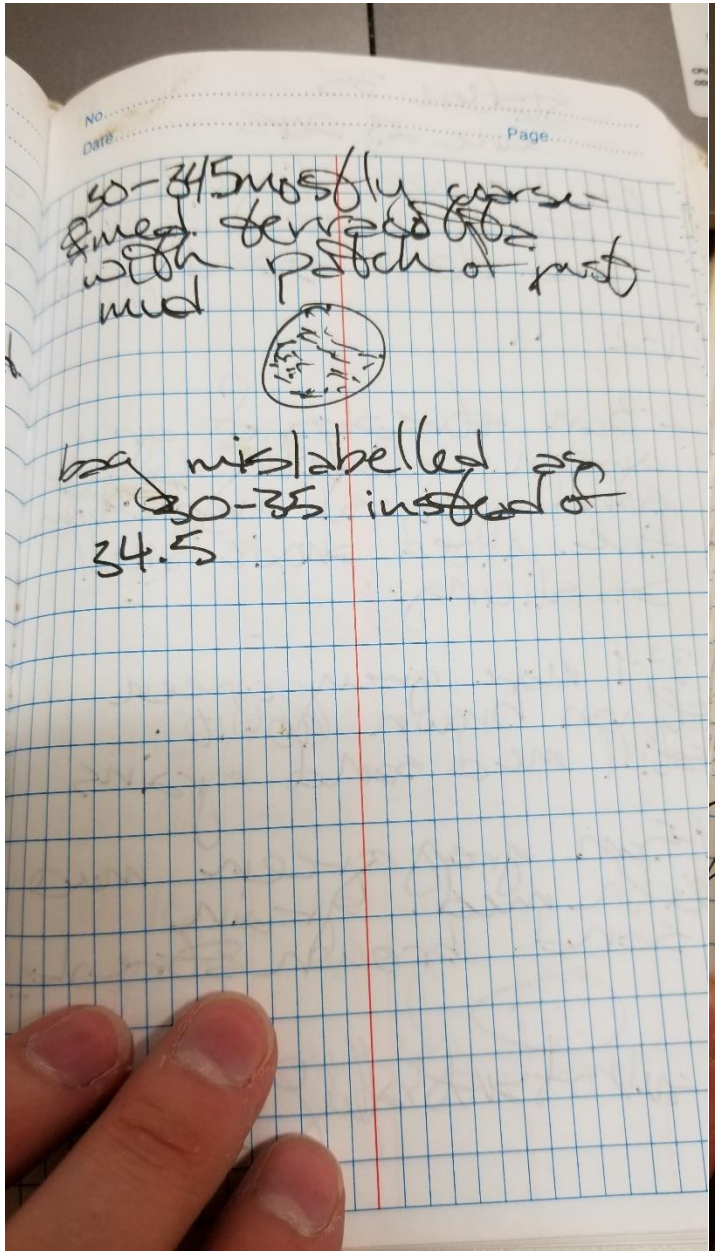
No.
Date
Page
30-34.5 mostly coarse & med. sand with patch of mud
bag mislabelled as 30-35 instead of 34.5

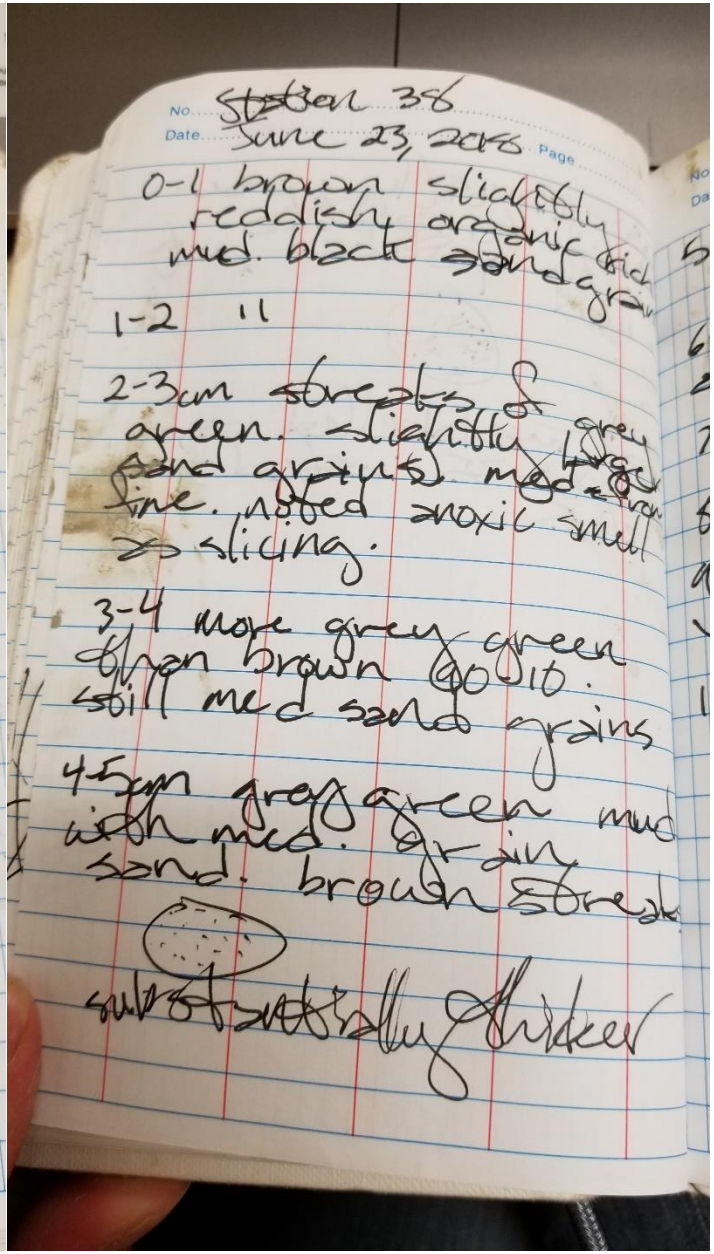
No.
Date
Page
Station 36
June 23, 2018
0-1 brown slightly reddish organic rich mud. black sand grains
1-2 "
2-3cm streaks of green. slightly grey sand grains med-coarse. fine. noted anoxic smell on slicing.
3-4 more grey green than brown 90/10. still med sand grains
4.5cm grey green mud with med. sand. brown streaks

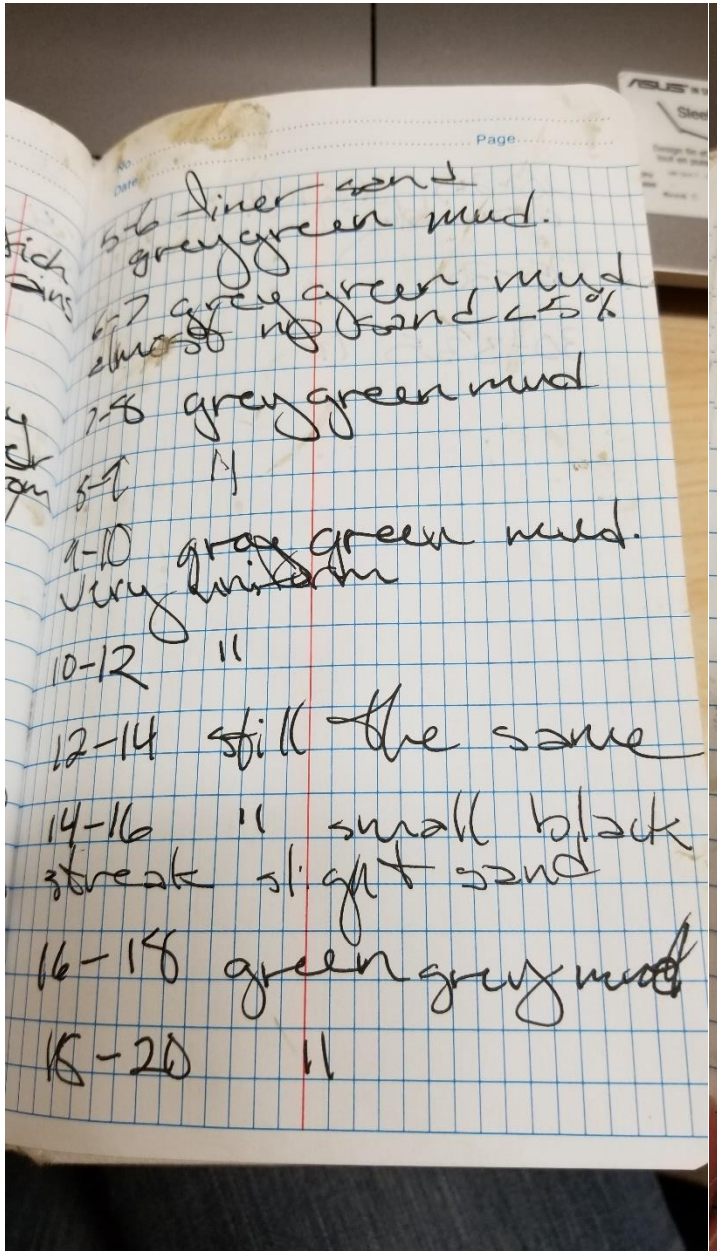

5-6 liner sand grey green mud.
6-7 grey green mud
slight no sand <5%
7-8 grey green mud
8-9 "
9-10 grey green mud. very fine
10-12 "
12-14 still the same
14-16 " small black streak slight sand
16-18 green grey mud
18-20 "

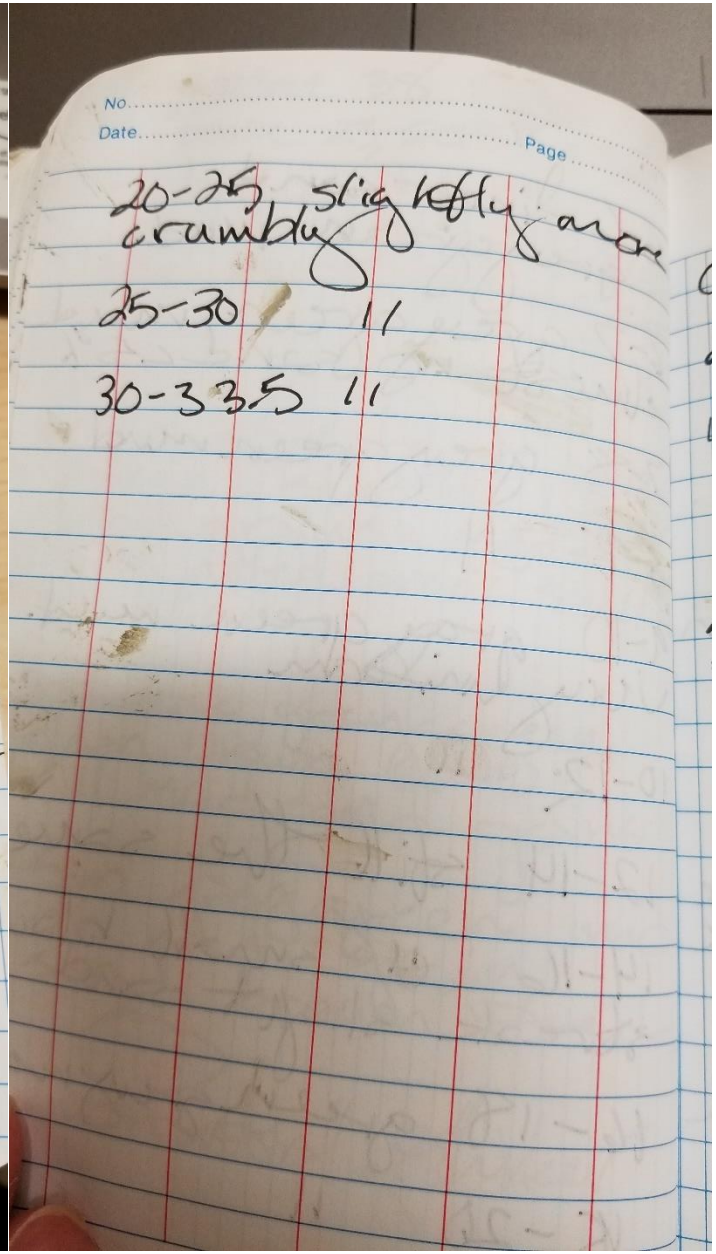

20-25 slightly crumbly
25-30 "
30-33.5 "

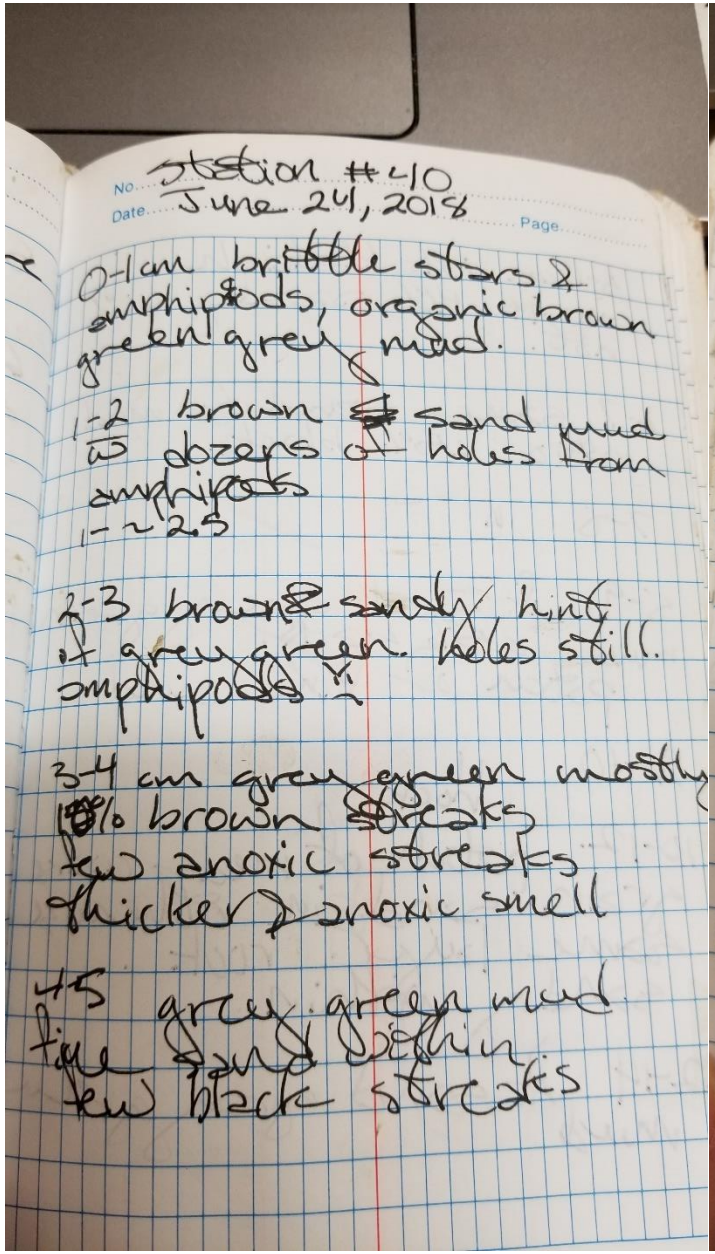

No. station #410
Date June 24, 2018 Page

0-1cm brittle stars & amphipods, organic brown green grey mud.

1-2 brown sand mud
~ dozens of holes from amphipods
1-~2.5

2-3 brown sandy, hint of grey green. holes still. amphipods ~

3-4 cm grey green mostly
~10% brown streaks
few anoxic streaks
thicker > anoxic smell

4-5 grey green mud
fine sand within
few black streaks

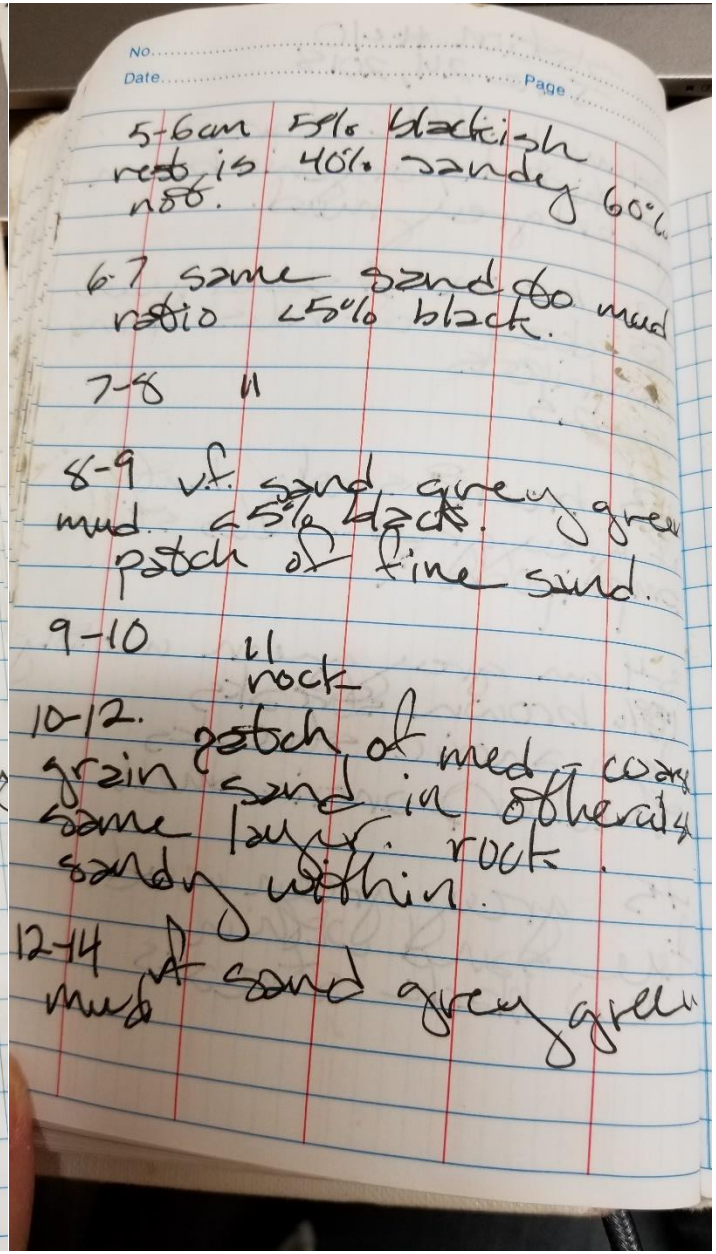

No.
Date Page

5-6cm 5% blackish
rest is 40% sandy 60%
mud.

6-7 same sand:mud
ratio <5% black.

7-8 "

8-9 v.f. sand grey green
mud. <5% black.
patch of fine sand.

9-10 " rock

10-12. patch of med - coarse
grain sand in otherwise
same layer. rock
sandy within.

12-14 sand grey green
mud

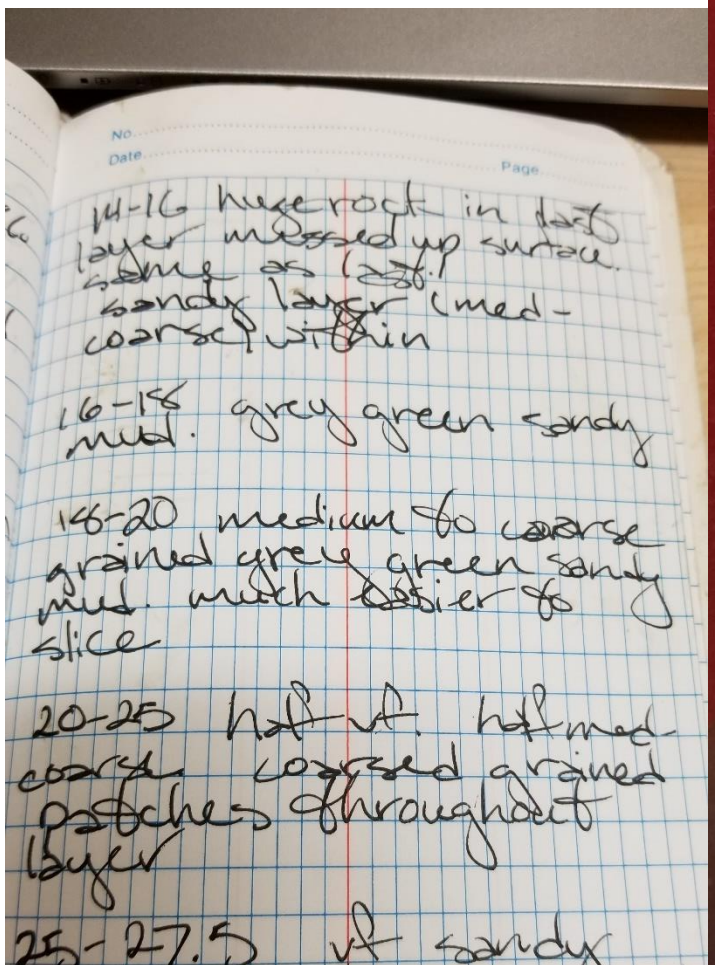
No.
Date
Page
14-16 huge rock in dark layer messed up surface. same as last.
sandy layer (med-coarse) within
16-18 mud. grey green sandy
18-20 medium to coarse grained grey green sandy mud. much easier to slice
20-25 half v. fine half med coarse coarse grained patches throughout layer
25-27.5 v. sandy

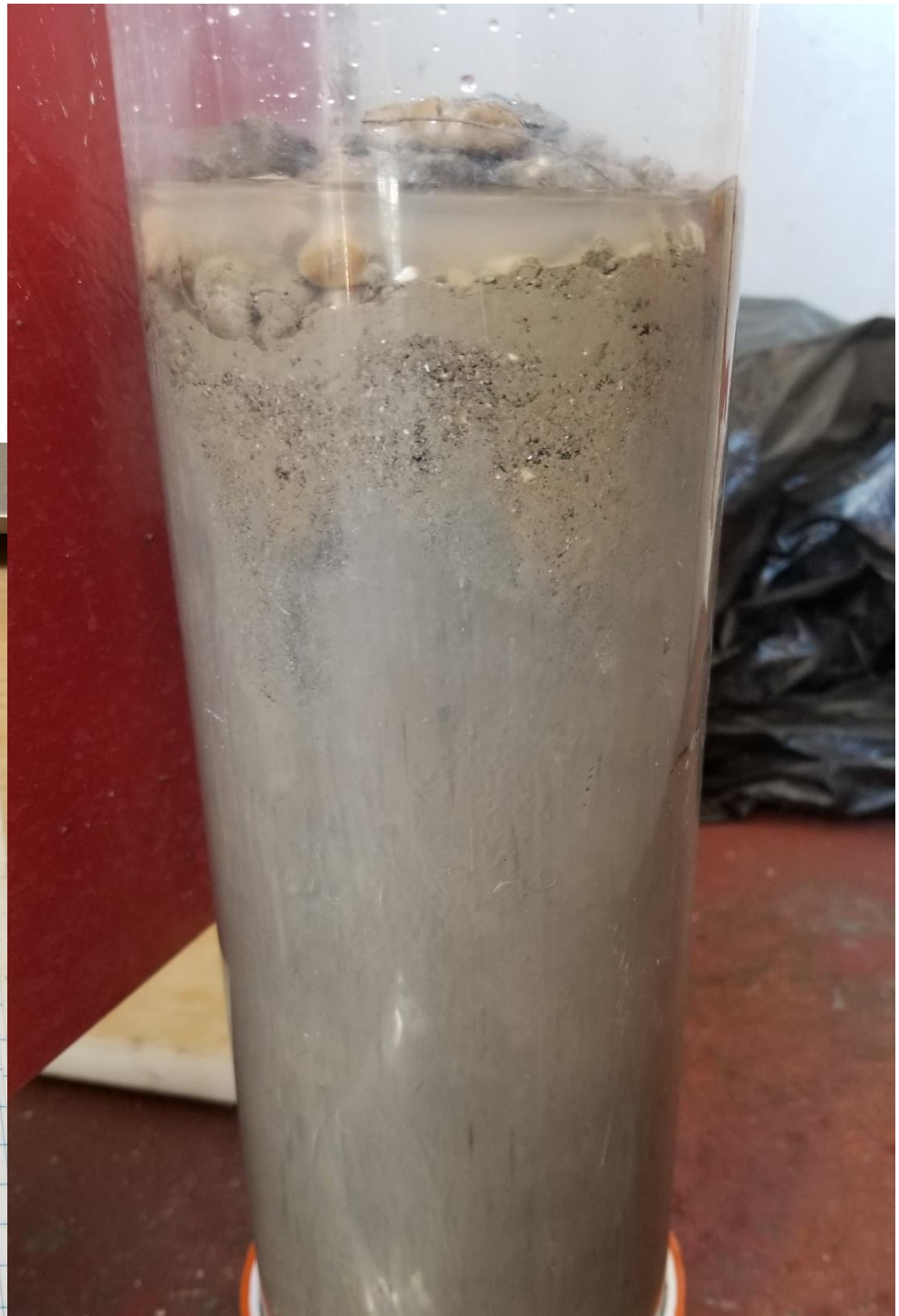


Nasco WHIRL-PAK
0-1cm

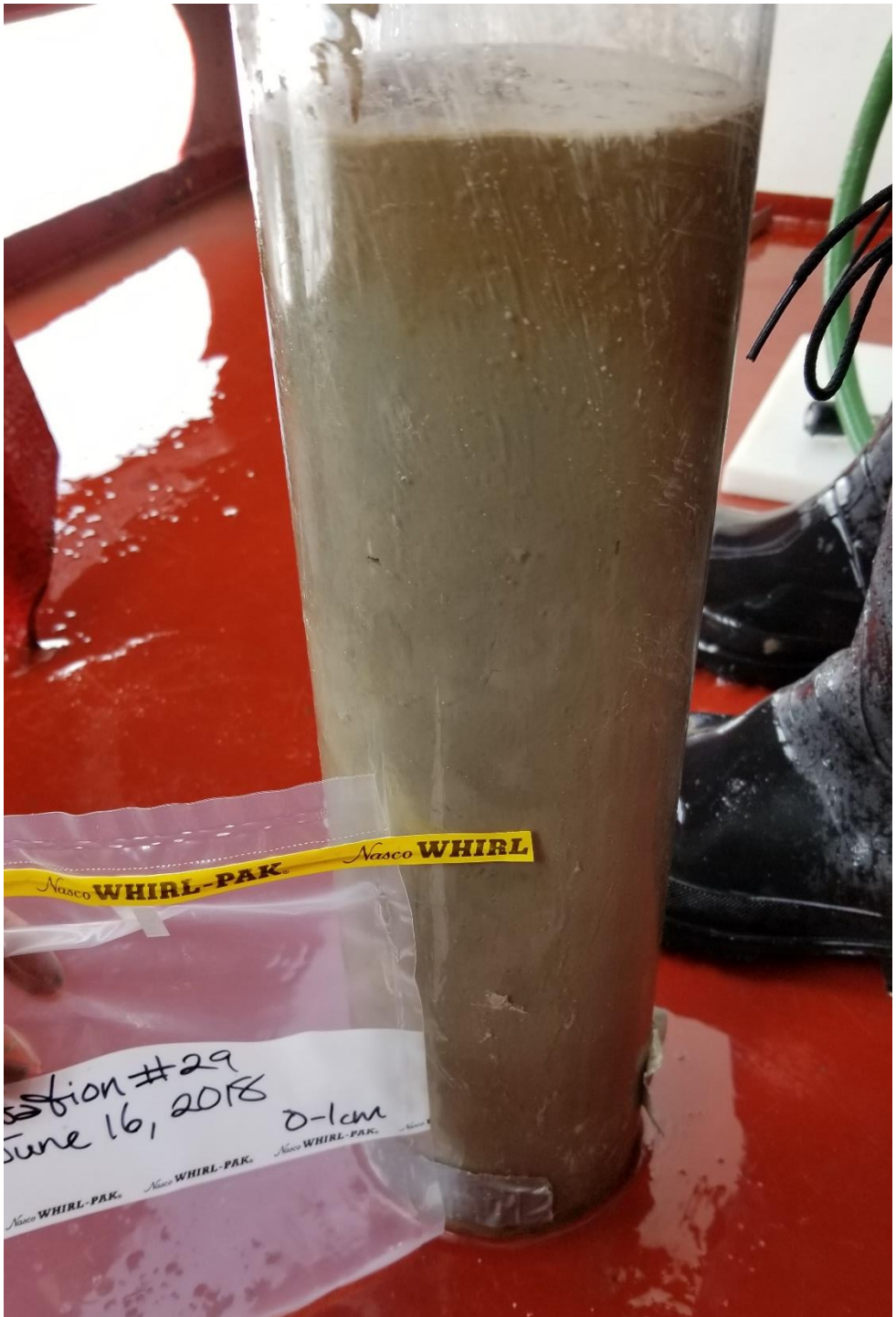
Nasco WHIRL-PAK
Nasco WHIRL
0-1cm
Nasco WHIRL-PAK
Nasco WHIRL-PAK
Nasco WHIRL-PAK


WHIRL


WHIRL-PAK
WHIRL-PAK
WHIRL-PAK
WHIRL-PAK
WHIRL-PAK

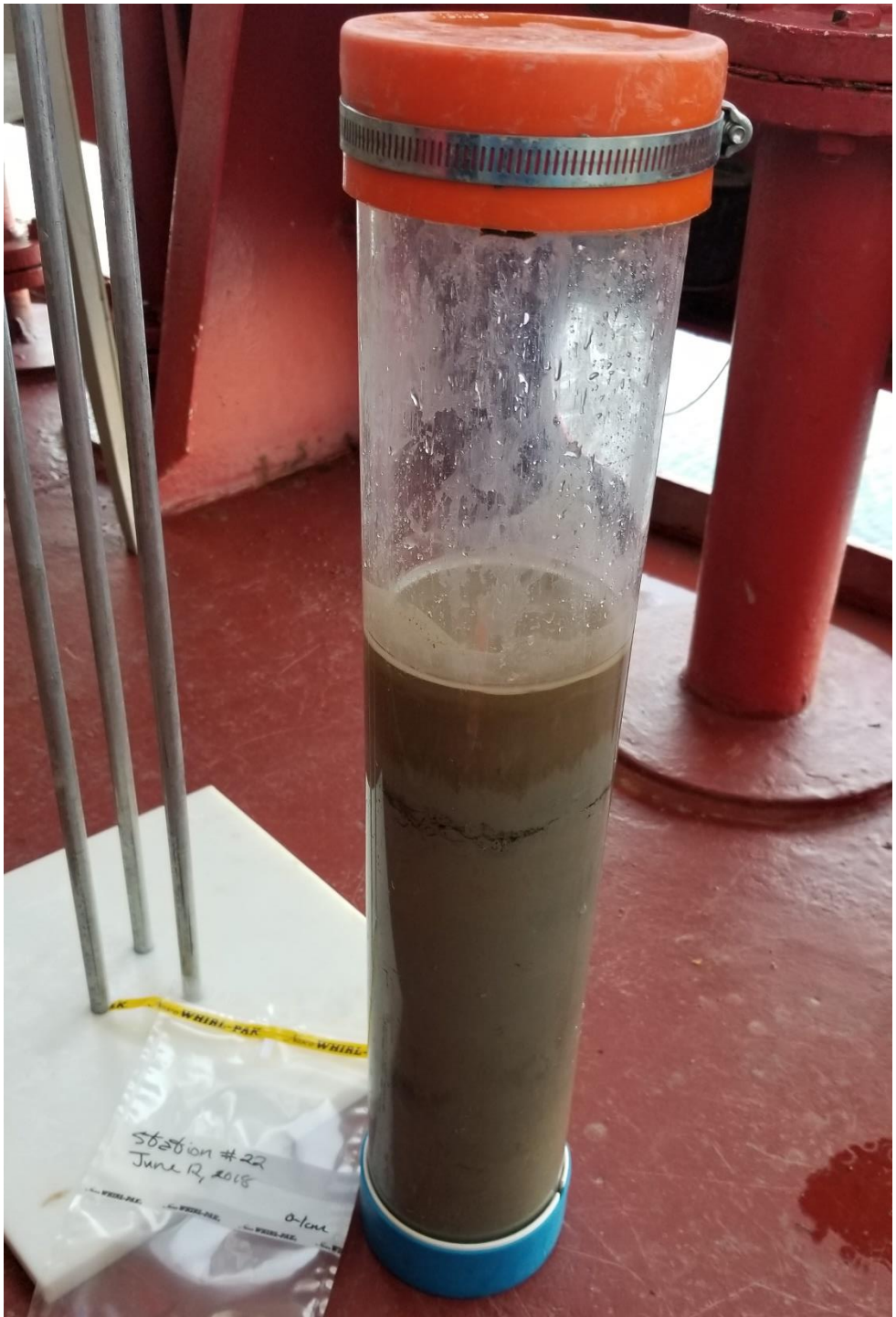
WHIRL-PAK
Station #22
June 9, 2018
0-1cm

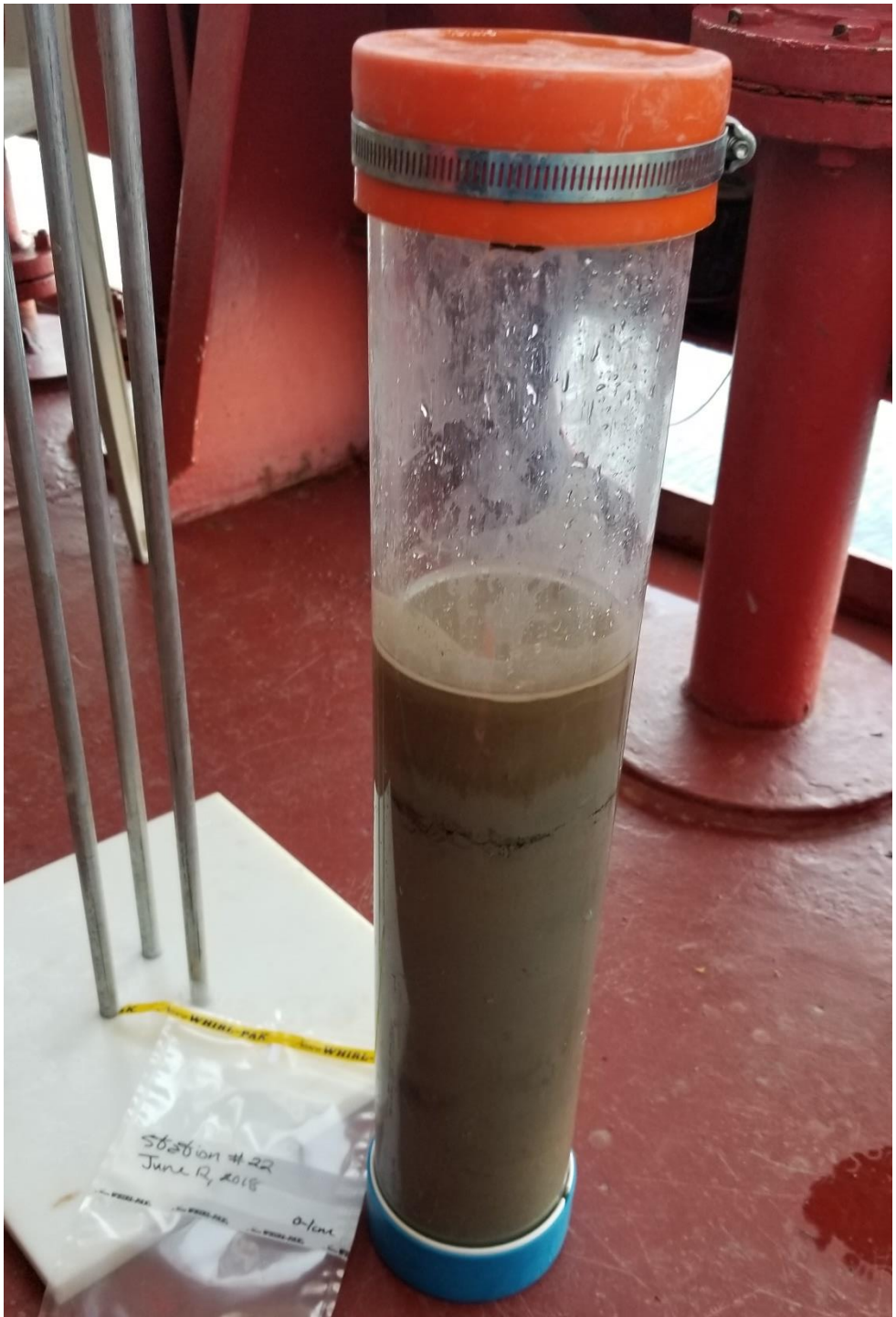
WHIRL-PAK
WHIRL-PAK


PAK
Nasco WHIRL-PA

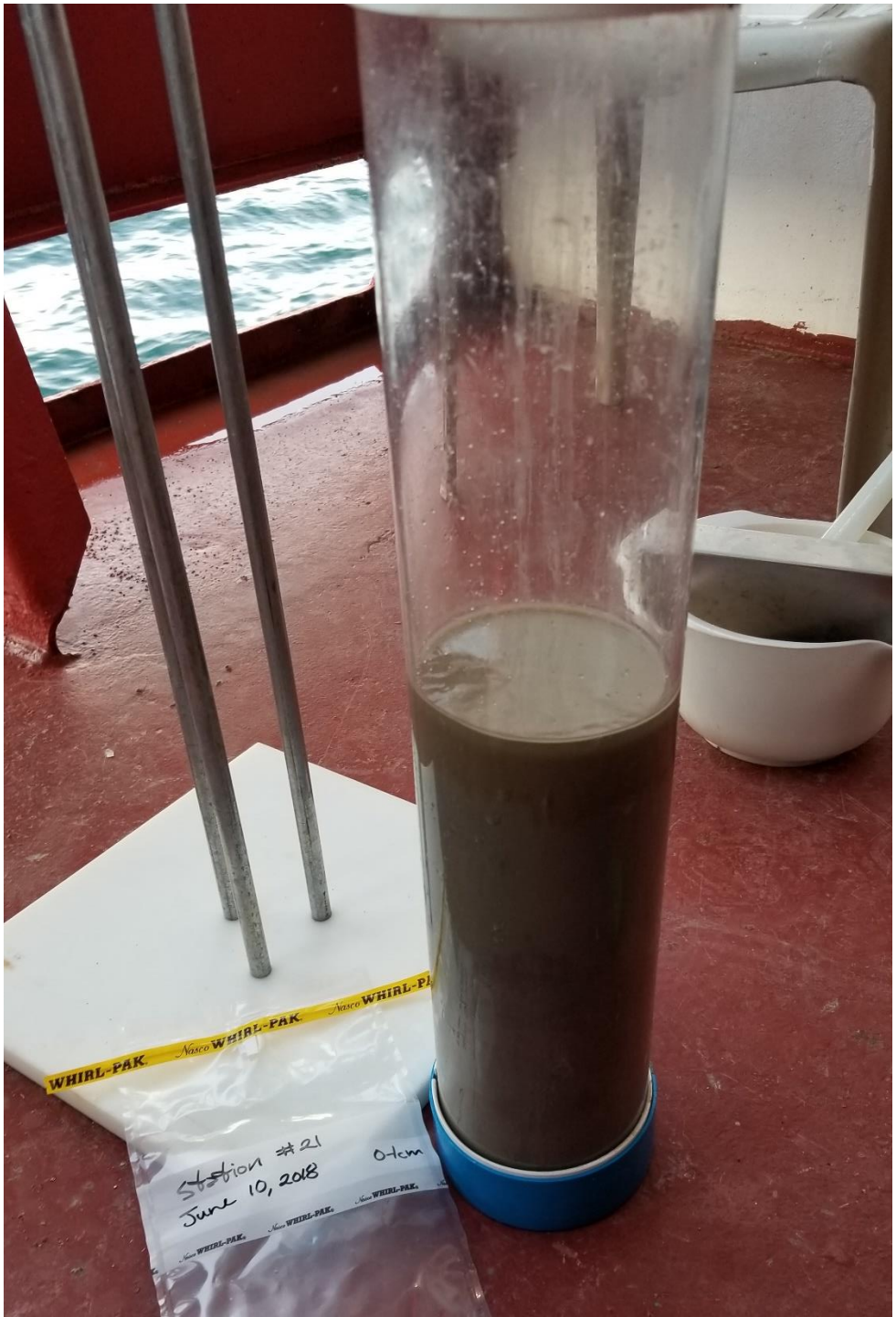
WHIRL-PAK
Nasco WHIRL-PAK
Station #21
June 10, 2018
0-1cm

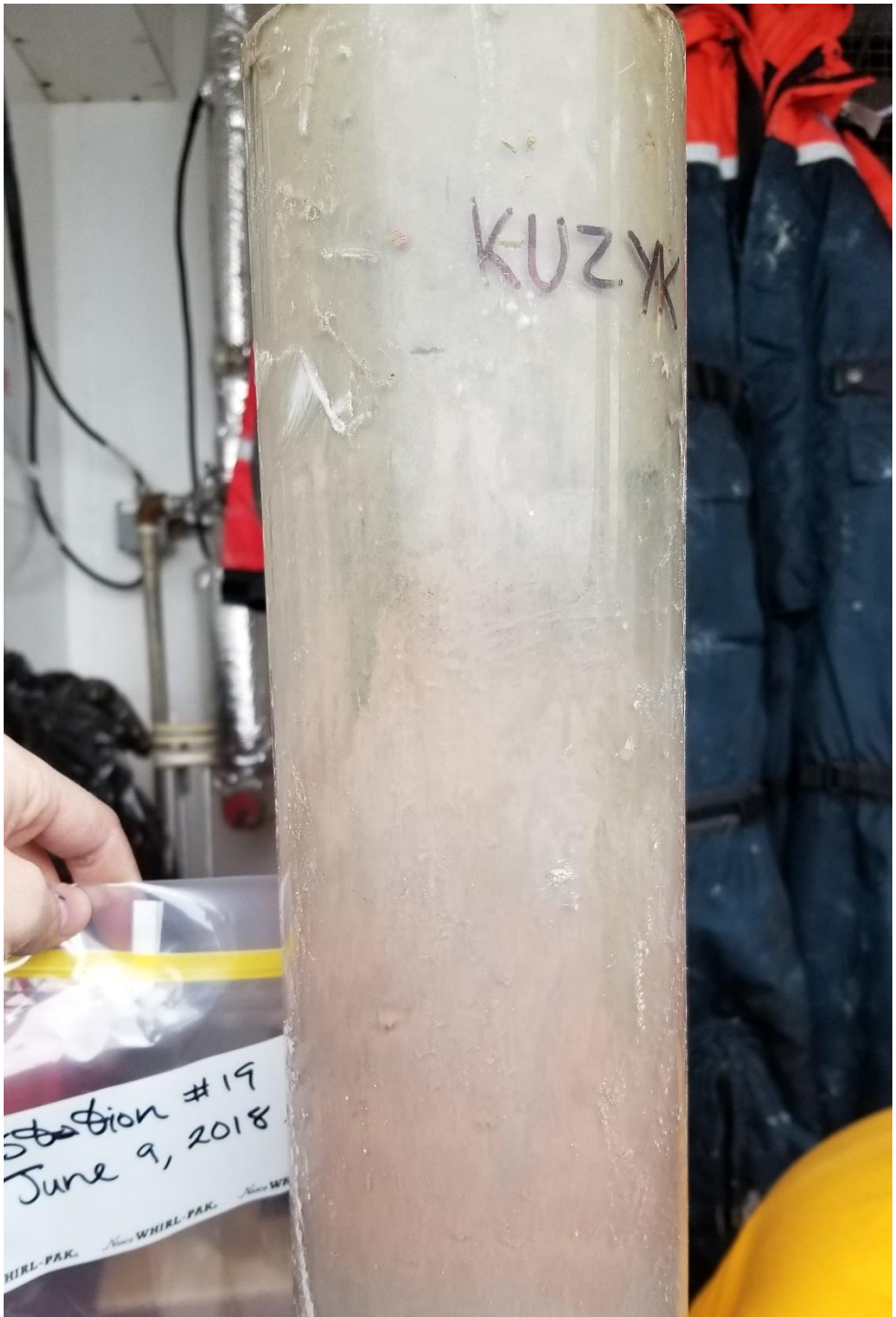
KUZYK
Station #19
June 9, 2018
WHIRL-PAK
WHIRL-PAK


KUZY


Nasco WHIRL-PAK
Station #18
June 8th 2018
0-1cm

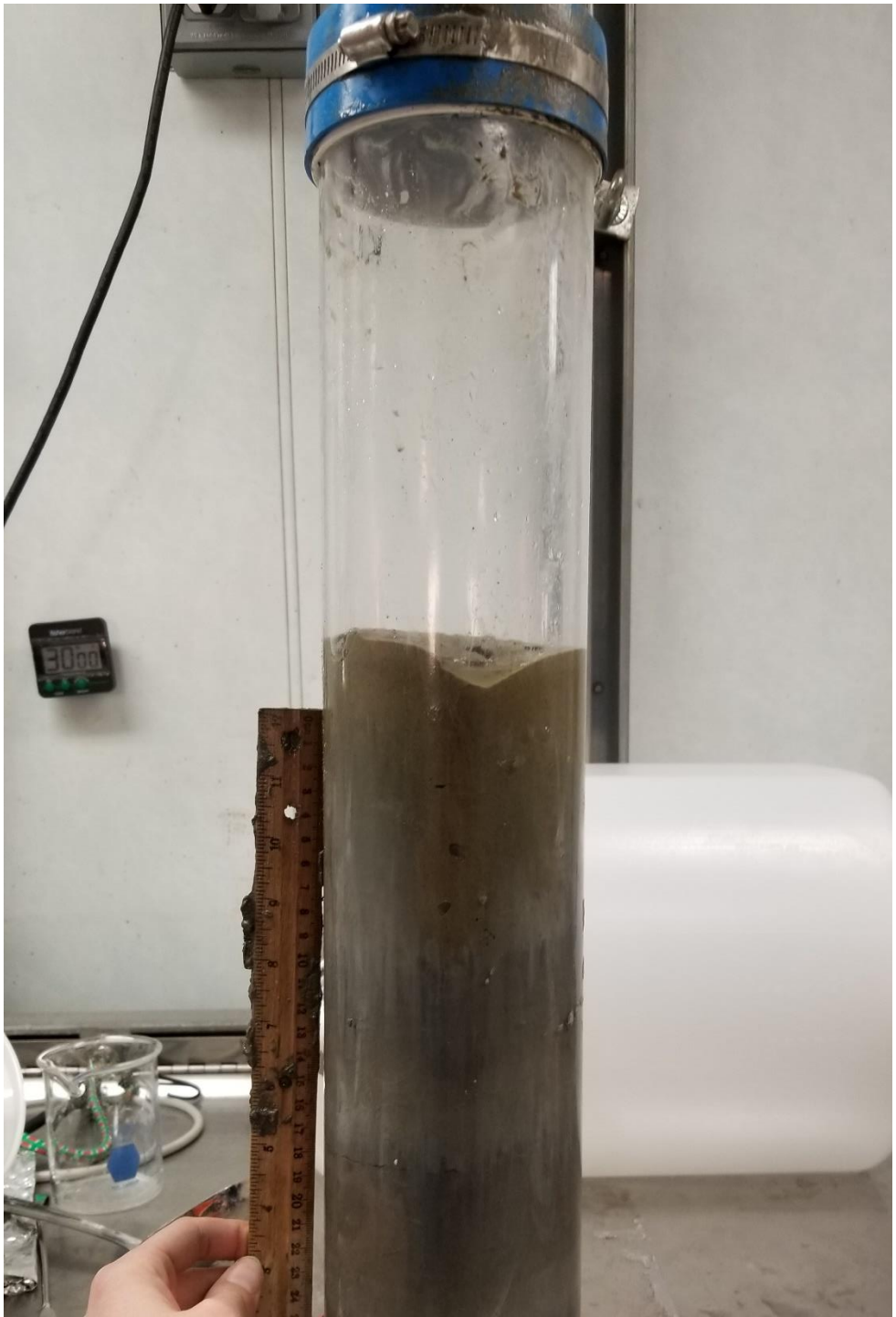


WHIRL-PAK
Station #10
June 4th 2018


Section #3
June 22nd, 2018
0-4cm